POLITECNICO DI MILANO

Facoltà di Ingegneria Industriale e Dell'Informazione

Dipartimento di Energia

Corso di Laurea Magistrale in Ingegneria Energetica con Orientamento Idrocarburi

Laboratory and Field Data Investigation on Disproportionate Permeability Reduction to Mitigate Water Production in Oil Industry

Relatore: Prof. Gianpiero GROPPI

Co-Relatori: Ing. Elisa di BIASE, ENI
Ing. Giuseppe RIPA, ENI

Tesi di Laurea Magistrale di:
Riccardo MORLACCHI
Matr. 801253

Anno Accademico 2013 - 2014

Ignoranti quem portum petat, nullus suus ventus est
A cului che non sa verso quale porto è diretto, nessun vento gli è favorevole.
He who does not know which port he's sailing to, has no favorable wind
(Lucius Annaeus Seneca)

Alla mia mamma, Romana,

al mio papà, Enzo,

e a mio fratello, Marcello.

RINGRAZIAMENTI

Il primo sentito e doveroso ringraziamento va a Elisa, Ing. di Biase, la mia ottima tutor aziendale, che mi ha assistito e sostenuto nella stesura della mia tesi. La ringrazio soprattutto per la sua pazienza nel chiarire tutti i miei dubbi.

Un grosso grazie anche all'Ing. Giuseppe Ripa che, inseguito a mattinate e pomeriggi passati a ponderare mille concetti e teorie, mi ha aiutato a risovere i quesiti che mi ero posto.

Ringrazio molto anche il Prof. Gianpiero Groppi per avermi dato l'opportunitá di svolgere questo lavoro e per la fiducia che ha riposto in me.

Ci tengo inoltre a ringraziare tutte le persone con le quali ho avuto il piacere di lavorare in questi mesi. L'Ing. Martin Bartosek, che mi ha assistito in tutti i frangenti durante il periodo di tempo passato ai laboratori ENI. L'Ing. Jose R. Vielma che spesso e volentieri mi dava consigli e libri per completare la mia tesi. Un grazie anche tutti gli altri colleghi che mi hanno aiutato: Vanessa, Salvatore, Giorgio e, in generale, tutto l'ufficio TEOP!

Questa laurea é dedicata ai alle mie nonne, che tanto sono orgogliose del mio lavoro, ai miei nonni, che sarebbero dovuti essere qui.

Grazie a tutti i miei amici che hanno sempre creduto in me. Soprattutto a te, Peppe, per la nostra amicizia senza tempo che supera qualsiasi distanza.

Grazie a tutti i miei compagni di avventura, di studio e sopratutto di risate per questi anni al Poli. Caro Max, o dovrei dire Montesquissimo, un grazie anche a te per avermi spalleggiato in questa odissea, e per le telefonate rincuoranti quanto tutto sembrava perduto nelle notti prima degli esami, anche se durante il primo anno ci odiavamo perché io ero un capellone e tu un pel di carota.

RIASSUNTO ESTESO

Questo documento si prefissa l'obiettivo di stabilire l'efficacia dei trattamenti effettuati con modificatori di permeabilità relativa, atti a ridurre la produzione d'acqua in giacimenti ad olio o a gas, identificando, con test di laboratorio e dati di produzione,quali sono i parametri e le variabili che influiscono e regolano il loro comportamento. Questi trattamenti sono effettuati tramite l'iniezione "bullhead" in pozzo di soluzioni acquose di polimeri o di gel debolmente legati. Una volta che questi prodotti raggiungono la formazione che si trova nelle immediate vicinanze del pozzo, si adsorbono sulla superficie dei pori della roccia esecitando un'azione selettiva di riduzione della permeabilità: la permeabilità effettiva all'acqua viene ridotta in una proporzione molto maggiore rispetto a quella degli idrocarburi. Un altro aspetto di cruciale importanza che si prefigge questa tesi, è quello di raccogliere tutte le considerazioni fatte per ottenere una guida che fornisca indicazioni sia per la selezione dei migliori pozzi candidabili ad un eventuale trattamento, sia istruzioni per la corretta esecuzione del trattamento stesso. Quindi, attraverso queste linee guida, punta ad incrementare le possiblità di successo per futuri trattamenti. Per raggiungere tali obiettivi, si sfrutta un'analisi incrociata di dati ottenuti attraverso prove sperimentali, propedeutiche ai trattamenti, e dati raccolti durante la fase di produzione di quattro differenti pozzi a gas locati nel mar Adriatico, sottoposti a trattamenti per la riduzione selettiva di permeabiltà.

La tesi è complessivamente strutturata in cinque capitoli. Nel primo capitolo si discute ampiamente sullo stato dell'arte della tecnologia e si introducono i maggiori prodotti utilizzati nell'industria petrolifera, per la modificazione della permeabilità relativa; sono inoltre descritti i principi fisici secondo i quali operano queste sostanze. In tale direzione si è anche dimostrato come la riduzione della permeabilità all'acqua, in una limitata area nell'intorno del pozzo, causi un abbassamento piezometrico della pressione favorendo la

produzione di idrocarburi. Tuttavia non è stato possible effettuare una verifica di campo per via della mancanza di dati che permettano un'analisi numerica di questo tipo. Infine si è discusso riguardo quali sono i fattori presenti a fondo pozzo che possono influenzare questi prodotti, sia da un punto di vista chimico, sia da un punto di vista fisico.

Il secondo capitolo si prefissa l'obiettivo di definire il comportamento di questi polimeri, o gel, una volta entrati in contatto con la formazione, attraverso una serie di prove di laboratorio. La prima serie di prove consiste in test di viscosità, effettuati con un viscosimetro con una geometria di couette, che si focalizzano sulla caratterizzazione reologica delle soluzioni acquose di polimero. Questi test si prefissano l'obiettivo di caratterizzare tali soluzioni sotto il punto di vista della stabilità meccanica, sotto il punto di vista della stabilità chimica e anche sotto il punto di vista della stabilità termica, in relazione alle condizioni di fondo pozzo. La caratteristica più rilevante di questi prodotti, ottenuta tramite i test, come è logico aspettarsi per una soluzione polimerica, è il loro comportamento pseudoplastico. Il seguente grafico dà un'idea dei risultati ottenuti:

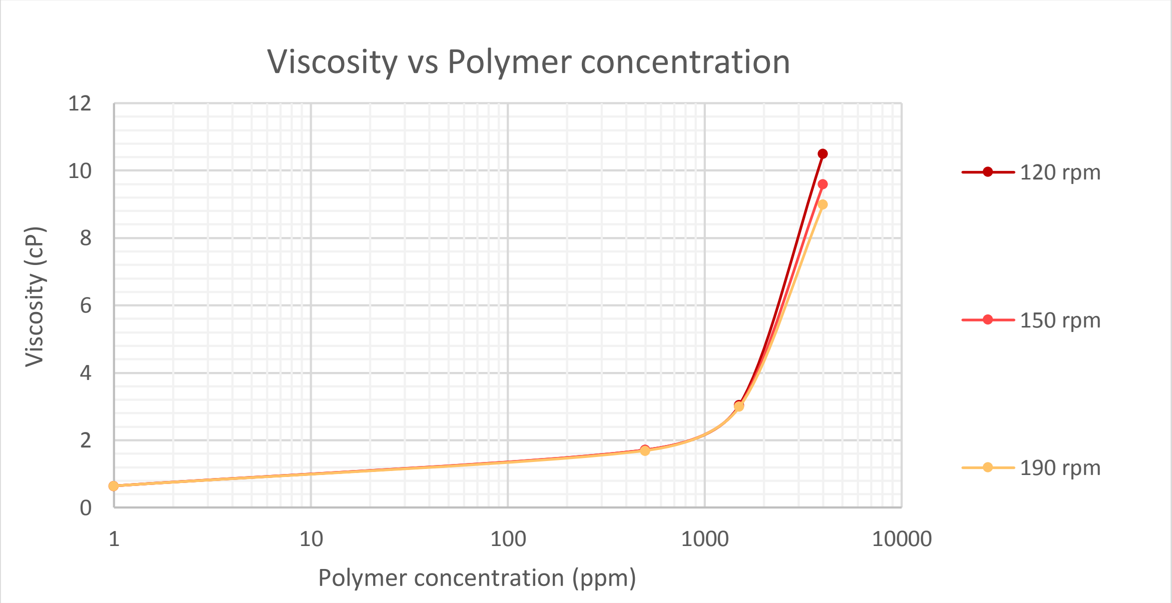

Figure 0-1: comportamento reologico della soluzione polimerica; Il grafico illustra la variazione della viscosità in seguito alle variazioni sia della concentrazione del polimero in soluzione, sia dello shear-rate imposto dal viscosimetro.

Tuttavia, la concentrazione delle soluzioni polimeriche durante i trattamenti, per la riduzione della produzione d'acqua, si aggira intorno ai $1500\ ppm$, massiche. Ovvero nella regione del grafico nella quale il comportamento dilatante non è ancora apprezzabile. Questo è il motivo per il quale, in questo documento, le soluzioni polimeriche vengono assimilate a fluidi Newtoniani.

I test di viscosità sono immediatamente seguiti da una serie di prove di flocculazione, eseguite con dei campioni di sabbia provenienti dagli stessi pozzi a gas sottoposti a trattamento. Questa serie di prove sono necessarie a stabilire quantitativamente il grado di interazione tra polimero e sabbia. Da essi si percepisce come il polimero sia estremamente attivo nell'adsorbirsi sulle particelle di fini diminuendo il loro tempo di deposizione fino a $5/6$ volte. Un altro aspetto molto importante che è stato evidenziato, è la possibilità di sfruttare la capacità di conglomerazione del polimero, nei confronti dei grani di sabbia, per esecitare un'azione agglomerante sulla formazione sabbiosa, e quindi di diminuire la produzione di sabbia. Questo comportamento è stato anche confermato dai dati di produzione e conferma la possibilità di utilizzare questo prodotto anche in pozzi che producono elevate quantità di fini in superficie.

Nella terza e ultima sezione del capitolo secondo, si discute dei test di flussaggio in carota. Questi ultimi servono a formire i dati più importanti per l'interpretazione dei dati di campo, ovvero: l'iniettività del prodotto, il grado di adsorbimento del polimero e l'efficacia nel ridurre selettivamente la permeabilità all'acqua lasciando inalterata quella agli idrocarburi. Questi test sono effettuati in condizioni di flusso stazionario e sfruttano campioni di una carota proveniente da uno dei pozzi in Adriatico. Essi consistono nel flussaggio alternativo di acqua, gas e ancora acqua, prima e dopo l'iniezione della soluzione polimerica.

L'uso di campioni provenienti da un solo pozzo è giustificato dal fatto che tutti i pozzi trattati presentano una certa omogeneità nelle caratteristiche della formazione e, inoltre, sarebbe estremamente dispendioso e ineconomico effettuare dei carotaggi su ciascun pozzo col fine di prelevare dei campioni.

Il seguente grafico fornisce un riassunto dei risultati ottenuti da questi test in termini di permeabilità effettiva al fluido flussato.

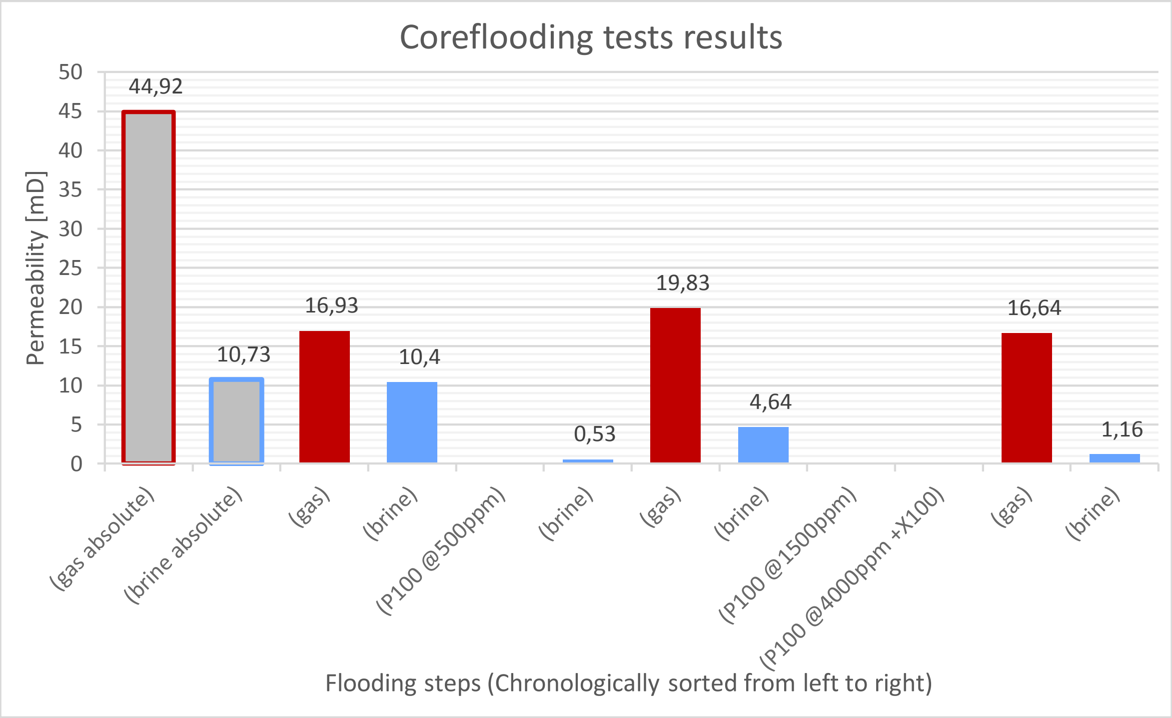

Figure 2: Grafico riassuntivo dei risultati delle prove di coreflooding eseguite nei laboratory ENI.

Il grafico evidenzia chiaramente come la permeabilità effettiva all’acqua è diminuita, mentre la permeabilità effettiva al gas è lasciata inalterata.

Infine, è utile accennare al fatto che test simili a quelli condotti nei laboratori ENI, prima del trattamento dei pozzi con soluzioni polimeriche, sono sempre effettuati anche dalle compagnie di servizio incaricate, e servono a verificare la fattibilità del trattamento stesso. Tuttavia, le compagnie petrolifere tendono a ripetere test simili, o del tutto differenti, sia per verificare i risultati forniti dalle compagnie di servizio, sia per ottenere ulteriori informazioni che sono indispensabili per consolidare il know-how.

Il terzo capitolo è dove si analizzano nel dettaglio i quattro pozzi a gas, perforati in roccia in arenaria, sui quali l’ENI ha effettuato i trattamenti con soluzioni polimeriche. I pozzi sono esaminati uno dopo l’altro dando innanzitutto una visione generale delle caratteristiche del pozzo, partendo dalla messa in produzione, fino allo schema di completamento. Successivamente, sono introdotti i dati raccolti durante la fase di iniezione del polimero con l'ausilio di un grafico che mostra, sull'asse delle ascisse il tempo richiesto dal trattamento, mentre sugli assi delle ordinate la pressione a testa pozzo, la portata istantanea di fluido iniettato e il loro rapporto. I dati raccolti dall'attività di campo, vengono poi direttamente confrontati con quelli raccolti e rielaborati durante i test condotti in laboratorio, allo scopo di evidenziare l'eventuale scostamento nel passaggio dalla scala di laboratorio a quella di campo. Successivamente viene presentata e trattata la storia produttiva del pozzo sia prima, sia dopo il trattamento, in modo da avere una chiara visione del suo esito. Alla fine di ogni paragrafo è presente un più completo confronto, con l'ausilio della legge di Darcy e un grafico che mostra delle proiezioni di produzione, tra i dati provenienti dalla storia di produzione dei pozzi e i dati provenienti dai test di laboratorio. In questo modo è possibile ottere un ottimo confronto tra dati sperimentali e i dati pratici, col fine di valutare l'esito del trattamento.

Il quarto capitolo è dove sono presentate le linee guida, di cui si è fatto accenno in precendenza, che forniscono non solo le informazioni necessarie per la selezione dei pozzi candidati, ma anche indicazioni sulla procedura operativa da utilizzare per ottimizzare il trattamento e per una corretta valutazione dell'effetto del polimero, o del gel.

Nell'ultimo capitolo sono illustrate alcune considerazioni generali, ad esempio il fatto che l'aumento della concentrazione della soluzione polimerica, durante il trattamento dei pozzi, non sembra sempre causare evidenti variazioni di iniettività, ovvero di perdita di pressione, mentre nei test di laboratorio, ad ogni aumento della concentrazione del polimero, corrisponde un aumento della pendenza della curva pressione-tempo, a parità di portata. Questo effetto potrebbe essere legato ad un'eterogeneità della formazione rocciosa nella pay-zone. Un'altra considerazione riguarda il fatto che i trattamenti acidi eseguiti sui pozzi, prima del trattamento con soluzione polimerica, non sembrano influire sul comportamento del polimero stesso, tuttavia potrebbero essere sfruttati per rimuovere il fattore di Skin e ottenere una più alta produzione.

In ogni caso, tralasciando queste ultime considerazioni, e nonostante le molte variabili esogene presenti nello studio della risposta a questo tipo di trattamenti, è stato possibile determinare che il successo di un trattamento per la riduzione della permeabilità relativa risiede, sia in una corretta selezione del pozzo candidato, in termini di struttura litologica del giacimento, sia in una corretta selezione del polimero utilizzato, in relazione alla permeabilità relativa media del giacimento

EXTENDED ABSTRACT

The aim of this document is to establish the effectiveness of the relative permeability modification treatments to reduce water production in oil industry, thus to identify which are the variable that contribute to their success. These treatments are carried out with a bullhead injection of polymer solution, or weakly crosslinked gel solutions, in the near wellbore area. The injected chemicals adsorb on the surfaces of the rock pores and alter the permeability of the near wellbore reservoir, selectively reducing the water permeability without affecting the oil or gas permeability. Another crucial objective of this dissertation is to collect all the deduced information into some useful guidelines, which provide indication on the selection of the most suitable candidate wells, and give general information on the procedure to implement the treatment itself, thus they aim at increasing the chances of success of any permeability reduction treatment.

To accomplish these purposes this thesis used a cross analysis of the data obtained both from experimental laboratory tests, and data collected from four different gas fields in the Adriatic sea, which were recently submitted to a water mitigation treatment with RPM products.

The structure of the thesis comprises five chapters. The first chapter includes a literature review describing the most common chemicals used to achieve water mitigation treatment, and also a thorough discussion about the physical principles that regulates them, along with a description of how the behavior of these products can be affected by physical or chemical interaction within the reservoir. Concerning the physical mechanism behind these chemicals, it has been demonstrated their application causes an increase in the drawdown pressure of the well. Still, it was not possible to prove this theory due to a partial lack of data from the gas field. These information are very important to understand every single chapter that follow.

The second chapter addresses the behaviour of the relative permeability modifier polymers, or gels, within the reservoir through a series of laboratory tests. The first set of tests are performed with a Couette geometry viscometer, and they are focused on the rheological behavior of the polymer, or gel, solutions, meaning that they aim at evaluating different aspects of these substances such as the mechanical resistance to shear stress, the thermal stability, and the chemical interaction of the gel solution with the surrounding environment. The most interesting aspect observed after these tests, as it was expected, is the shear-thinning behavior of the polymer solution which can be appreciated from the following plot:

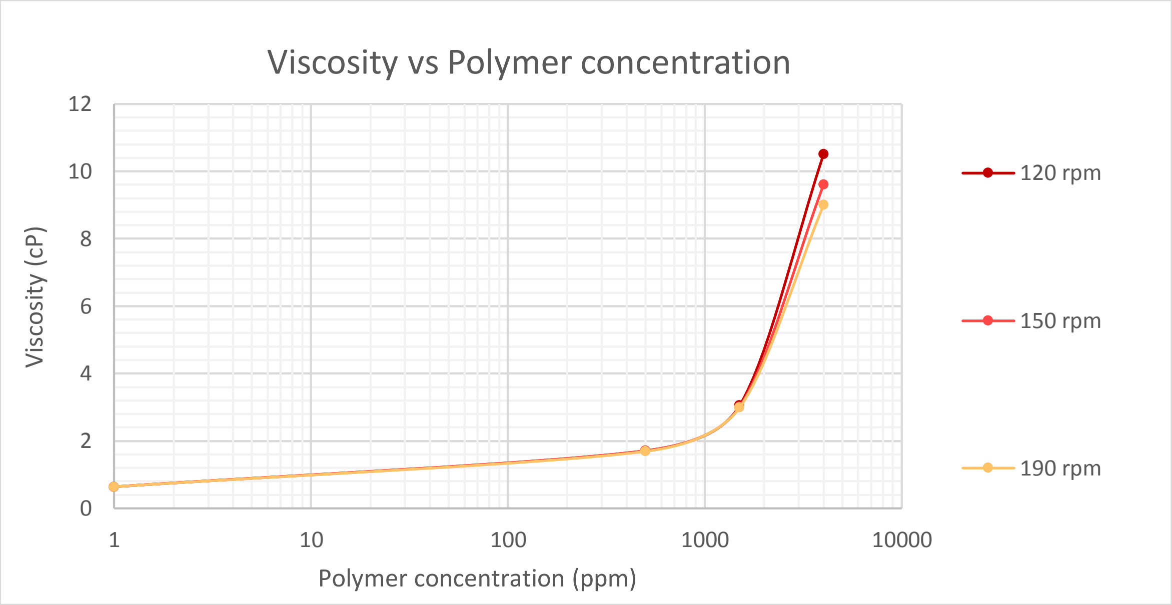

Figure 0-1: polymer behaviour; viscosity vs Polymer concentration at different shear rate.

Anyway, the concentration of the polymer during any water mitigation treatment is around $1500\ ppm$, where the shear-thinning effect can be neglected. That is the reason why, in this document, the behavior of any polymer solution is considered Newtonian.

These test are immediately followed by a series of quantitative flocculation tests carried out with sand obtained from the gas wells treated with the polymer. The flocculation tests are necessary to evaluate the attraction between the sand and the polymer. These test proved not only that the polymer solution, at every concentration used, greatly diminishes the settling time of the sand particle, from 5 to 6 times, but also that is plausible to expect that a product with these good flocculating properties, could also operate some sort of sand control. Indeed the process of adsorption and the coating of the pore surfaces could prevent the release of small grain fines during the production.

Finally a sequence of coreflooding tests provide the most important and useful parameters for a RPM treatment: the injectivity, the degree of adsorption and the effectiveness of the product in selectively reducing the water effective permeability. These last set of tests are performed in a steady-state equilibrium, using plugs of a core coming from one the gas wells in the Adriatic Sea. With a very simple explanation, the tests consisted in alternatively flushing water, gas, and again water, through the core itself, before and after the polymer treatment, until all the effective permeability were obtained. The fact of using sample coming from a single gas well is justified by the facts that it is thought to be representative of all the other wells, due the homogeneity of the Adriatic Sea formations, and that is economically unbearable to collect samples and perform tests on every single well

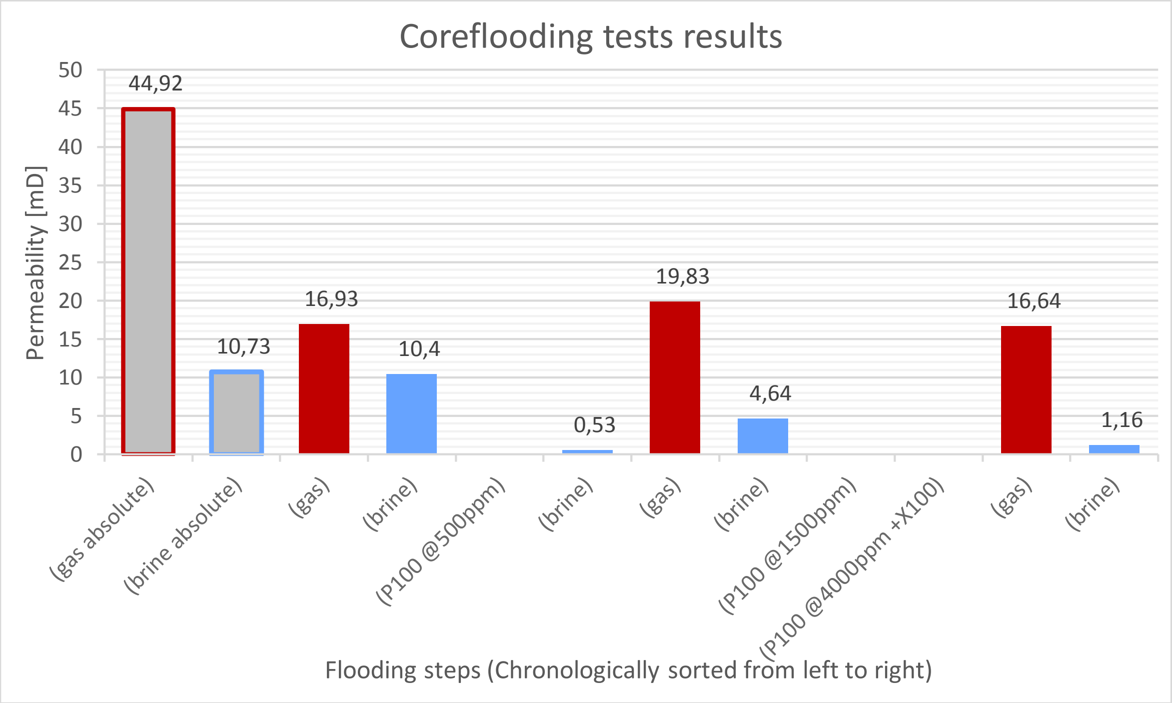

Figure 2: overview of the coreflooding tests results

candidate for a water mitigation treatment. The following plot summarizes the result of the coreflooding tests:
The plot evidently shows that the water effective permeability before and after the treatment is greatly diminished, while the gas effective permeability is almost left untouched.
Still, it must be noted that tests similar to these ones are always carried out by the acting service company, before the water mitigation treatment is implemented, to verify the feasibility of the treatment itself. Nevertheless, as in this case, oil companies always repeat some of these tests, introducing minor modifications, or perform completely different tests, in order to verify the reliability of the first one, and to gain further information that provide solid know-how basis.

The third chapter is used to discuss the four ENI wells that have been treated with the RPM. The structure of the description is the following. First, the characteristic of each one of them, such as the formation and the completion specific, will be largely discussed. Then the data collected during the polymer injection will be presented and argued using a collapsed plot showing the registered well head pressure against time, the injection rate against time, and also their ratio versus time. The last argued information are the production histories of gas and water, both before and after the RPM treatment, used to understand the outcome of the treatment. In the end of this chapter, a broad discussion and comparison between the field data and the results of the laboratory tests, aided by calculations implemented using Darcy's law, allow to depict, as clearly as possible, the outcome of the well treatment, and how it resulted accordingly to the experimental results on the core plug.

Indeed the fourth chapter draws some inferences, deduced from the cross analysis performed in the previous chapter, concerning the selection of the best candidate for a future water mitigation treatment with RPM, and outline the best practice to perform it.

The final chapter highlights the main aspect and conclusion of the thesis. As a matter of fact, in this section of the thesis, are introduced different consideration such as the fact that the increase of polymer concentration, during the field treatment, does not cause any variation in the injectivity pressure response, while during laboratory experiments, it evidently origins a rise of the slope of the injectivity curve. This effect may be related to the heterogeneity of the reservoir formation, in opposition with the homogeneity of the core plug used for tests. Furthermore it is stated that the acid treatment, performed before any polymer injection, does not affect the polymer behavior itself, but it could be of great use to remove any skin factor and obtain a higher production post job.

Anyway, aside from these considerations, and despite the many uncertain variables that regulate the behavior of a gas well, with which the oil industry is accustomed, it has been possible to understand that the key for the success of a disproportionate permeability reduction treatment, lays in a correct selection of both the candidate well, in relation with the lithology of the reservoir, and the relative permeability modifier product, in relation with the permeability of the reservoir.

List of Contents

List of Figures XXIII

List of Tables XXIX

Sommario XXXIII

Abstract XXXV

Introduction 1

Disproportionate permeability reduction overview 5

    1.1 - Introduction on the RPM usage 5

    1.2 - Basic description of RPM polymers and polymers gel 7

        Inorganic gels 9

        Organic Gels 10

        Microgels 13

        Mixed Inorganic and Organic Gels 14

    1.3 - Theories behind the operating principles of RPM 14

    1.4 - Inquiries on possible operating principles for gels 17

        Relation between drawdown, permeability reduction and productivity 19

        Possible role of capillary and elastic forces inside the pore throat 24

    1.5 - RPM behavior changes due to external conditions 26

        Electrostatic and Ions in Solution effect 27

        Temperature effect 28

        Rock wettability effect 29

Rock permeability effect 30

RPM characterization: laboratory tests and results... 31

2.1 - Rheological behavior of RPM...32

Basic rheological behavior of RPM 32

Viscosity: laboratory tests and results 34

2.2 - Interaction between RPM and rocks 40

Flocculation: laboratory tests and results 41

2.3 - RPM injectivity and permeability reduction effect..43

Coreflooding: equipment layout 45

Coreflooding: test overview 47

Coreflooding: tests and results.. 51

Coreflooding: Test overview and inference 77

Analysis of ENI treated wells 81

3.1 - Case 1: Pozzo 1 C 83

3.2 - Case 2: Pozzo 2 C 92

3.3 - Case 3: Pozzo 3 L...99

3.4 - Case 4: Pozzo 4 L...106

RPM usage guidelines... 115

4.1 - Candidate selection 115

Single hydrocarbon producing zone.. 116

Multiple producing intervals when crossflow exist. 117

Multiple producing intervals without crossflow. 118

Other aspects regarding multi-layered reservoir... 119

Water coning 121

4.2 - RPM treatment procedure and evaluation 121

RPM treatment procedure 121

RPM post treatment evaluation 124

Conclusion 127

Appendix A - Reservoir Conformance A–1

Appendix B - Focus on chemical aspects of polymers Gels B–1

Focus on synthetic polymers B–1

Focus on Biopolymers B–2

Other kind of synthetic polymers B–3

Symbols I

Acronym Glossary V

Bibliography VII

LIST OF FIGURES

Figure 0-1: Conceptual picture of water influx in reservoir during gas takeout. Fonte: http://www.geoexpro.com/articles/2013/12/using-gravity-to-enhance-recovery 2

Figure 1-1: well log, Pozzo 1 C. Schlumberger, Well Evaluation Conference. 1987 6

Figure 1-2: diagram showing main Gels Technologies used in disproportionate permeability reduction. Black dashed lines lead to gels that are not used as RPM. Red thick solid lines lead to gels that can be used as RPM. 8

Figure 1-3: partially hydrolysed polyacrylamide crosslinking process by Chromium acetate metallic crosslinker. Images taken from: A.H. Kabir, SPE 72119, Chemical Water and Gas shutoff Technology – An Overview, 2001; Chan K. et Al.: “Pushing Out Oil with Conform 11

Figure 1-4: monomers used in WSO treatments. 12

Figure 1-5: (a) linear polymer chain; (b) high crosslinked density small microgel; (c) high crosslink density big microgel; (d) low crosslink density big microgel; New Microgels for EOR - From Laboratory to Field Applications. D. Rousseau et al. 2007 14

Figure 1-6: schematic representation of the entanglement between flowing and adsorbed polymer. C.A. Grattoni et. Al. Journal of Petroleum Science and Engineering 45 (2004) 233-245. 15

Figure 1-7: on the left: RPM effect on water flow; On the right; oil pathways creation. Image adapted from R.D. Seright, Annual report PRRC 2006, Chapter 3, Mechanism for dispoportionate permeability reduction. 17

Figure 1-8: forces equilibrium applied to dehydration/displacement theory in the throat of a large pore. 18

Figure 1-9: left: permeability curves before RPM treatment. Right: permeability curves after the treatment 21

Figure 1-10: detailed figure of RPM effect on relative permeability curves. 22

Figure 1-11: contact angle in a water wet reservoir. Left: wetting phase is increasing (imbibition). Right: wetting phase is decreasing (drainage). L. P. Dake; Fundamentals of Reservoir Engineering. 24

Figure 1-12: hypothesized Capillary pressure curve variation after a RPM treatment 26

Figure 1-13: calcium Divalent ion bridging equally charged polymer and surface 27

Figure 2-1: viscosity test result for brine. 36

Figure 2-2: viscosity test result for RPM solution at 500ppm concentration of polymer, filtered at 5 µm. 37

Figure 2-3: viscosity test result for RPM solution at 1500ppm concentration of polymer, filtered at 5 µm. 38

Figure 2-4: polymer behaviour; viscosity vs Polymer concentration at different shear rate. 39

Figure 2-5: aspects of sand particles before the contact with the microgel, on the left, and after, on the right. Zaitoun et Pichery, New Polymer Technology for Sand Control Treatments of Gas Storage Wells; SPE 121291; Texas; April 2009; 41

Figure 2-6: flocculation tests results at three different polymer concentration. 42

Figure 2-7: coreflooding oven and Hassler cell at ENI laboratories. 44

Figure 2-8: volumetric pump, pressure transducers and pump controller at ENI laboratory 44

Figure 2-9: disassembled Hassler cell, core sample and rubber sheath 45

Figure 2-10: System schematic of the coreflooding equipment used in ENI laboratories for testing P100. 46

Figure 2-11: the plot illustrates the phase of stabilization of the pressure transducers necessary to find their zeroes. 51

Figure 2-12: transducers pressure response during test 1, gas core flooding. 52
Figure 2-13: transducers pressure response during test 2, brine core flooding. 55
Figure 2-14: transducers pressure response during test 3, gas core flooding. 57
Figure 2-15: transducers pressure response during test 4, brine core flooding. 60
Figure 2-16: pressure response at the inlet pressure transducer during the injection of P100 at a concentration of 500 ppm w/w. 62
Figure 2-17: transducers pressure response during test 6, brine core flooding. 64
Figure 2-18: transducers pressure response during test 6, backflow brine core flooding. 66
Figure 2-19: transducers pressure response during test 7, gas core flooding. 68
Figure 2-20: pressure response at the inlet pressure transducer during the injection of P100 at a concentration of 1500 ppm w/w. 72
Figure 2-21: pressure response at the inlet pressure transducer during the injection of P100, first, at a concentration of 1500 ppm w/w, then, at a concentration of 4000 ppm w/w with an organic crosslinker called X100, in the end, the same as the latter but with reduced flow rate. 73
Figure 2-22 overview of the coreflooding tests results 77
Figure 3-1: Pozzo 1 C seismic log schematic, the orange highlighted areas indicates the perforated interval. Image from ENI archives. 85
Figure 3-2: Injection rate, well head pressure and their ratio during the polymer injection phase of Pozzo 1 C. Data provided by ENI. 86
Figure 3-3: Pozzo 1 C production history. The blue line refers to water, the red line refers to gas, while the black line indicates the top well head pressure. The yellow shaded area indicated the treatment period. The dotted vertical line indicates the backflow of all the injected water from the polymer solution. Data provided by ENI. 88
Figure 3-4: Pozzo 1 C pressure drop across the near wellbore reservoir before and after the treatment. The Shaded area indicates the expected pressure drop range. 91

Figure 3-5: Pozzo 2 C seismic log schematic; orange highlighted areas indicates perforated interval. Image from ENI. 93
Figure 3-6: Injection rate, well head pressure and their ratio during the polymer injection phase of Pozzo 2 C. Data provided by ENI. 95
Figure 3-7: Pozzo 2 C production history. The blue line refers to water, the red line refers to gas, while the black line indicates the top well head pressure. The yellow shaded area indicated the treatment period. The dotted vertical line indicates the backflow of all the injected water from the polymer solution. Data provided by ENI. 96
Figure 3-8: Pozzo 2 C pressure drop across the near wellbore reservoir before and after the treatment. The Shaded area indicates the expected pressure drop range. 98
Figure 3-9: Pozzo 3 L seismic log schematic, the orange highlighted areas indicates the perforated interval. Image from ENI archives. 101
Figure 3-10: Injection rate, well head pressure and their ratio during the polymer injection phase of Pozzo 3 L. Data provided by ENI. 102
Figure 3-11: Pozzo 3 L production history. The blue line refers to water, the red line refers to gas, while the black line indicates the top well head pressure. The yellow shaded area indicated the treatment period. The dotted vertical line indicates the backflow of all the injected water from the polymer solution. Data provided by ENI. 103
Figure 3-12: Pozzo 3 L inflow performance near wellbore before and after the treatment. The Shaded area indicates the expected pressure drop range. 105
Figure 3-13: Pozzo 4 L seismic log schematic, the orange highlighted areas indicates the perforated interval. Image from ENI archives. 107
Figure 3-14: Injection rate, well head pressure and their ratio during the polymer injection phase of Pozzo 4 L. Data provided by ENI. 109

Figure 3-15: Pozzo 4 L production history. The blue line refers to water, the red line refers to gas, while the black line indicates the top well head pressure. The yellow shaded area indicated the treatment period. The dotted vertical line indicates the backflow of all the injected water from the polymer solution. Data provided by ENI. 110
Figure 3-16: Pozzo 4 L inflow performance near wellbore before and after the treatment. The Shaded area indicates the expected pressure drop range. 112
Figure 4-1: Illustration of the conditions of diffuse flow in a single layer of a reservoir, where the water vertical saturation is uniform. 120
Figure A-1: Generalized matrix-rock and high-permeability anomaly conformance problem. Sydansk, Robert D. e Romero-Zeron, Laura. Reservoir Conformance Improvement. A–1
Figure A-2: A Waterflood in a 5-spot well pattern displaying both poor vertical and areal sweep efficiency. Sydansk, Robert D. e Romero-Zeron, Laura. Reservoir Conformance Improvement. A–2
Figure B-1: Illustration of two polymer molecules: Polyacrylamide and Hydrolyzed Polyacrylamide. Images taken from A.H. Kabir, SPE 72119, Chemical Water and Gas shutoff Technology – An Overview, 2001. .... B–2
Figure B-2: RPM system base polymer; the hydrophobic modifications allow the polymer to build up because of the association of the hydrophobic groups. Vasquez J., Eoff L., A Relative Permeability Modifier Water Control: Candidate Selection, Cases Histories, and Lessons Learned after more than 3'000 Well Interventions, 2013, SPE 165091. .... B–4

LIST OF TABLES

Table 2-1: viscosity tests list and description. 35

Table 2-2: characteristic of the core sample from Pozzo 1 C. 45

Table 2-3: zeroes of the pressure transducer during the test 1, gas coreflooding 52

Table 2-4: average registered pressure at the inlet and outlet transducers during test 1, gas flooding 53

Table 2-5: flow rates measured during test 1, gas flooding. 53

Table 2-6: the table illustrates the computed permeability after test 1, gas flooding, as K_1, K_2, and K_3. The last row contains the average absolute permeability to gas of the core sample. 54

Table 2-7: average registered pressure at the inlet and outlet transducers during test 2, brine flooding, with the respective flow rate 56

Table 2-8: the table illustrates the computed permeability after test 2, brine flooding, as K_1 and K_2. The last row contains the average absolute permeability to brine of the core sample. 56

Table 2-9: average registered pressures at the inlet and outlet transducers during test 3, gas drainage. 58

Table 2-10: flow rates measured during test 3, gas flooding 58

Table 2-11: the table illustrate the computed permeability after test 3, gas flooding, as K_1, K_2, and K_3. The last row contains the average absolute permeability to gas of the core sample. 59

Table 2-12: irreducible water saturation of the sandstone core before the polymer injection. 59

Table 2-13: average registered pressure at the inlet and outlet transducers during test 4, brine flooding, with the respective flow rate. 61

Table 2-14: the table illustrate the computed permeability after test 4, brine flooding, as K_1 and K_2. The last row contains the average absolute permeability to brine of the core sample. 61
Table 2-15: average registered pressure at the inlet and outlet transducers during test 6, brine flooding, with the respective flow rate. 64
Table 2-16: the table illustrates the computed permeability after test 6, brine flooding, as K_1, K_2…K_6. The last raw contains the average absolute permeability to gas of the core sample. 65
Table 2-17: average registered pressure at the inlet and outlet transducers during test 6, backflow brine flooding, with the respective flow rate. 67
Table 2-18: the table illustrate the computed permeability after test 6, brine flooding, as K_1, K_2. The last raw contains the average absolute permeability to brine of the core sample. 67
Table 2-19: flow rates measured during test 7, gas flooding 69
Table 2-20: the table illustrate the computed permeability after test 7, gas flooding, as K_1, K_2, and K_3. The last row contains the average absolute permeability to gas of the core sample. 69
Table 2-21: average registered pressure at the inlet and outlet transducers during test 8, brine flooding, with the respective flow rate. 70
Table 2-22: the table illustrates the computed permeability after test 6, brine flooding, as K_1, K_2 and K_3. The last raw contains the average absolute permeability to brine of the core sample. 70
Table 2-23: flow rates measured during test 10, gas flooding 74
Table 2-24: the table illustrates the computed permeability after test 10, gas flooding, as K_1, K_2, and K_3. The last row contains the average absolute permeability to gas of the core sample 75
Table 2-25: irreducible water saturation of the sandstone core before the polymer injection. 75

Table 2-26: average registered pressure at the inlet and outlet transducers during test 11, brine flooding, with the respective flow rate. ... 76

Table 2-27: the table illustrates the computed permeability after test 11, brine flooding, as K_1, K_2 and K_3. The last raw contains the average absolute permeability to brine of the core sample. ... 76

Table 2-28: Gas residual resistance factor evaluated both after the polymer injection, at 500 ppm, and after the gel injection ... 78

Table 2-29: Water residual resistance factor evaluated both after the polymer injection, at 500 ppm, and after the gel injection ... 78

Table 3-1: Pozzo 1 C preliminary properties. ... 84

Table 3-2: Pozzo 1 C production parameters before and after the RPM treatment. ... 89

Table 3-3: Pozzo 1 C computed parameters before and after the polymer treatment. ... 90

Table 3-4: Pozzo 2 C preliminary properties. ... 93

Table 3-5: Pozzo 2 C production parameters before and after the RPM treatment. ... 97

Table 3-6: Pozzo 2 C computed parameters before and after the polymer treatment. ... 97

Table 3-7: Pozzo 3 L preliminary properties. ... 100

Table 3-8: Pozzo 3 L production parameters before and after the RPM treatment. ... 104

Table 3-9: Pozzo 3 L computed parameters before and after the polymer treatment. ... 104

Table 3-10: Pozzo 4 L preliminary properties. ... 107

Table 3-11: Pozzo 4 L production parameters before and after the RPM treatment. ... 111

Table 3-12: Pozzo 4 L computed parameters before and after the polymer treatment. ... 112

SOMMARIO

Nel settore dell’industria petrolifera, il controllo dell’acqua prodotta da giacimenti ad olio o a gas è uno degli aspetti che più impattano sui costi, influenzando pesantemente la redditività attraverso sia una riduzione del volume di idrocarburi prodotti, sia un aumento dei costi associati al trattamento e alla gestione dell’acqua stessa. Vi sono tuttavia molte vie percorribili per risolvere il problema, che si dividono principalmente in due categorie: metodi che sfruttano dispositivi meccanici, e metodi basati sull’uso di polimeri o di gel, che esercitano un’azione più o meno sigillante. Questi ultimi agiscono secondo il meccanismo di riduzione di permeabilità sproporzionata, DPR, altresì conosciuti come RPM, modificatori di permeabilità relativa. Il loro corretto utilizzo può portare ad una significativa riduzione della produzione d’acqua lasciando inalterata la produzione di olio o gas.

L’obiettivo di questa tesi è dunque quello di fornire una panoramica su queste sostanze chimiche, analizzando le principali sfide legate al loro utilizzo e, in seguito, con un'analisi incrociata dei dati ottenuti da test di laboratorio e dati raccolti dai pozzi di gas, capire quali sono le variabili che influiscono sul loro comportamento. Di conseguenza si passa alla stesura di linee guida che forniscano sia un know-how per la selezione di pozzi trattabili, sia delle istruzioni per eseguire il trattamento stesso. Le prove di laboratorio effettuate a tal fine sono eseguite su campioni prelevati dagli stessi giacimenti di gas che forniscono i dati di campo, e consistono in una serie di test di viscosità, di flocculazione e di flussaggio di carota. Con i dati ottenuti in queste prove, messi in relazione con i dati produttivi dei giacimenti di gas, è stato possibile dedurre l’insieme completo di regole prima citato, che possono essere sfruttate al fine di aumentare le possibilità di successo per i futuri trattamenti di mitigazione acqua, lasciando ampio spazio per ulteriori sviluppi futuri.

Parole chiave: riduzione selettiva della permeabilità; modifica della permeabilità relativa; riduzione della produzione d’acqua; polimeri; gel polimerici; linee guida;

ABSTRACT

Controlling water production from oil and gas reservoirs, in oil industry, is an objective of primary importance. Water production could heavily affect the profitability of producing wells due to reduced productivity of hydrocarbons and increased costs associated with water treatment and handling. In long term scale it could lead to premature well abandonment, thus in money loss.

Many methods are available to mitigate water production: chemical approaches or mechanical approaches. Among chemical methods both sealing and non-sealing system have been in use for many years. Usually the non-sealing systems act accordingly to the phenomena of Disproportionate Permeability Reduction, DPR, and consequently they are known as RPM, Relative Permeability Modifiers. Although their usage may lead to a significant decrease in the water to hydrocarbons ratio, it is fundamental to understand where and when they can be successfully used.

This dissertation aims at giving an insight on these chemicals, analysing the main challenges related to their usage, and the solutions deduced by a cross analysis of data collected from laboratory tests and data collected from gas fields. The laboratory tests are performed over samples collected from the same gas fields, and they consist of viscosity, flocculation and coreflooding experiments. While from the gas field production history, interpreted with the results obtained in laboratory, is possible to deduce a complete set of rules, or guidelines, aimed at increasing the chances of success for future water mitigation treatments. This final guide will encloses information necessary to select candidate wells and implement the process of polymer injection, but will leave some space for further development on the topic.

Key words: disproportionate permeability reduction; relative permeability modifier; water mitigation; polymers; weakly crosslinked gels; guidelines;

INTRODUCTION

Most oil or gas reservoir, at some point of their lifetime, start to produce water. Water production could happen early in time, like at the beginning of the production, or delayed, when the field is already mature. Whenever this phenomena occurs, it always comes with some related problems, such as decreased hydrocarbon production, sand production, disposal and handling concerns, and the corrosion-erosion of tubular and surface equipment. As a matter of fact water often comprise more than 50% of the produced fluids: the average water oil production ratio in oil industry, is of about three or more barrels of water for each barrel of oil produced. The quantity of produced water can be related to the quantity of produced oil through a parameter of a paramount importance in oil industry, "Water cut", shortened as "WC". The latter is defined as the ratio of produced water compared to the volume of total liquid production, from a given well.

The reasons which lead to water production are multiple. The most common is related to reservoir depletion. To clarify this concept it necessary to consider a closed container filled with liquid. When this liquid is removed from the container without being replaced by another fluid, the volume of the container itself must change. A reservoir can be approximately related to a container that cannot substantially change its shape, thus when hydrocarbons are produced, another liquid must fill the vacuum created. This is what happen in a reservoir when water, coming from a deeper aquifer, invades the reservoir itself until it reaches the production tubing, starting water production.

Figure 0-1 shows three different stages of water gradually replacing the hydrocarbons in the reservoir exploited with a horizontal well, black solid line. This will ultimately lead to water break through and high quantity of produced water.

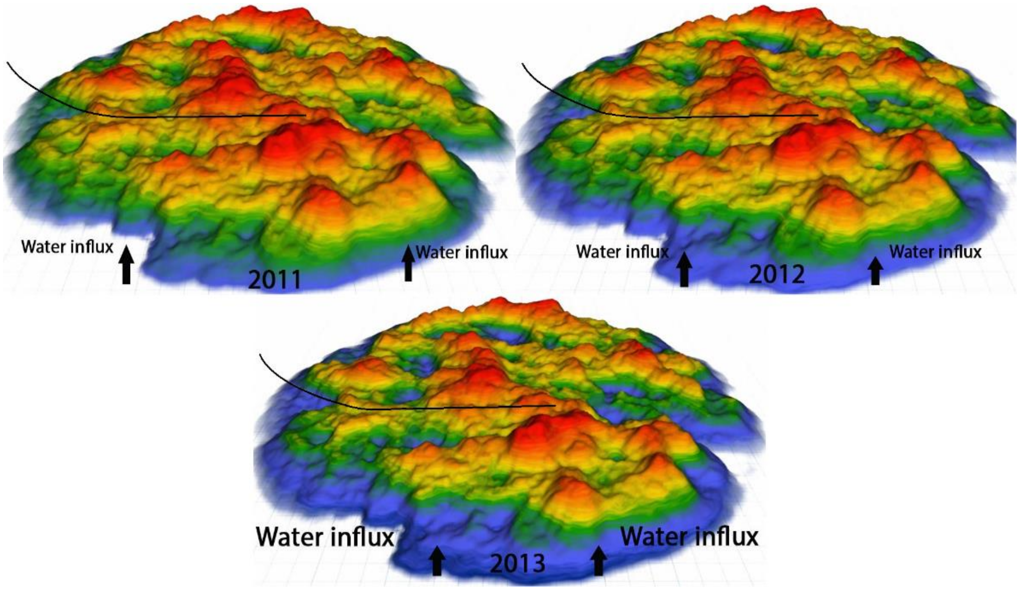

Figure 0-1: Conceptual picture of water influx in reservoir during gas takeout. Fonte: http://www.geoexpro.com/articles/2013/12/using-gravity-to-enhance-recovery

Another reason leading to water production is the process of coning due to bottom water drive, that is the change in oil-water contact or gas-water contact profiles as a result of drawdown pressures drop during production. Coning occurs in vertical or slightly deviated wells and is affected by the characteristics of the fluids involved, and the ratio of horizontal to vertical permeability.

One more reason is water breakthrough from high permeability, watered-out layers. This happens during water displacement, where the water injected to maintain reservoir pressure via injection wells, breaks through one or more of the producing wells.

These are some of the reasons why water is produced from oil wells. A detailed discussion of the mechanism by which water can reach the producing tube is beyond the scope of this thesis, thus will not be further argued.

Obviously, the higher is the water cut of a well, the lower is its economical profitability. As a matter of fact, produced water not only reduces the oil or gas production, but also requires handling and treatment. These last two processes, which often shorten the economic life of a well, are especially expansive on offshore platforms, where environmental concerns are very important. In fact, on these structures, there is little availability of space, thus water treatment plant are very expensive and difficult to install.

These are the causes why oil companies have great interest in trying to reduce water cut as much as possible, especially in mature fields where it reaches very high values. For example, reducing the water cut from 90% to 70% or 60% is already an incredible success. The operation of reducing water production from oil wells is called “Water shutoff”, shortened as “WSO”, or even better, but less common, “Water mitigation”. In this document the term water shutoff, or its acronym, will be used to denote the procedure to reduce water production from a well.

In pursuing WSO, oil companies have found many solutions to this problem. One of them is the DPR, disproportionate permeability reduction, which is a phenomenon whereby polymers or polymer gels injection reduce the permeability to water flow to a greater extent than to oil or gas flow. RPM, relative permeability modification, also refers to selective water permeability reduction. Practitioners argues whether one terms should be used for strong polymers gels that cause a strong permeability reduction, while the other term ought to be used with weaker and more soft polymer gels [1]. For the sake of clarity, in this document, the terms DPR and RPM will be used as synonyms.

Given a brief introduction on the problems related to excessive water production, and one of their possible solutions through disproportionate permeability reduction treatment, it is possible to provide a description of the content of this dissertation, related to this topic. As a matter of fact, the aim of this document is to establish the effectiveness of the relative permeability modification treatments, and which are the parameters the mainly impact on their success. On top of this, some useful guidelines, aimed at increasing the chances of success of any treatment, will be delineated.

These goals are achieved with an analysis of the data obtained with a planned series of experiments performed in the laboratories of ENI, and the data collected from four different gas fields, located in the Adriatic Sea, previously submitted to a RPM treatment.

The first part of the document primarily focus on a description of the chemicals, used for water mitigation purposes, which act as relative permeability modifiers. Moreover, since their operating principles are yet to be fully understood, the main theories regarding the mechanism that should held responsible for causing a disproportionate permeability reduction are outlined, along with some recent developments and personal opinions of the author. The first chapter ends with a description of how the behavior of these product can be affected by physical or chemical interactions within the reservoir, thus to define the correct laboratory tests necessary to establish which precautions should be used during the treatment implementation. These experiments comprehend a series of viscosity, flocculation, and coreflooding tests, and they are introduced, explained and analyzed in the second chapter. Furthermore, these tests are very similar to the one performed by the service company that provides the RPM products, and they are also used to confirm the data provided by them. The tests the second chapter will mainly focus on, are a series of coreflooding tests. Indeed they provide the most important parameters to establish the degree of the permeability reduction effect, caused by these chemicals. These values, along with the other results are used to correctly read and interpret the production data of four different gas fields in the Adriatic Sea. This task is carried out in the third chapter, where a complete investigation over the production history of each gas field is completed, and from the collected data are extrapolated the significant variables used to evaluate the outcome of the RPM treatment. This is achieved by a thorough study on both the production parameters and the production history of each single well, followed by an analytical confrontation between the production data, collected before and after the treatment, with the data obtained in the laboratory tests.

All the remarks obtained from this investigation are put together in the fourth chapter, where a series of guidelines, regarding both the well candidate selection and the treatment procedure, are drawn down, with the aim of increasing the chances of success of future treatment.

In the last chapter, the thesis is concluded and discussed, providing an insight of the main inferences obtained throughout this document and their limitation. Additionally, some suggestions regarding possible future development to perfect and improve this document are argued.

CHAPTER 1

DISPROPORTIONATE PERMEABILITY REDUCTION OVERVIEW

1.1 - INTRODUCTION ON THE RPM USAGE

Relative permeability modifier, intended as either polymers or polymers gels, are not the only chemicals which can be used to mitigate water production from oil, or gas, wells. When oil companies deal with conformance improvement[1] due to excessive water production, they conventionally use strong and total water shut off products. The problem is that due to the completion techniques used in many wells, protecting the hydrocarbon interval is not always practical or cost-effective [2]. For example, when the water producing layer is very thin, as depicted in Figure 1-1, isolating a few centimeters, or a few feet of rock in a several hundred meters depth borehole, is incredibly difficult, plus the operation outcome in not always certain.

---

[1] To obtain further information on the topic, see ‘Appendix A’.

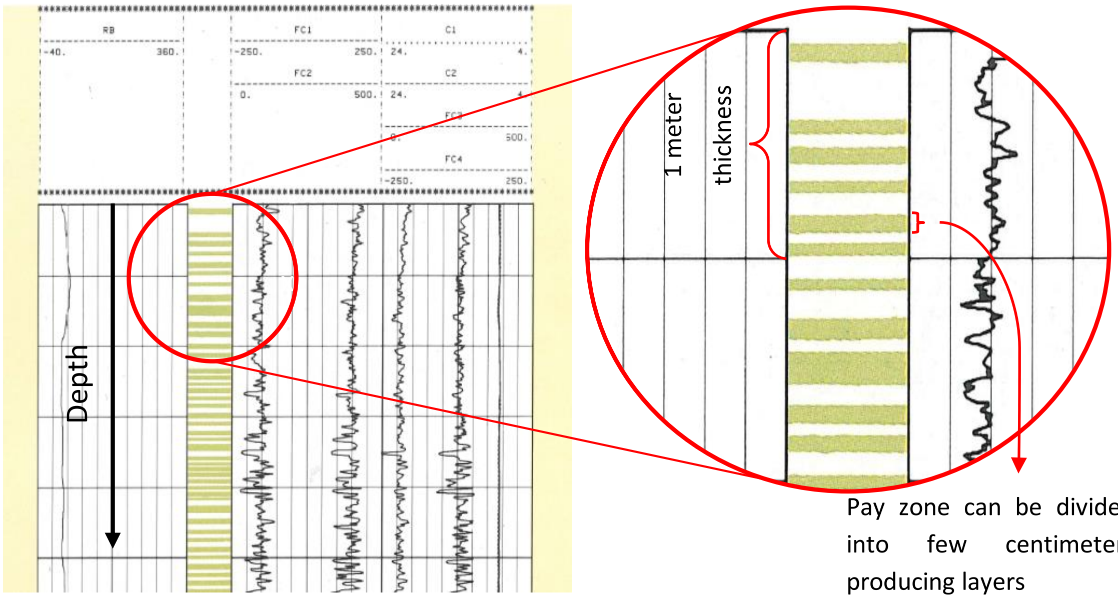

Pay zone can be divided into few centimeters producing layers

Figure 1-1: well log, Pozzo 1 C. Schlumberger, Well Evaluation Conference. 1987

Additionally, the use of mechanical zone isolation during water-shutoff-treatment placement is normally not feasible when the well is completer with a slotted-liner[2] or gravel-pack[3] or when the well involves a sub-sea tieback[4] flow line [1].

These are some of the reasons why oil companies are always more and more interested in developing technologies that do not require mechanical zone isolation. Particularly, this also explain the causes behind a rising interest, in the petroleum industry, regarding bullheadable DPR water-shutoff treatments.

Bullhead treatments imply pumping fluids from the well-head, straight into a formation; this operation is by definition quite easy. Though, bullheading is intrinsically risky. The primary risk in bullheading is the lack of control over the fluid flow direction within the

---

[2] Slotted-liner is a liner with multiple longitudinal slots, for example 2 mm x 50mm, spread across the length and circumference of each joint [30].

[3] A gravel pack consists of a steel screen which is placed in the wellbore while the surrounding annulus is packed with gravels of a specific size, designed to prevent the passage of formation sand. The primary objective is to stabilize the formation while causing minimal impairment to well productivity [33].

[4] A sub-sea tieback is a connection between a new oil and gas discovery and an existing production facility [31].

reservoir, as the fluid being pumped downhole has a tendency to enter the most permeable zones of the formation. In addition, if only shallow casing is cemented in the well, the bullheading operation can cause wellbore fluids to broach around the casing shoe and reach the surface. The liquids rising toward the surface have the effect of fluidizing and weakening either the soil or the subsea floor. Consequently this operation may cause from a simple formation damage, to a reservoir fracturing or, in the worst case scenario, to disastrous equipment impairment.

These risks can be diminished and entirely nullified. Essentially RPM treatments are aimed to the whole completed formation zone, thus what we previously defined as risk is actually an expected result. Furthermore it is possible to prevent any formation fracture by conducting an injectivity test[5] prior any bullhead operation. Hence the main advantages of RPM as a water mitigation treatment are:

- **Low cost**. The treatment does not require mechanical zone isolation and can be pumped in bullheading.
- **Low risk**. Formation fracture can be avoided using injection test before carrying out the treatment.

Furthermore RPM are also very effective. It is been reported that water permeability reduction, after a successful treatment, can be decrease tens of times, leaving the oil permeability almost unaffected. Of course even oil permeability decreases slightly, but far less than the water one.

1.2 - BASIC DESCRIPTION OF RPM POLYMERS AND POLYMERS GEL

Gel technologies may be categorized accordingly to their properties. In this paragraph the reader is presented with an overview, focusing on the chemical aspects, of the types of gel

---

[5] The injectivity test is a procedure conducted to establish the rate and pressure at which fluids can be pumped into the treatment target without fracturing the formation. The test results give the key treatment parameters and operating limits for well operations.

currently available. Anyhow the contents will be limited the principal technologies: the list does not intend to be an exhaustive guide of them all, since this is beyond this document purpose.

Polymer gels were first use back in the 1970s, while inorganic gels dates even further back in time, and they have been object of study since then. Even so, the research started to focus on RPM only at the end of the 20th century, and at the beginning of the 21st century. This is the reason many scientists do not yet agree on a proper classification of them. Anyway, the following, Figure 1-2, shows an easy-to-read diagram sorting the main gels technologies.

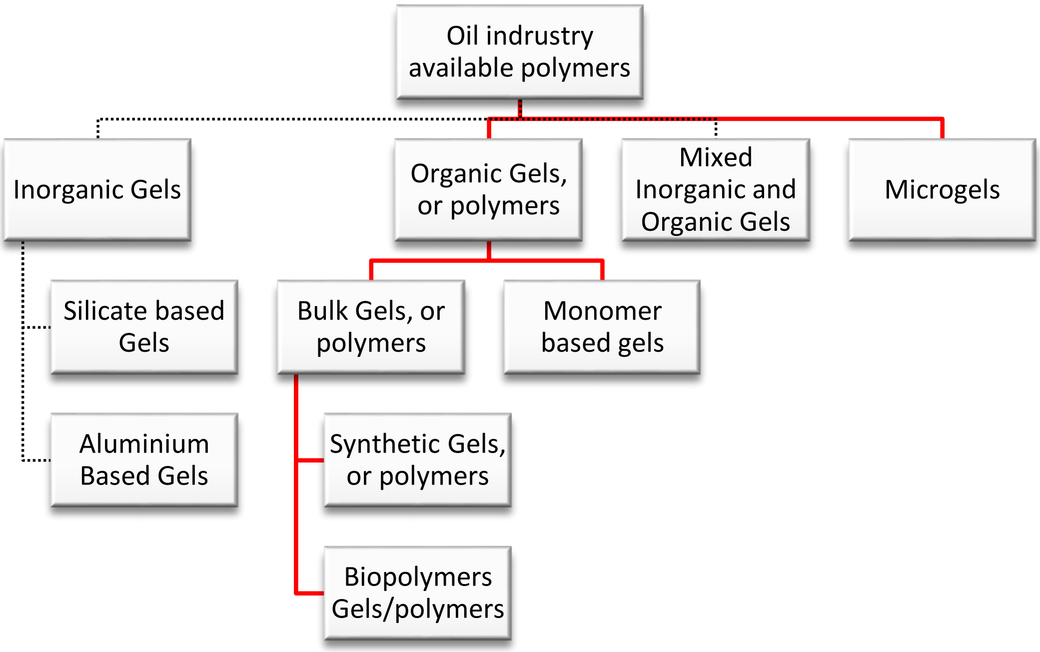

Figure 1-2: diagram showing main Gels/Polymer Technologies used in disproportionate permeability reduction. Black dashed lines lead to gels that are not used as RPM. Red thick solid lines lead to gels that can be used as RPM.

From an overall point of view, gels are fluid based system to which solid-like structural properties have been imparted [3]. These kind of substances are primarily aqueous based, meaning that they are largely made out of water, thus they preserve a certain elasticity despite their apparent solid structure. As a matter of fact the concentration of high molecular weight particles, whether organic or inorganic, is quite low. Generally polymer gels have a polymers concentration in the range of 1’500 to 100’000 ppm, but more commonly from 2’000 to 50’000, and most frequently in the range of 3’000 to 12’000 ppm

[3]. RPMs are also defined as weak gels solution, as their polymers concentration is of a few thousand part per million, or just simple polymer solution, when no crosslinker is used. Of course, not all of the presented chemicals can be used as RPM, but only few of them.

Inorganic gels

Inorganic gels are likely the oldest conformance improvement technology. As a matter of fact they were first introduced in 1920s, when they were used for plugging lost circulation, zone squeezing and consolidating weak formations [4]. As previously described they are aqueous based. Anyway they do not only contain the inorganic gelling matter, but they also contain an activator, which could be a hardening agent or a catalyst. The latter is responsible for triggering the gelation process in response to an external alteration of the environment condition, such as a temperature variation or a salinity rise. There are different reasons why these gels are falling into disuse. The main reason is that there is little control on the gelation time due to possible heterogeneity in the reservoir rocks, such as the presence of cations like Ca^{2+} [5]. The usage of gelation retardant could, in some cases, solves this problem. Nevertheless inorganic gels generally have a fragile structure and their contact to either acid or basic environments may result in an even feebler structure [4]. On the other hand inorganic gels have the capability to penetrate deeply in the rock matrix due to their low viscosity, plus they are resistant to higher temperature compared to organic polymer based gels. There are two main types of inorganic gels:

- Silicate based Gels. The most common ones are sodium silicate gels, also known as liquid glass, or waterglass. Generally, gelation time is positively related to temperature [4], thus an increase in the latter causes the gel to clot in less time. Its advantage is manly related to its high temperature resistance. Additionally it is a low cost product. The great disadvantage of this chemicals is associated to the fact that they immediately gel upon contact with divalent cations such as Ca^{2+}, Mg^{2+}, Fe^{2+} [4]..
- Aluminium based Gels. They have been introduced to overcome the problem related to instant geletion time typical of sodium silicate gel, the problem is that

they are destabilized by divalent anions like sulfates, SO_4^{2-}, and carbonates, CO_3^{2-} [4].

Inorganic gels have either been mentioned or tested for relative permeability reduction purposes. However they are currently only used as sealant, while they do not find application for RPM usages.

Organic Gels and polymers

Organic Gels can occur in two different forms that are bulk gels and monomer gels. The description of organic gel is based on the work of Sidansk, 2011 [3]:

- Bulk polymers, also referred as ‘polymers’, or are made up of repeated monomer units joined together to obtain long chains. Their physical aspect implies high molecular weight and chains whose size is in the micron scale, which is the same order of magnitude of pore throat width. Furthermore the gel form also contains a second chemical called cross-linker whose duty is to create interconnection between different polymers in order to entangle them in a three dimensional structure. The crosslinking process can be triggered by different events, such as the increase of the temperature. Crosslinking polymer molecules is necessary to increase gel viscosity, thus obtaining a total pore obstruction or, in some cases, a disproportionate permeability reduction. A very important aspect of these chemicals is the gelation time: a polymer which greatly increases its viscosity while is being pumped is not useful and it could cause problems during the pumping phases, especially to the pumping equipment. Thus, the control over the gelation time is a critical aspect of these substances.

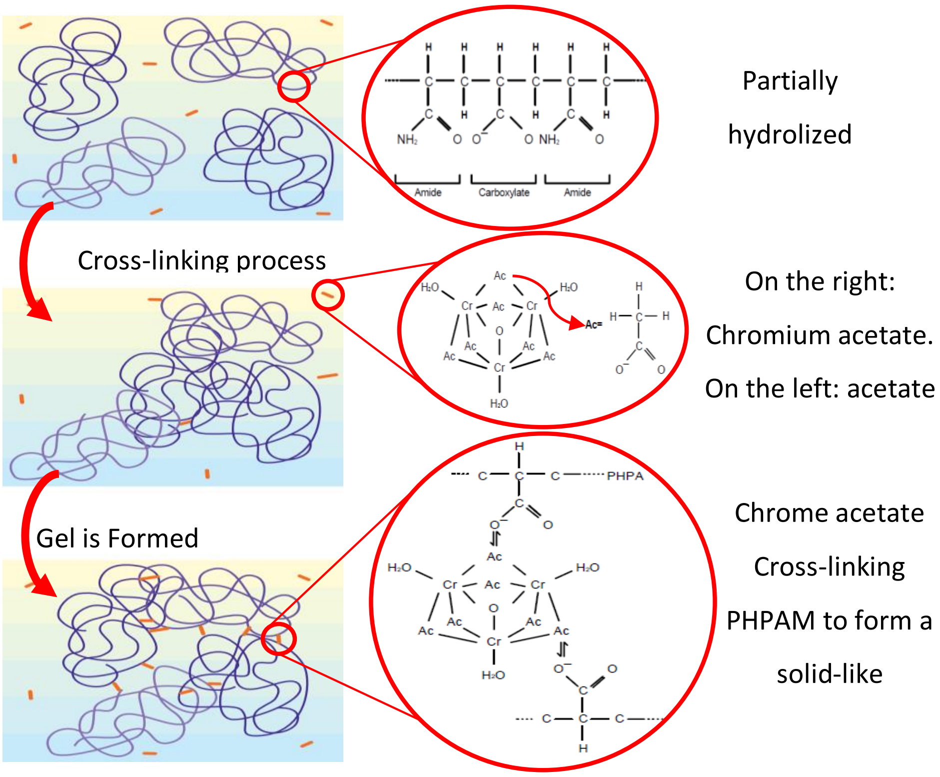

Figure 1-3: partially hydrolysed polyacrylamide crosslinking process by Chromium acetate metallic crosslinker. Images taken from: A.H. Kabir, SPE 72119, Chemical Water and Gas shutoff Technology – An Overview, 2001;

Figure 1-3 illustrates the interaction between a cross-linking agent and a synthetic polymer, partially hydrolysed polyacrylamide, to form a gel.

Additionally polymers, or polymer gels, are distinguished between biopolymers and synthetic polymers. The first ones have different advantages like the insensitivity to water salinity and the elevated hardness; the drawback is that they are quite expansive, plus they are subject to microbial attack. On the other hand, synthetic polymers, are less expansive, they resist microbial attack and they have better injectivity properties, meaning that it is easier to pump them into the formation. In contrast they are less resistant to elevated salinity and mechanical stress.

Further information about chemical aspects of polymers gel are exposed in the appendix B[6].

---

[6] Appendix B: For appendix B, go to the appendix section.

- Monomer gels are based on the in-situ polymerization of organic monomer to form gels inside the reservoir itself. Figure 1-4 shows a few examples of monomers that can be used as RPM:

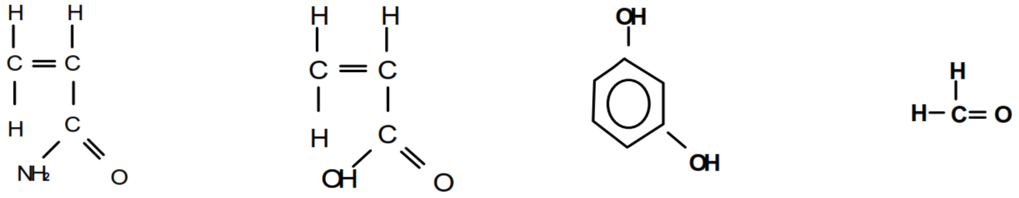

Amide Acrylic Acid Resorcinol Fromaldeid

Figure 1-4: monomers used in WSO treatments.

These chemicals have the drawback of showing little control on their gelation time: gelation is a free-radical initiated process that occurs very rapidly once initiated. Free radicals may be present in the rock formation. Thus, to avoid early gelation of the injected solution, it would be advisable to carefully check the cleanliness of the treatment zone [6]. Early monomer gel treatments were often based on the in-situ polymerization of acrylamide monomer, but this is seldom used presently due to toxicity and environmental concerns. Most recent conformance improvement monomer-gel technology for oilfield applications are based on the in-situ polymerization of relatively less toxic acrylate monomers. The main advantage of monomer injection is the low water-like viscosity of the gelant solution [3].

Organic gels, whether bulk polymers, bulk polymer gels, or monomer gels, can be used for both sealing and RPM processes. Of course, depending on the purpose of the treatment, the concentration of the chemicals within the injection fluid can be different. Anyway some polymers or monomers, are better suited for sealing action rather than RPM treatments, or vice versa. For example, hydrophobically modified polymers, presented in Appendix B, are best suited for reducing water relative permeability, and are now a day used for such purpose. Nevertheless simple polymer solution are also widely used as RPM, especially where low rock permeability would make gels incompatible.

Microgels

Microgels are gels synthetized at low polymer concentrations and at polymer concentrations below the polymer's critical overlap concentration[7] in the gel's makeup brine[8] [3]. As for bulk gels, they also have crosslinking interaction. The difference is that the intermolecular crosslinking happen more often on the same molecule, while in bulk gel the crosslinking interaction are more likely to occur among different molecules. Microgels ought to be an evolution of normal bulk gel in the direction of reducing or eliminating treatment failure associated with the latters. Ideal microgels for water shutoff or profile control should be: insensitive to shear and reservoir physic-chemical conditions, size-controlled, small enough to ensure a deeper treatment and large enough to reduce significantly water permeability, soft enough to be disproportionate relative permeability modifiers, strongly adsorbing onto pore surface for a long-term efficiency, and non-toxic for the environment [7]. Microgels properties depend on their manufacturing conditions and on polymer chain chemistry, and can thus be controlled. According to their crosslinking density and their estimated size, microgels are classified as 'big', for diameters in the order of magnitude of about 2μm, or as 'small', for diameters of about 0.3-0.4μm [8].

Figure 1-5 illustrates different kind of microgels structure according to the former classification.

---

[7] Critical concentration is identified as the concentration at which interaction or overlapping of the domains of polymer molecules in solution first occurs [32].

[8] In well completion, Brine is a water-based solution of inorganic salts, used as a well-control fluid during the completion and workover phases of well operations [33].

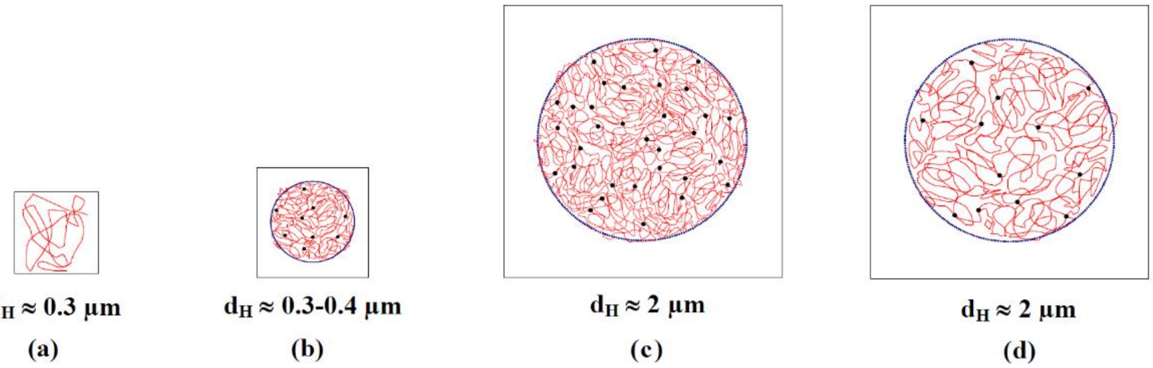

Figure 1-5: (a) linear polymer chain; (b) high crosslinked density small microgel; (c) high crosslink density big microgel; (d) low crosslink density big microgel; New Microgels for EOR - From Laboratory to Field Applications. D. Rousseau et al. 2007

Mixed Inorganic and Organic Gels

It was previously stated that inorganic gels are only used as sealant to completely isolate water-producing reservoir zones. Consequently any mix of organic and inorganic gels is more appropriate for total zones isolation.

1.3 - THEORIES BEHIND THE OPERATING PRINCIPLES OF RPM

Now a day there is no agreement on what mechanism should be held responsible for causing a disproportionate permeability reduction. One of the reasons for lack of consensus regarding the disproportionate permeability reduction mechanism is that it is recognized both for monomers and for crosslinked polymers. Anyway there are various know facts which have been proved in laboratory tests, about the effects that polymer gels have on the formation:

- Polymers, or polymer gels, injection increases the irreducible water saturation of the treated zone, diminishing the end point relative permeability of oil.
- Polymers, or polymer gels, are hydrophilic and, once injected, can alter rock wettability from oil wet to mixed oil and water wet.
- Polymers, or polymer gels, attach to rock surfaces through an irreversible adsorption process.

- The thickness of the adsorbed layer can increase thanks both to mechanical entanglement between polymers tails and to a crosslinking process operated by metallic or organic crosslinkers, or hydrophobic modifications.

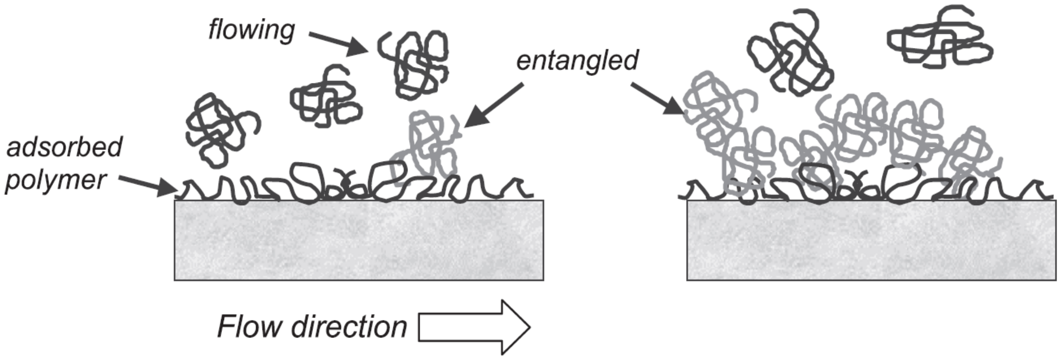

Figure 1-6: schematic representation of the entanglement between flowing and adsorbed polymer. C.A. Grattoni et. Al. Journal of Petroleum Science and Engineering 45 (2004) 233-245.

Figure 1-6, gives a visual representation of the adsorbed polymer and the mechanical entanglement that occurs during the flow of polymer.

On the other hand there are many hypothesis trying to explain their operating principles, and all of them come from experimental observations:

- Balance between the capillary forces and the elasticity of the adsorbed layers affect hydrocarbons and water flow differently [9].
- Polymers or Gels alter rock wettability [10].
- Lubrication effect [11]
- Wall Effect[9] [10].
- Pore blocking by gel droplets [12].
- Combined Wall Effect and Gel Droplet model [13].
- Segregated flow mechanism [14].
- Polymers, or polymer gels, dehydrate when oil is injected [15].

---

[9] Wall Effect occurs when, in a given pore, gels constricts water pathways more than oil pathways.

The truth is that all of these theories may be plausible explanations. As a matter of fact each one of them has been proved reasonable for a specific application. The personal opinion of the author is that they are not self-exclusive, thus they can coexist. Nevertheless in this paragraph are only described the presently most accepted ones, which seem to be inherent with the gel dehydration.

This theory was described by Seright et al. after a X-ray computed microtomography[10] had been used to understand why gels reduce permeability to water more than that to hydrocarbons [16]. A review of the investigated mechanism considered two conditions. First, it is assumed a situation immediately after the RPM placement in a porous media, in which the water base gel occupies all of the aqueous pore space and residual hydrocarbons may be trapped in the pore center in a water-wet rock, as illustrated in the Figure 1-7, on the left. If water or brine is injected, an extremely high resistance to water flow is observed [3]. This significant reduction of permeability to water is explained by the fact that the water must flow through the RPM matrix itself, which has an inherit permeability to water in the microDarcy range [3]. Consequently the fraction of flowing water is greatly reduced where the RPM has invaded the formation. The second condition assumes that the well is returned to production after the RPM placement and gelation, thus the hydrocarbons are the first fluids to contact the gel treated region. In Figure 1-7, on the right, is possible to observe this condition. During hydrocarbons flow, at a fixed pressure gradient, experimental observations indicate that the hydrocarbons open up pathways along the solid-like polymer, or gel, phase. Hence, the permeability to hydrocarbons is restored, and is followed by the reestablishment of the hydrocarbons flow across the region [3].

---

[10] X-ray Microtomography uses x-rays to create cross-sections of a physical object that can be used to recreate a virtual model (3D model) without destroying the original model.

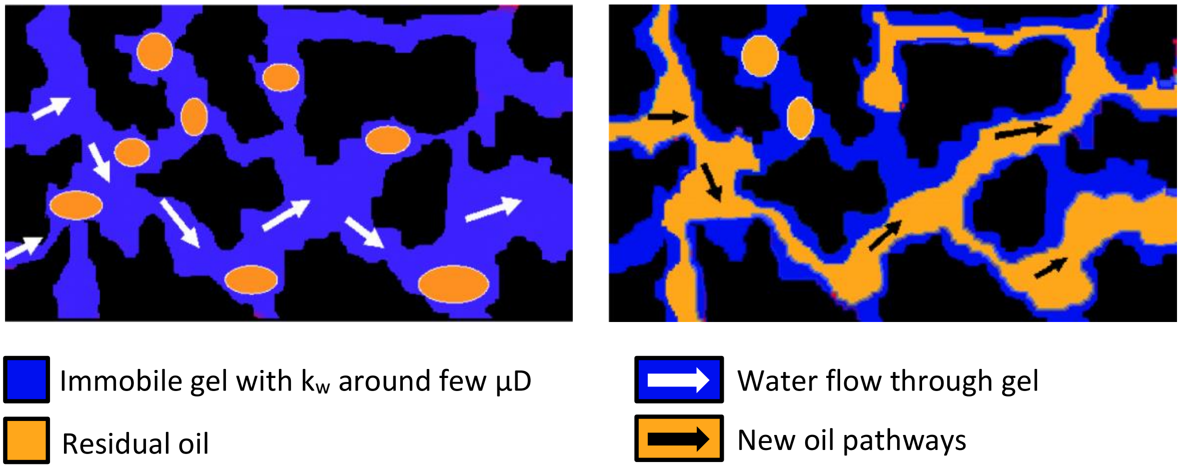

Figure 1-7: on the left: RPM effect on water flow; On the right; oil pathways creation. Image adapted from R.D. Seright, Annual report PRRC 2006, Chapter 3, Mechanism for dispoportionate permeability reduction.

These pathways are created by dehydration[11] [16] or, according to some other studies [17], displacement/destruction of the RPM matrix due to pressure gradient imposed during hydrocarbons flow. Nevertheless tests that support the DPR solution displacement over its dehydration were conducted over a sandstone core with a permeability ranging from 4 to 5 μm^2(meaning 4 to 5 Darcys), vice versa the tests supporting dehydration over displacement considered a sandstone core showing an average permeability of 0,5 μm^2(meaning 0,5 Darcys). This may suggest that different mechanisms apply for different sandstone permeability.

Given this explanation it is clear that there is a main theory explaining the disproportionate permeability reduction, alas an analytical demonstration of the phenomena is not yet available.

1.4 - INQUIRIES ON POSSIBLE OPERATING PRINCIPLES FOR GELS

It is personal opinion of the author that an explanation of the mechanism, presented in the previous paragraph, could be linked to an equilibrium of capillary forces, gel elasticity, and

---

[11] Gel dehydration is defined as the process of removing water from gel by imposing a pressure gradient on the gel itself that cause its concentration, thus its volume reduction.

water and oil, or gas, saturation of the pores. Probably a lubrication effect may also be implied. Figure 1-8, illustrates a sketch with different conditions of a pore throat, after polymer flooding and gelation, that connect two large pores in a water wet reservoir. It shows a possible behavior of the flowing fluids as the rock saturation in water and oil changes.

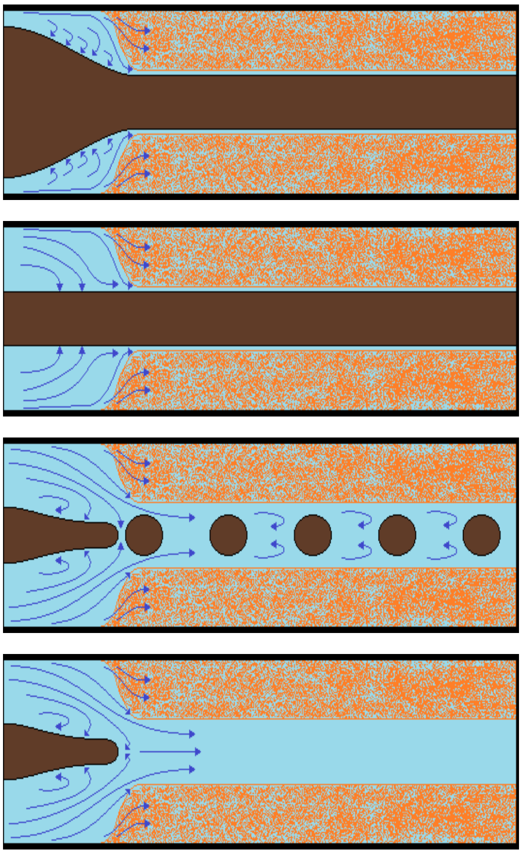

Oil flows through the pore and squeezes water inside the RPM matrix. Higher capillary pressure ensured by RPM elasticity permits this effect.

Capillary pressure is still high enough even though oil, or gas, saturation is reduced. Oil, or gas, still flows with stable equilibrium.

A further drop in capillary pressure cause a non-equilibrium situation in which hydrocarbons can, unstably, manage to flow.

Capillary pressure drops again and oil, or gas, flow stops. Water is no longer squeezed into the RPM matrix. Without the RPM, hydrocarbons could still flow.

Figure 1-8: forces equilibrium applied to dehydration/displacement theory in the throat of a large pore.

From basic knowledge of reservoir it is known that the three main forces acting in a reservoir are: gravity forces, capillary forces and forces caused by macroscopic pressure differences. The first consideration to make is that gravity is very unlikely to affect the flow on a pore scale level. Thus, the reason why hydrocarbons manages to break through the gel matrix, create stable pathways, and maintain a certain flow rate despite its reduced permeability, should be related to drawdown forces and capillary forces.

Relation between drawdown, permeability reduction and productivity

As stated at the beginning of this paragraph, one of the effects of polymer/gel injection, is to rise the irreducible water saturation level, diminishing the end point relative permeability to hydrocarbons. This could also cause a drop in hydrocarbons relative permeability, and consequently a productivity reduction. Then again is possible to demonstrate that drawdown pressure increases, and this effect compensates the latter. First it is necessary to consider the rock pore as a two-phase, one dimensional system in which water wet the surface of the rock. Additionally, to simplify the analysis, the hypothesis of linear, mono-dimensional and diffuse flow[12], and horizontal reservoir will be considered valid. One last condition requires that the Darcy's equation can be applied:

$$v_o = k\frac{k_{r,o}(S_w)}{\mu_o}\frac{\partial P_o}{\partial x} \tag{1.1}$$

$$v_w = k\frac{k_{r,w}(S_w)}{\mu_w}\frac{\partial P_w}{\partial x} \tag{1.2}$$

Where: 'o' stands for oil; 'w' stands for water; v_i is the superficial velocity of the considered fluid; k is the absolute permeability of the porous media; $k_{r,i}$ is the relative permeability of the considered fluid; S_i is rock saturation in the considered fluid; and P_i is the pressure of the considered fluid. It is now possible to introduce the fraction of flowing water, f_w, defined as:

$$f_w = \frac{q_w}{q_t} = \frac{v_w}{v_w + v_o} \tag{1.3}$$

---

[12] Diffuse flow means that the fluids do not separate accordingly to densities. This kind of flow undertakes that dynamic forces prevail over gravity forces, thus the latters are negligible.

In equation (1.3) it is also possible to simplify the volumetric flow rate, q_w and q_t, assuming the pore section area is maintained constant. Replacing Darcy's equations for oil and water in the latter one gives:

$$f_w = \frac{\frac{k_{r,w}(S_w)}{\mu_w}}{\frac{k_{r,w}(S_w)}{\mu_w} + \frac{k_{r,o}(S_w)}{\mu_o}} \tag{1.4}$$

It is now introduced the term, *WOR*, which is the ratio of the flowing water and the flowing oil:

$$WOR = \frac{q_w}{q_0} = \frac{f_w}{1 - f_w} = \frac{\frac{k_{r,w}(S_w)}{\mu_w}}{\frac{k_{r,o}(S_w)}{\mu_o}} \tag{1.5}$$

Equation (1.5) shows that even the producing water oil ratio is a mere function of the water rock saturation, if the considered hypothesis are valid. Introducing the mass conservation equation for a thin mono-dimensional horizontal slice of reservoir:

$$dV\,\phi \frac{\partial S_w}{\partial t} = -\frac{\partial q_w}{\partial x} dx = -\frac{\partial v_w}{\partial x} dA\, dx \tag{1.6}$$

Where ϕ is the rock porosity. Replacing the water superficial velocity with the fractional flowing water, and simplifying the volume terms gives:

$$\phi \frac{\partial S_w}{\partial t} = -\frac{\partial (f_w v_t)}{\partial x} \tag{1.7}$$

But the total superficial velocity, v_t, must be constant since the fluid is considered to be incompressible. Then it is possible to write:

$$\phi \frac{\partial S_w}{\partial t} = -v_t \frac{\partial (f_w)}{\partial x} \tag{1.8}$$

A new necessary hypothesis implies a steady state flow, thus the derivative of water saturation with respect to time is null. This gives that the fraction of flowing water, consequently the producing water to oil ratio, must be constant along the *x-axis*. Now it is necessary to consider that before a treatment with RPM, the fraction of flowing water is different than after the treatment and, since it is only a function of the water saturation, the reservoir saturation in water must shift accordingly to the new value of WOR. Furthermore, it is also known that the treatment leaves the oil relative permeability intact. The only way this could happen is that the water relative permeability curve is shifted and/or tilted downward. Figure 1-9, below, illustrates the expected relative permeability curve modification of a generic reservoir:

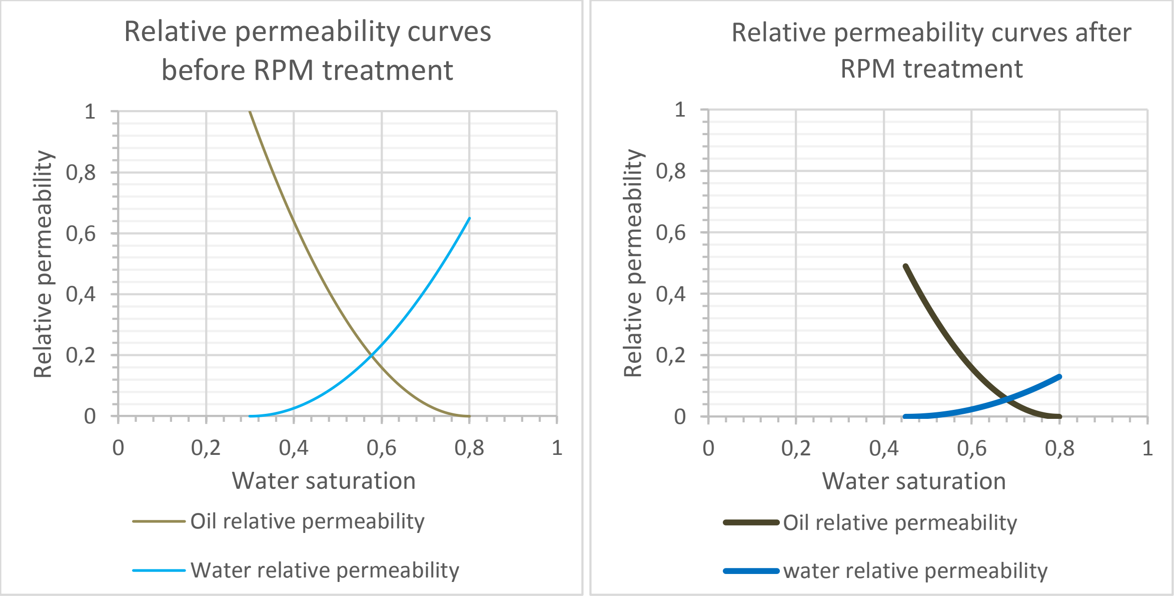

Figure 1-9. left: permeability curves before RPM treatment. Right: permeability curves after the treatment

Overlapping the two plots, as in Figure 1-10, makes it easier to give an interpretation of the occurring phenomena:

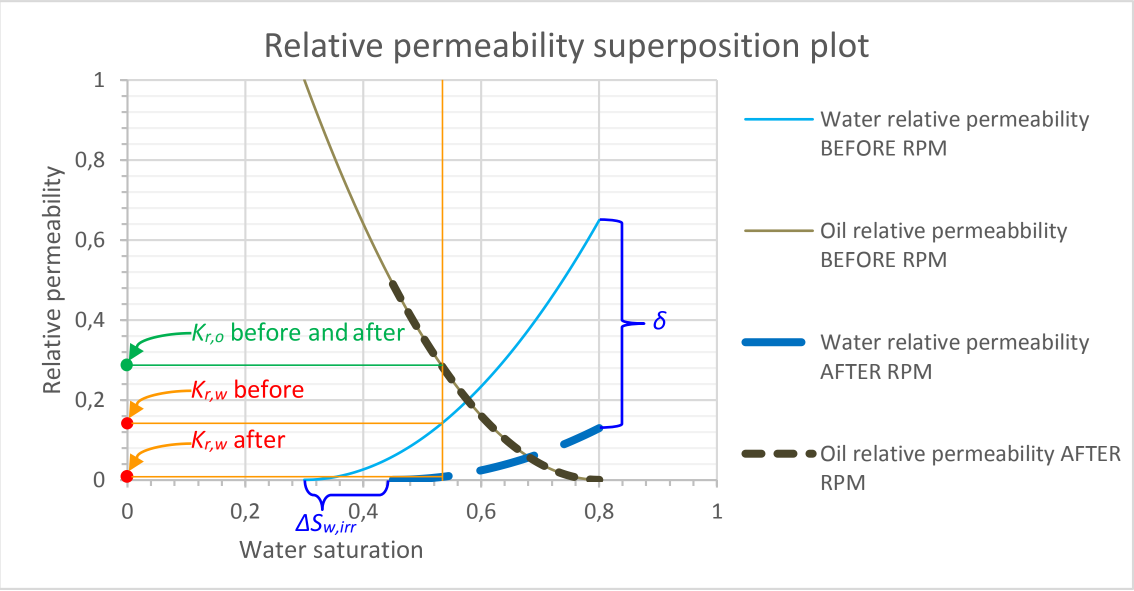

Figure 1-10: detailed figure of RPM effect on relative permeability curves.

Always Figure 1-10 shows that the permeability reduction to water causes an increase in the value of the irriducible water saturation, $\Delta S_{w,irr}$, which must be considered together with an overall scalation of the water permeability curve by a factor δ. Figure 1-10 also displays that the oil relative permeability is unchanged, but this is true as long the sum of $\Delta S_{w,irr}$ and $S_{w,irr}$ is lower than the actual water saturation before the treatment. Otherwise the oil permeability will be reduced to the new and lower level, corresponding to the post treatment oil end point relative permeability. If this is the case the well would require a higher pressure gradient to maintain constant production. The limit case, complete shutoff, is achived when $\Delta S_{w,irr}$ is very large and δ is close to the unit, thus the oil saturation of the reservoir tend to the residual oil saturation. Consequently the treatment must aim at reducing water relative permeability without affecting oil relative permeability, which is the considered case. Given these consideration the new producing water to oil ratio would be:

$$WOR = \frac{\frac{\delta\, k_{r,w}\left(S_w - \Delta S_{w,irr}\right)}{\mu_w}}{\frac{k_{r,o}(S_w)}{\mu_o}} \qquad (1.9)$$

Again it has already been stated the fluids are considered incompressible thus, accordingly to Darcy's equations, the reduction in water relative permeability causes a lower water superficial velocity, hence less water production. On the other hand, if the total velocity must be constant the oil superficial velocity ought to be increased. Still, this is only possible, since all the other parameters are constant, when oil pressure gradient in the reservoir grows. This reasoning also applies in the case of gas producing wells. This fact is of capital importance since it explains the cause of higher drawdown after RPM treatment. Regrettably the previous reasoning seems a little simplistic for several reasons:

- Fluids flow inside the reservoir is hardly ever in a steady state. In the simple situation outlined, for instance, buildup of water saturation in the treated zone must be a transient process; however, if the treated zone is small in volume compared to the bulk of the reservoir, this transient period is short compared to the time scale of production [18].
- The assumption of constant saturation away from the treated zone may sometimes be quite unrealistic. With a varying saturation, $S_w(x)$, steady state will generally not prevail. However, the point remains that the reservoir at large determines the *WOR* delivered to the treated zone, because water and oil everywhere are at the same pressure gradient. After (the rapid) buildup of water saturation in the treated zone, that *WOR* must also be delivered to the well [18].

Furthermore is necessary to notice that, in long term production, the build up of water saturation would cause a rising value of *WOR.* A high water saturation in an untreated region corresponds to large *WOR* flow out of that region and into the treated zone [18]. The above given explanation may not seems totally convincing. Simulations that prove what previously stated are not the aim of this document and won't be further discussed, anyway additional information can be found in the SPE-50983 journal article, see ref. [18].

Possible role of capillary and elastic forces inside the pore throat

Still, is not clear how gel can effectively reduce water relative permeability more than oil relative permeability. A possible explanation might be related to a balance between capillary forces and gel elasticity. Capillary pressure is one of the main forces that operates within the reservoir. It is defined as the difference in pressure between the interfaces of two immiscible fluids; in this case the two fluids are oil and water:

$$P_{cow} = P_o - P_w \qquad (1.10)$$

Where P_{cow} is the capillary pressure. This pressure difference is strictly related to Young-Laplace equation, and defines how oil and water are placed within the rock pore. In point of fact the Laplace equation, when the rock porosity can be simplistically represented by a capillary tube boundle can be written as follow:

$$P_{cow} = 2\frac{\sigma\, cos(\vartheta_c)}{r} \qquad (1.11)$$

Where: σ is the interfacial tension between oil and water; ϑ_c is the contact angle between a water drop and the rock surface; and *'r'* is the average pore radius. Figure 1-11, gives a better explanation of the terms in the equation of Laplace.

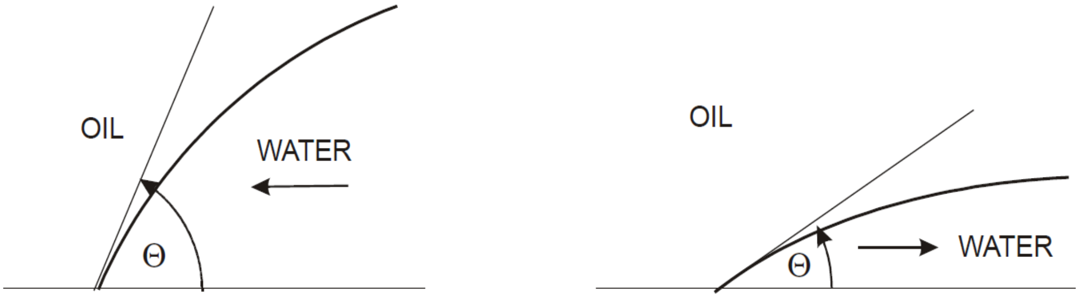

Figure 1-11: contact angle in a water wet reservoir. Left: wetting phase is increasing (imbibition). Right: wetting phase is decreasing (drainage). L. P. Dake; Fundamentals of Reservoir Engineering.

After an RPM treatment the polymers adhere on the rock surface. Through X-ray computed microtomography it is known that the polymers creates a layer that merges with the water wetting layer. This new RPM layer, is thicker than the original water one since, as emerged from the previous demonstration, the irreducible water saturation has increased. Additionally, from the oil point of view, it acts reducing the pore diameter, thus increases the oil water capillary pressure. Furthermore the adsorption process creates a soft, solid-like configuration within the RPM matrix. This new structure tends to occupy as much space as it can inside the pore, and shows, as many polymers, prominent elastic properties. It is plausible that the force, thus pressure, yielded by the polymer, aided by its hydrophilic properties and supported by oil superficial tension, is sufficient to push the water within its matrix. Consequently the water is forced to flow within the gel matrix itself rather than in the space between the oil surface and the gel surface. The problem may rise when the capillary pressure drops under a certain level and the water starts to flow outside the gel, preventing the oil flow. If this is the case RPM treatment would only be advisable where oil saturation is still elevated and mobility ratio is favorable. Similar consideration has been reached by Liang J.T. and Seright R.S. [19], and can also be applied when considering gas reservoir.

Figure 1-8, previously presented, shows the above described effect through a series of reservoir oil depletion stages.

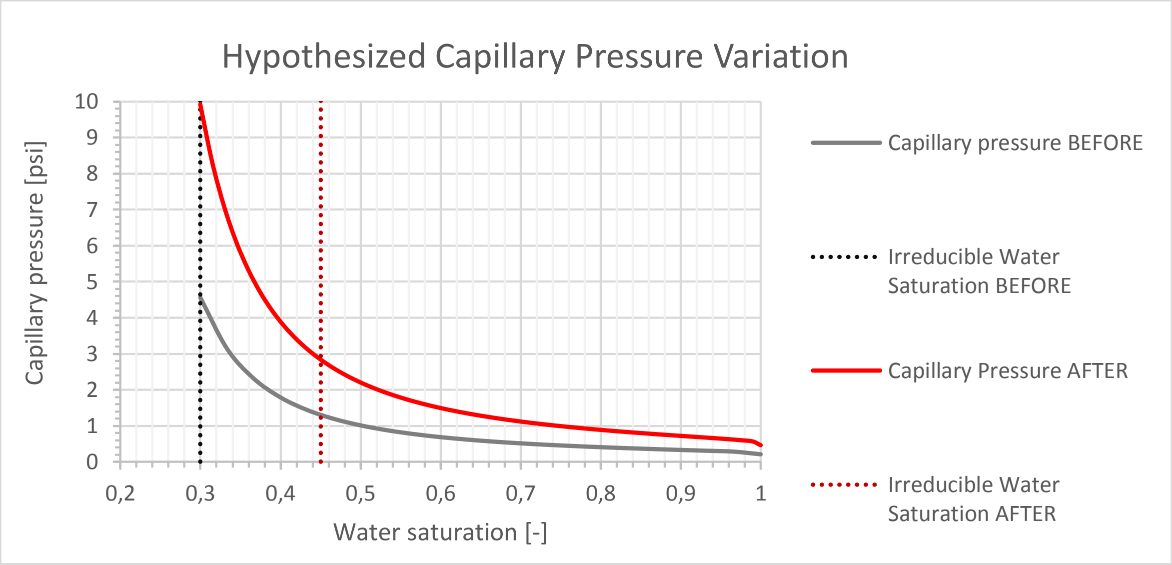

Figure 1-12: hypothesized Capillary pressure curve variation after a RPM treatment

Figure 1-12, illustrates a possible effect of RPM treatment on capillary pressure curves during imbibition process in a water wet system. It is clear that at a given water saturation of the reservoir, before and after the treatment, the capillary pressure is rised by the disproportionate permeability reduction gel.

The plot in Figure 1-12 is obtained by using Hawkins, Luffel and Harris capillary pressure correlation which appears to be reasonably accurate. This correlation is based on water saturation, porosity and permeability. Although the permeability was kept constant for the sake of simplicity, the result are similar to the experimental one obtained by Barrufet M. A. and Ali L. (1994, Texas University).

1.5 - RPM BEHAVIOR CHANGES DUE TO EXTERNAL CONDITIONS

RPM behavior is affected by many different aspects of the reservoir, such as the temperature, but also the salinity, the rock wettability, the electric behavior of the substrate, the porosity, etc. For example a successful treatment of a given reservoir with low salinity, does not imply that a treatment of an identical reservoir, with the same RPM, but characterized by a different salinity leads to identical results. Of course each polymer gels reacts differently depending on its surrounding environment, thus an exhaustive analysis would consider each chemical, one by one. Though the aim of this paragraph is to present the reader with some knowledge about how different conditions can in general modify RPM performance, without being too specific.

Electrostatic and Ions in Solution effect

Electrostatic interactions between polymers and solution ions can largely affect the behavior of disproportionate permeability reduction substances. For example the content of carbonates has a direct effect on the reservoir brine pH, thereby the gelation time [20]. On the other hand divalent ions, released by carbonates in solutions, can increase polymers adsorption due to bridging of negatively charged polymer molecules to negatively charged grain surface. This effect can be appreciated in Figure 1-13.

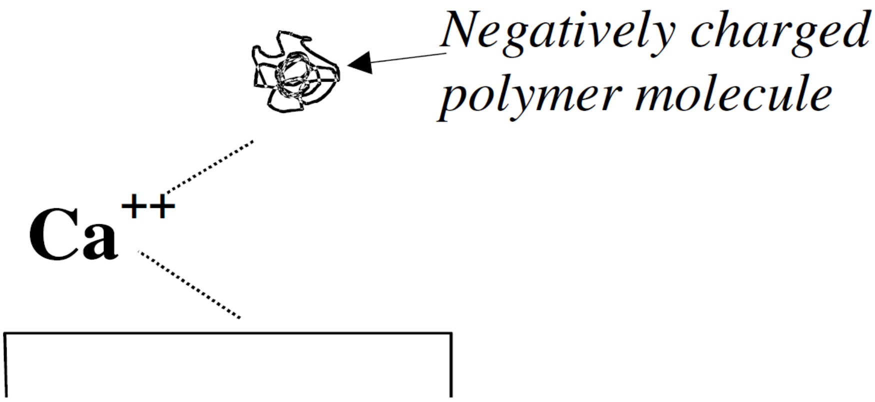

Figure 1-13: calcium Divalent ion bridging equally charged polymer and surface

The salinity of a reservoir must be thoroughly considered when dealing with synthetic polymers since it plays a dominant role in the adsorption, while it is not very important when considering biopolymers. The different behaviors induced by salinity are due to the arrangement of polymer molecules on the surfaces and their interaction. When there is no, or little, salt present the polymer molecules have a larger hydrodynamic size, which induces a low surface coverage. Thus the overall effect of salt is to increase the surface coverage, with a larger dense domain made of loops-trains close to the surface and a dilute layer consisting of more stable tails extending in the solution [21]. Furthermore polyacrylamide can be modified, to obtain cationic PAM, by attaching some positively charged chemicals groups to some of the polymer’s pendant amide groups. This modification provides cationic PAM with a strong tendency to adsorb onto rock reservoir surfaces, especially sand and sandstone which are negatively charges. Other kind of minerals which are characterized by high surface area that is negatively charged, such as clay, will be predominant during the process of adsorption. Thus, in a field treatment the adsorbed polymer will be prevalently concentrated on the clay minerals, which may result in a non-uniform coverage [22]. Secondary effect induced by carbonates and the presence of oxygen must also be considered. For example if carbonate, such as iron (II) carbonate, $FeCO_3$, is present the reservoir in a sufficiently high concentration, it generates divalent iron ions. The oxidation of these ions to trivalent iron generates free radicals which can cause severe polymer degradation [20].

Given these facts, it is possible to make some inferences about ions effect on RPM chemicals:

- Negatively charged polymers are best suited to be adsorbed on positively charged porous media, vice versa positively charged polymers are better adsorbed on negatively charged surfaces.
- The presence of divalent ions can increase the concentration of adsorbed polymer through bridging. Alas, in some cases, it can also cause polymer degradation.
- Saltiness of a reservoir connate water can influence the surface coverage during polymer flooding. Never the less this is a parameter that requires punctual analysis since the combined effect of salinity together with other substances must be checked in laboratory tests.

These are just some of the effects of ions on the RPM chemicals, but they outline the fact that before any field application, scrupulous laboratory test should be performed.

Temperature effect

Temperature is another parameter of great importance since it directly affects gel stability. For instance acrylamide polymers undergo a process of hydrolysis when exposed to high temperature. A certain degree of hydrolysis is accepted, as in HPAM, but when it becomes too great it causes a shift in gel behavior: crosslinking level raises too much and RPM effect is replaced by a total shutoff effect and, subsequently, syneresis[13]. Nevertheless polymer temperature resistance can be improved modifying their chemical structure: copolymers containing 2-acrylamido-methyl-propanesulfonic acid monomers, AMPS, and acrylamide monomers can resist to higher temperature. What is important is to acknowledge the operating downhole temperature and carry out long term laboratory stability test. For example the considered solution of polymers could be matured, under anaerobic conditions, in an oven at the temperature of the reservoir for a month. Biopolymers used to be substantially much more resistant to elevated temperature, but the evolution of synthetic polymers during the last years has levelled this difference.

Rock wettability effect

Wettability of the reservoir rock is another factor that requires considerations before application of a disproportionate permeability reduction treatment [1]. Experiments clearly show that polymer adsorption always occurs, whatever the wettability conditions are [23]. Another important result is that adsorption kinetic is also affected by rock wettability: total polymer adsorption on rock surfaces require a larger volume of polymer injection when shifting the wettability from total water-wet, through mixed oil-water-wet, to oil-wet [23]. Furthermore, during core flood experiments, polymer injection in mixed oil-water wet cores or in total oil-wet cores, leads to additional oil recovery [23]. Such a behavior has never been observed in strongly water-wet cores. These observation suggest that the polymer adsorption causes a wettability inversion, from oil-wet to water-wet. During this process the previous wetting oil becomes part of the non-wetting phase and, as a result, can be produced. Furthermore it has been observed that after RPM had been injected in an oil or in a mixed oil-water wet cores, water relative permeability reduction decreased slightly but oil relative permeability was kept constant. If this is the case, relative

---

[13] Syneresis is a collapse in gel structure, generally characterized by a loss of adhesion, reduction of volume and water expulsion.

permeability modification effect seems less pronounced when rock wettability to water decreases [23]. It is then possible to infer that:

- RPM polymers can be used regardless the fact that the reservoir is water-wet, mixed oil-water wet, or oil wet.
- RPM effect in strongly water-wet systems is greater than in any other system.
- Polymers adsorption on oil-wet systems or mixed oil-water-wet systems may cause a wettability inversion, increasing the water-wetting phase.
- Oil-wet or partially oil-wet systems requires larger volume of polymer solution.

However it is unlikely that a water soluble polymer will adsorb at an oil-wet surface. It may be that the claimed oil-wettability is more of a mixed or fractional wettability where there still are some water-wet pathways [14].

Rock permeability effect

RPM can only penetrate in porous media with pore diameter matching their size. Depending on the precise lithology, RPM with big diameter, such as big microgel, will not propagate in formations of permeability lower than a few Darcy (few μm^2), whereas RPM with small diameter, as for small microgel, the same permeability threshold is of a few milliDarcy (few $10^{-3}\ \mu m^2$) [8]. Furthermore it has been observer that the disproportionate permeability reduction effect is greater where the permeability is lower. This could be explained by the fact that, with growing pore throat size, the polymer plugging effect will decrease since the polymer effective diameter is finite. The more the pores throat diameter grows, the more the ration between the latter and the effective thickness of the polymer deposited layer will be small. Thus the water will be able to create larger flowing pathways between the gel layer and the oil flow pathway.

Therefore, before an RPM operation, it is necessary to evaluate the treatment zone permeability, and choose the correct polymer dimension for such permeability.

CHAPTER 2

RPM CHARACTERIZATION: LABORATORY TESTS AND RESULTS

Addressing the behaviour of the RPM polymers or gels within the reservoir is extremely important if a water mitigation treatment seeks to be successful. Before each RPM treatment, it is necessary to characterize the polymer, or gel, which are about to be used. But the mere knowledge of a product, along with its rheological aspects, is just not sufficient to predict its behaviour within a real reservoir. Therefore punctual laboratory tests are due to assess these and other information, and increase the possibilities of a successful treatment.

The good interaction between the formation rocks and the product is the first information to gain. The flocculation test provides such knowledge and, once is confirmed that polymer has a certain affinity with the formation, it is necessary to establish the long-term stability of the polymer at reservoir conditions. This operation is carried out with an aging test. In the end it is crucial to understand whether the polymer gel can be easily injected, thus propagate, through the pores, and how much polymer is required to treat a certain volume of near-wellbore formation. Lastly, after all these tests, it is possible to gauge the mobility and permeability reduction. All of these information can be evaluated with a specific sequence of coreflooding tests.

Still the prerequisite of any of these tests, imply the knowledge of the reservoir characteristics: ranging from the temperature to the formation water composition.

All these tests are always carried out by the acting service company, before the water mitigation treatment is implemented, to verify the feasibility of the treatment itself. Nevertheless, oil companies always repeat some of these tests in order to verify their reliability, and to gain further information that provide solid know-how basis. Within this document, and particularly in this chapter, are therefore illustrate the most important tests, viscosity tests and coreflooding tests, that outline the key information for a successful RPM well treatment.

Consequently, the following chapter illustrates and explains, one by one, the tests required to characterize any relative permeability modifier and acknowledge its behavior. Then, when it is necessary, it presents and explains the results of the tests performed in the ENI Laboratory. These tests were performed with sands and on a core sample coming from Pozzo 1 C, which is representative of all the other wells of the Adriatic Sea, and they are fundamental for an exhaustive comprehension of the cases history studied in the following chapter. Indeed, the information gathered in this chapter lay the foundation for a correct interpretation of the RPM treatment, on the four wells of the Adriatic Sea, which are discussed in Chapter 3.

2.1 - RHEOLOGICAL BEHAVIOR OF RPM

The first step toward the definition of any relative permeability modifier properties is a study focused on the rheological behavior, meaning that it is necessary to evaluate different aspects of these substances such as the mechanical resistance to shear stress, the thermal stability, and the chemical interaction of the RPM solution with the surrounding environment.

Basic rheological behavior of RPM

The first set of tests that any RPM product are submitted to, should be focused on a broad viscosity inquiry. These viscosity tests can be performed, regardless the RPM product being used, with a low and a high, shear rate viscometer. The goal is to have an idea of the order of magnitude of the product viscosity at reservoir temperature. It is also very important to define the reservoir brine viscosity at reservoir temperature, which will be very useful during the coreflooding experiment.

The following lists introduce other important tests carried out with a viscometer:

- Mechanical stability.

  Mechanical stability can be inquired by subjecting the RPM solution to a viscosity test with a high shear rate viscometer for a long period of time. If the product is mechanically stable, at a fixed shear rate, it shear rate should be constant. On the other hand, a product that is not stable, would show a decreasing viscosity over time.
- Thermal stability.

  There are two different types of thermal stability tests, but they have in common the procedure of aging the RPM product inside an oven at reservoir temperature, under vacuum condition, for a period ranging from one to three months. The first test consist in a simple quantitative observation of the aged test tube to verify that the polymer or gel particles do not degrade, settling on the bottom of the test tube itself. The second test imply, once more, a viscosity measurement of the product after it has been properly aged. It would also be advisable to verify once more the mechanical stability after the aging test. Of course, if the viscosity registered after the test is somewhat lower than the previous one, it means that the polymer underwent some sort of degradation.
- Chemical stability.

  Chemical stability is again a measurement of the RPM viscosity in a harsh environment: viscosity test are performed on a solution of the relative permeability modifier that also contains the aggressive substances present in the reservoir, for example hydrogen sulfide. Viscosity measurements after the test should relate to the previous ones, otherwise the RPM has been, somehow, compromised.

Viscosity: laboratory tests and results

Viscosity tests performed in ENI Laboratories consist of a basic viscosity analysis of the brine and of the RPM solution, used in four different gas wells in the Adriatic Sea, which will also be useful for some consideration in the following paragraph. Other viscosity tests has not been performed since the reservoir conditions of these wells are quite mild. As a matter of fact the least temperature resistant RPM that was used, is a monomer polyacrylamide based RPM, whose name cannot be divulged to respect a disclosure agreement, thus will be referred as P100, who is stable up to 60-70°C while the reservoir temperature is around 45°C. These four wells are chemically inert since they do not contain any acid, like hydrogen sulfide. They also have a quite low production rate over a long completed interval, meaning that the fluid velocity around the well is moderate.

The tests were conducted using a low shear rate viscometer with Couette geometry, and the data were gathered after some time from the beginning of the experiment. This would imply a steady state condition. The first step toward the execution of the tests is the preparation of the RPM solution. Viscosity tests were performed on three solution of brine-P100 at different mass concentrations: $500\ ppm$, $1500\ ppm$, and $4000\ ppm$. Furthermore the brine-polymer solution, when the concentration of the polymer is $1500\ ppm$, were tested before and after filtering in order to verify the presence of big size agglomerate of polymer, which would cause problems during the coreflooding test, thus the injection phase (plugging). The following table gives on overview of the tests performed:

Viscosity test at reservoir temperature, 43°C	
Test number	Note
1	Evaluation of brine viscosity.
2	Evaluation of the viscosity of the brine-P100 (500 ppm) solution. Solution filtered at 5µm.
3	Evaluation of the viscosity of the brine-P100 (1500 ppm) solution. Solution not filtered.
4	Evaluation of the viscosity of the brine-P100 (1500 ppm) solution. Solution filtered at 5µm.
5	Quick evaluation of the viscosity of the brine-P100 (4000 ppm) solution. Solution not filtered.

Table 2-1: viscosity tests list and description.

During the evaluation of the brine viscosity, the composition of the make-up water is set a 2% weight in KCl, meaning $20\,{}^{g}/_{L}$ of potassium chloride. The following plot, Figure 2-1, illustrates the results of the viscosity test, conducted at 43°C, for the synthetic brine.

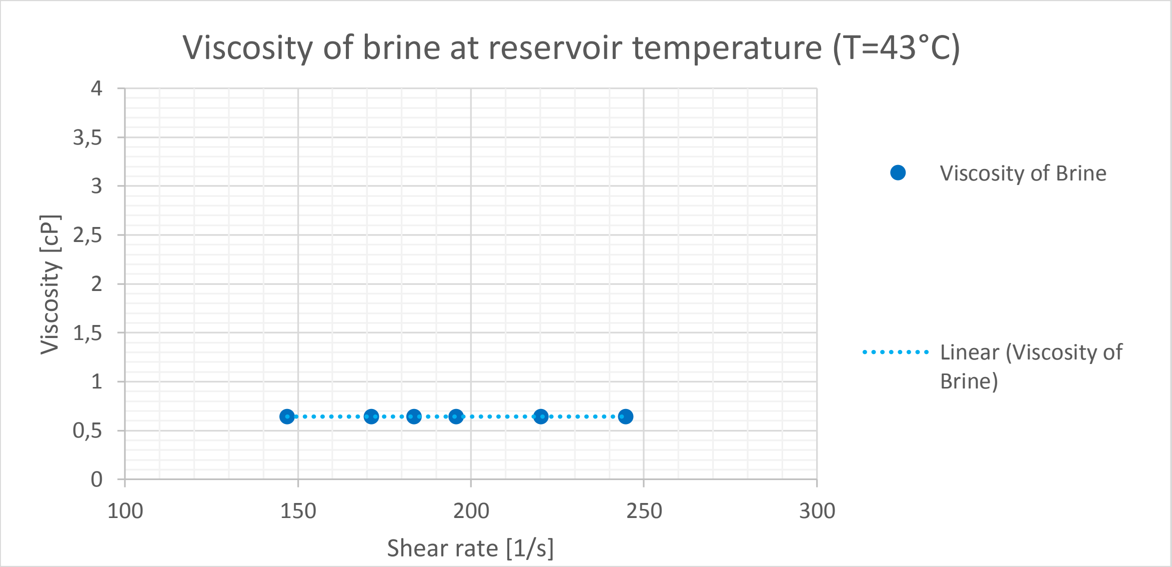

Figure 2-1: viscosity test result for brine.

From Figure 2-1 it is possible to see that the make-up water has perfectly normal newtonian behaviour as the interpolating trend is clearly linear and the r-squared value is higher than 0.995. This result meet the expectation since the viscosity of non-salty water at standard condition is around $0,65\ [cP]$. The value of the formation water viscosity is very important for the implementation of Darcy's equation during both the coreflooding tests, see paragraph 2.3, and the evaluation of the ENI study cases, see Chapter 3.

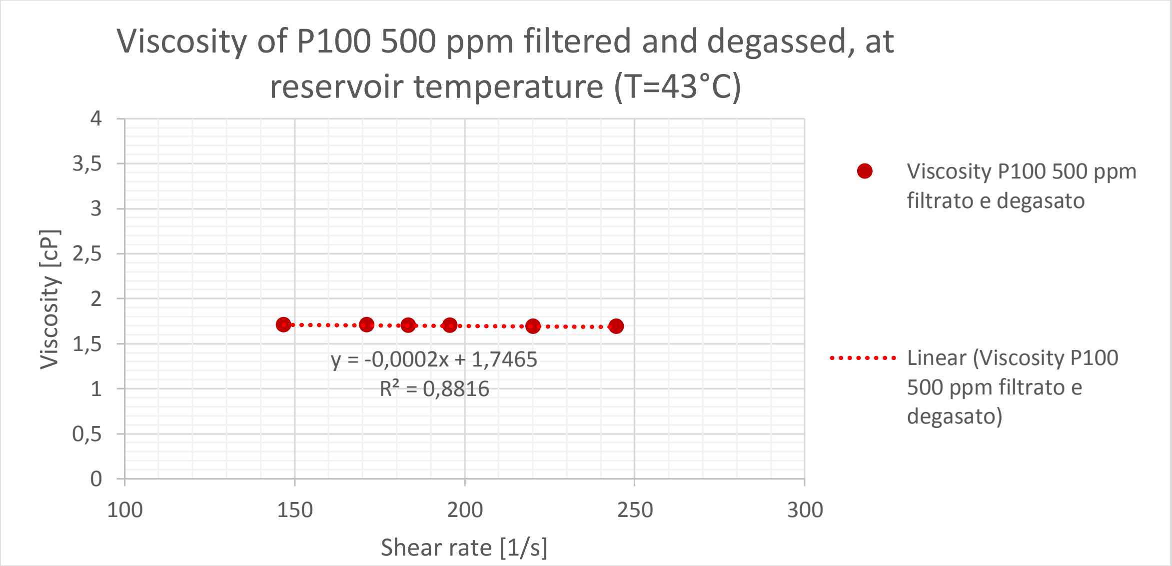

Figure 2-2: viscosity test result for RPM solution at 500ppm concentration of polymer, filtered at 5 µm.

Figure 2-2 illustrates the viscosity test of the brine-P100 solution at 500 ppm, filtered at 5 µm, and at reservoir temperature 43°C. It shows how the viscosity of polymer solution is only slightly higher than the brine viscosity: the average brine viscosity is $0{,}65\ [cP]$, while in this case the average viscosity is about $1{,}7\ [cP]$. At first glimpse it would appear that the polymer solution behaves like a Newtonian fluid. Anyway the r-squared of the trendline, $R^2 = 0{,}882$, leave some doubts about the linear trend. Indeed it appears that the experimental points would be better approximated by a logarithmic trendline. If that is the case the solution would behave more like a pseudoplastic, or shear-thinning, fluid, which would be the expected behaviour for a polymer solution. Additionally, viscosity versus shear rate plots generally have a logarithmic horizontal axis. Anyway, the Couette viscometer used in ENI laboratories can only operate in a limited range of round per minutes, meaning that a logarithmic plot wouldn't be very different from the one above.

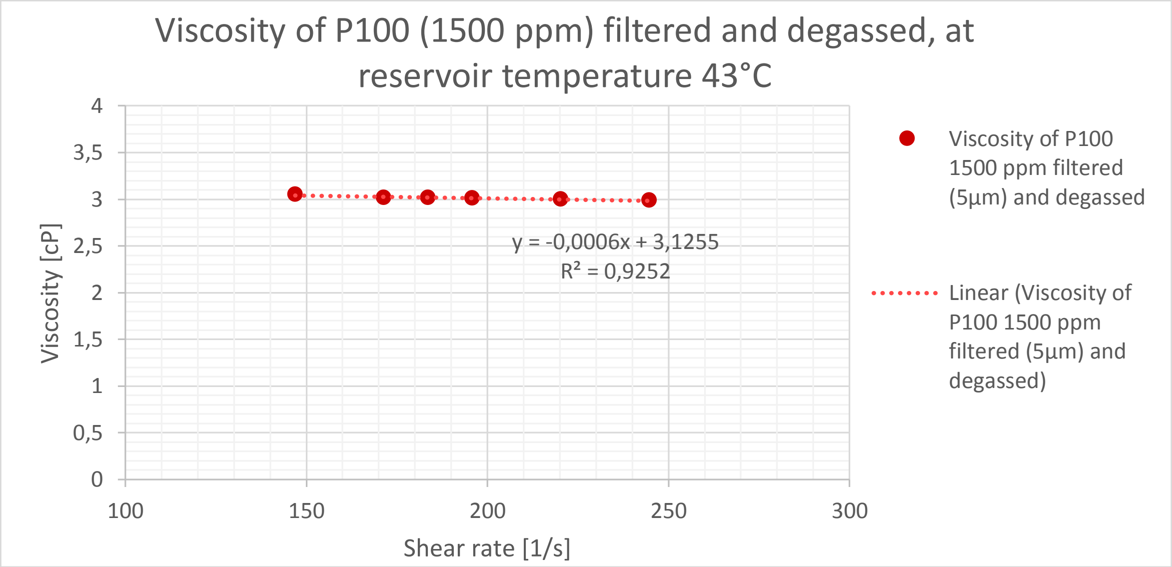

Figure 2-3: viscosity test result for RPM solution at 1500ppm concentration of polymer, filtered at 5 µm.

Just like Figure 2-2, Figure 2-3 plots the results for the viscosity test for the brine-P100 solution at 1500 ppm, filtered at 5 µm, and at reservoir temperature 43°C. The viscosity is a bit more elevated than the previous case, it shifted from 1,7 $[cP]$ to 3 $[cP]$, due to a higher mass concentration of the polymer. Once again the experimental points seem very likely to relate to a linear trend, though the r-squared of the trendline is not so high. This suggest once more a shear-thinning behavior.

To verify that P100 does not coagulate in big polymer cluster, which would plug the free face of the core during a coreflooding, the viscosity test is repeated for a P100 solution at 1500 ppm not filtered. Results from this test are extremely close to the ones obtained for a filtered solution, suggesting that there are none, or very little, polymer agglomeration bigger than 5 µm.

Viscosity test for a non-filtered solution has also been performed for a solution with polymer concentration of 4000 ppm, and the observations for this last case are exactly the same as the previous one.

The following plot summarizes all the data gathered from the viscosity tests and provides a clearer overview of the RPM solution behavior:

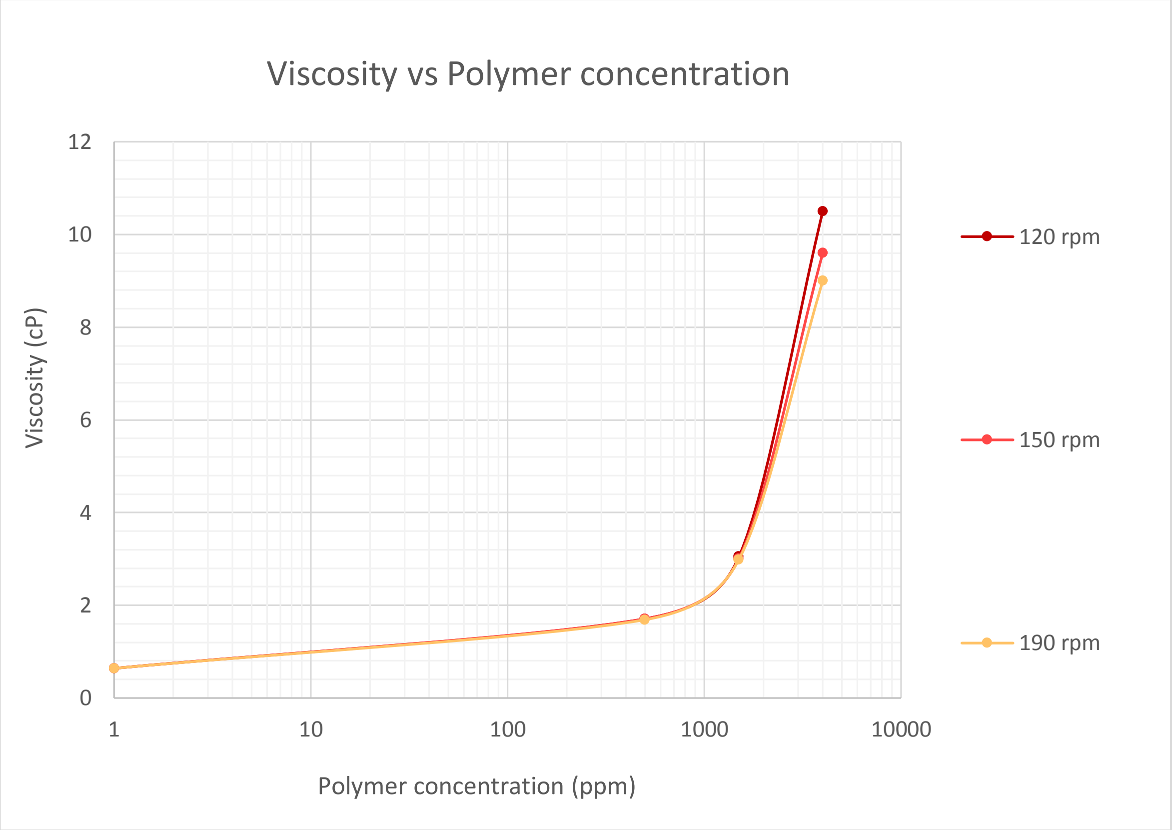

Figure 2-4: polymer behaviour; viscosity vs Polymer concentration at different shear rate.

Each curve in Figure 2-4 represents the registered viscosity, at different polymer concentration, for a defined value of the shear rate. The shear rate is directly related to the angular speed of the viscometer: a higher value of rpm (round per minute), produce a higher value of the shear rate. The plot highlight that solutions with elevated polymer concentration, especially with mass concentration higher than $2000 - 3000\ ppm$, have lower viscosity at high shear rate. This situation confirms the previous emphasized shear-thinning properties, and consequently it also suggests that the addition of more polymer to the RPM solution enhances its pseudoplastic properties. This aspect would require to investigate the shear rate during the coreflooding test, and also during the field treatment, since it may affect the pressure response, to injection, in both cases. Anyway the highest concentration of polymer used in the field treatments in about $2500\ ppm$, where the pseudoplastic effect of the solution is extremely low. Thus the polymer solution will be considered as a pseudo-newtonian fluid with constant viscosity.

2.2 - INTERACTION BETWEEN RPM AND ROCKS

To evaluate the attraction between the sand of the area near the wellbore and the polymer it is possible to perform a flocculation test. Flocculation is the process in which colloids aggregates, or come together, to form large particles called flocs by the addition of a chemical called flocculant. In this case the flocs are the sand particles produced from the reservoir, while the flocculant is the polymer itself. This kind of test can be performed using either high precision machinery, such as the Turbiscan, or in more simple way. In ENI laboratory, since the objective of this test is not to accurately investigate the flocculation properties of the P100, but to obtain a general information about its behaviour, the flocculation is carried out in a with a very simple, but effective, test. This test, always performed at reservoir condition, consists in mixing a given quantity of sand with the polymer solution in a graduated ampoule having two graduations to detect flocculation time. Once the two components are mixed together the ampoule should be gently reversed, or the liquid should be stirred, to optimize the blending. Then everything should be allowed to settle. Flocculation time, which is the required parameter, is simply measured as the time needed for the solid/liquid interface to sink below the lowest graduation line. As a first approximation, it is possible to assume that the shortest the flocculation time, the highest the ability of the polymer to coagulate the sand, thus to coat it.

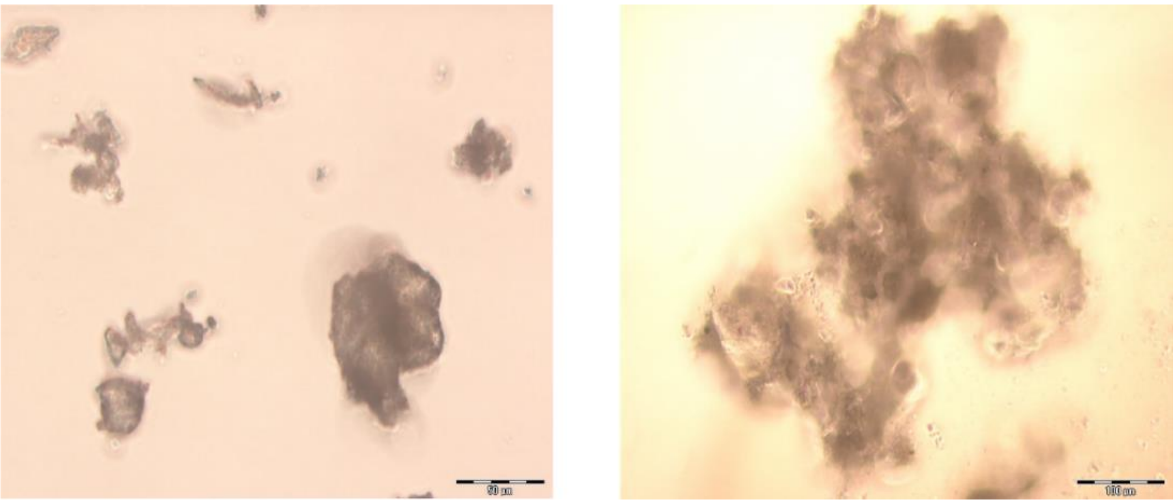

Figure 2-5: aspects of sand particles before the contact with the microgel, on the left, and after, on the right. Zaitoun et Pichery, New Polymer Technology for Sand Control Treatments of Gas Storage Wells; SPE 121291; Texas; April 2009;

Figure 2-5 shows two electronic picture of sand particles before and after the contact with an RPM solution during a flocculation test. The picture on the right is an example of how a good flocculant should aggregate sand particles and fines.

Flocculation: laboratory tests and results

The procedure followed to perform a flocculation test in ENI Laboratories is the one described above, completed stirring the solution, with the only difference that the test has been repeated at different contact times and different concentrations of P100. Repeating the test at different contact times allow the measurements of the degradation of the flocculation properties of the polymer. The make-up water is the same that has been used for the viscosity test.

The evolution of the settling times during flocculation test with and without polymer is shown in the following plot:

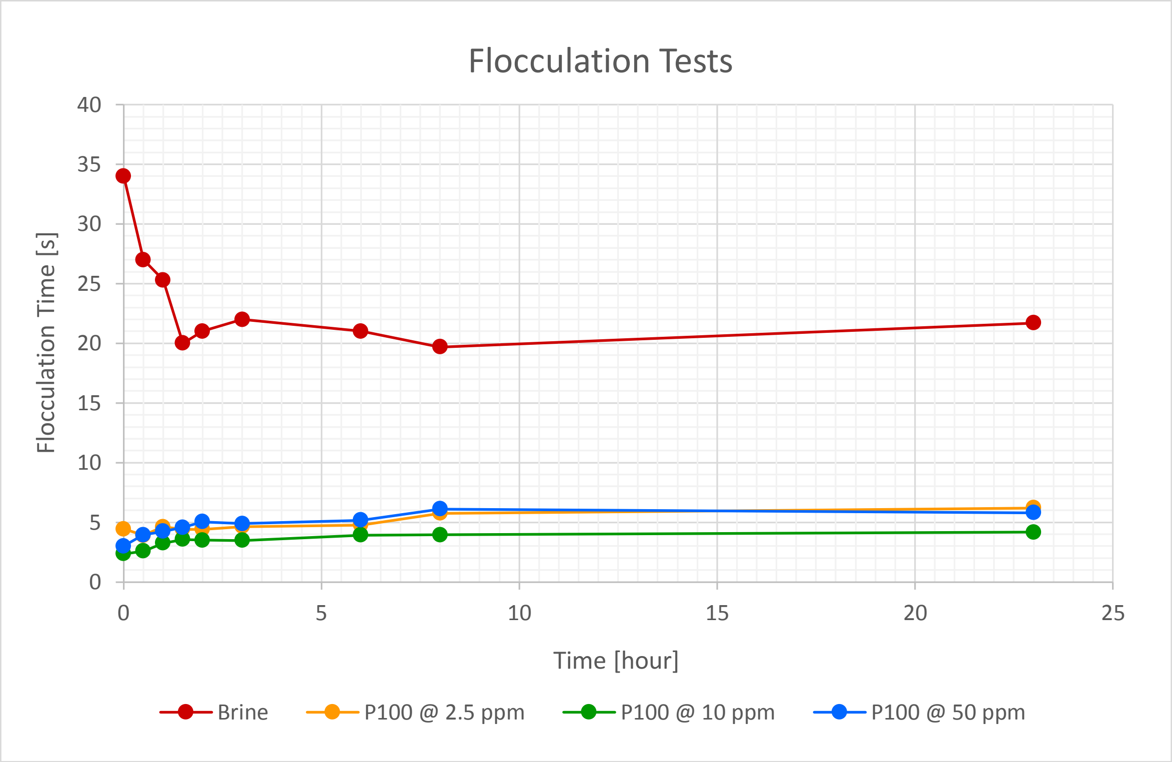

Figure 2-6: flocculation tests results at three different polymer concentration.

Form Figure 2-6 it is clear that the polymer solution, at every concentration used, greatly diminishes the settling time of the sand particle. Indeed all the flocculation tests result in a settling time 5 to 6 times lower to the brine case. Furthermore, the degradation of the polymer appear to be very little and it doesn’t increase as the quantity of polymer itself increases. Eventually is possible to state that the P100 solution is reasonably stable and it has a good interaction with the sand of the treated wells. Anyway this test could lead to wrong considerations, as a higher polymer concentration induces a higher settling time for flocculated particles. This is the reason why such low concentration of polymer were used during this test: if a solution has very good flocculant properties at low mass concentration of polymer, it is expected to have even better properties when the polymer mass concentration is increased.

Additionally, regarding the problem of sand production, it is plausible to expect that a product with these good flocculating properties, could also operate some sort of sand control. Indeed the process of adsorption and the coating of the pore surfaces could prevent the release of small grain fines during the production. This aspect is extremely interesting for the well treated by ENI in the Adriatic Sea since all of them suffers from sand production. Besides, no test will be performed to assess this aspect, which will be anyway discussed in the following chapter where the real case of RPM treatment are argued.

2.3 - RPM INJECTIVITY AND PERMEABILITY REDUCTION EFFECT

Once the rheological behavior of the RPM is assessed, and its good interaction with the formation rock is verified, it is possible to test the most important and useful parameter for a RPM treatment: the injectivity, the degree of adsorption and the efficacy of the product in selectively reducing the water effective permeability. A correct sequence of coreflooding tests can provide such information. The coreflooding test mainly consists in flushing a fluid, or a combination of fluids, through a rock sample and analyze their interaction. The equipment necessary to perform this test consist of:

- Core sample, or more than one if it is necessary to test multiple different wells.
- A core holder, Hassler cell, which is the heart of the machine. It encloses the core sample and is capable of withstand the pressure during the test.
- An oven which is require to condition the temperature of the Hassler cell at the reservoir temperature.
- A high pressure liquid chromatography pump used to flush the fluid through the Hassler cell at a constant rate.
- Various pressure transducer to register the pressure at the inlet and at the outlet of the cell.
- A pump controller used to operate another pump, necessary to maintain a fixed confining pressure around the core.
- A flowmeter used to measure the gas flow rate at the outlet of the cell.
- Tubes necessary to connect all the devices together. The tubes must be of a high pressure resistant material, and they also need to be have a high thermal

conductivity so that the flowing fluid reaches the reservoir temperature before entering the Hassler cell.

The equipment used for such a test in ENI laboratories is the one depicted in the following figures:

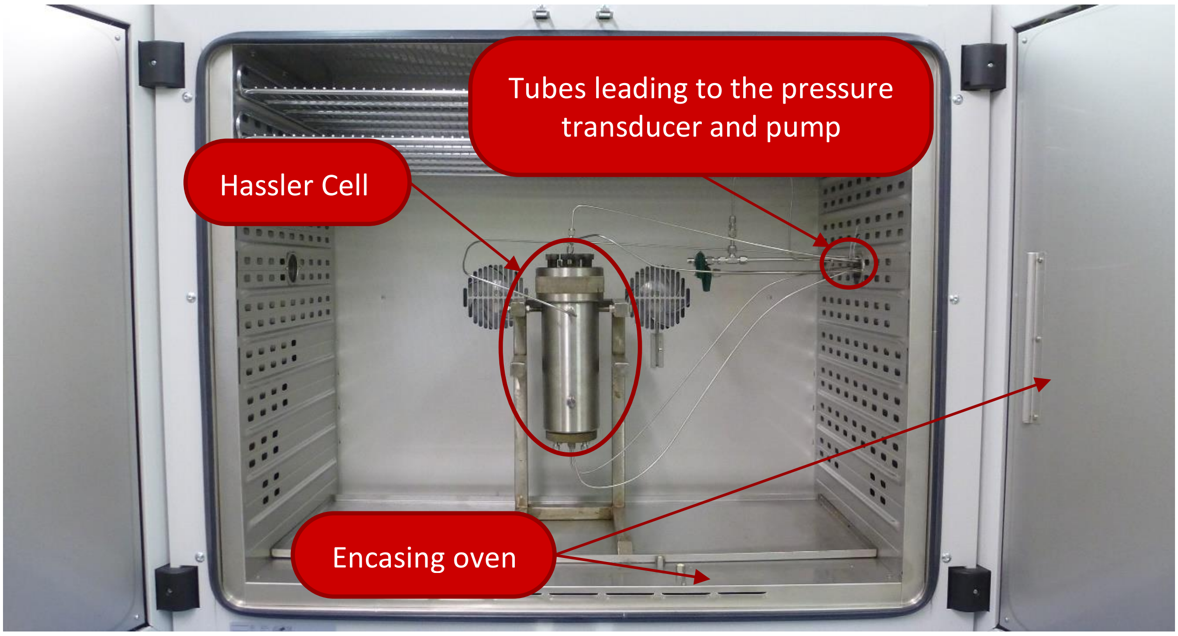

Figure 2-7: coreflooding oven and Hassler cell at ENI laboratories.

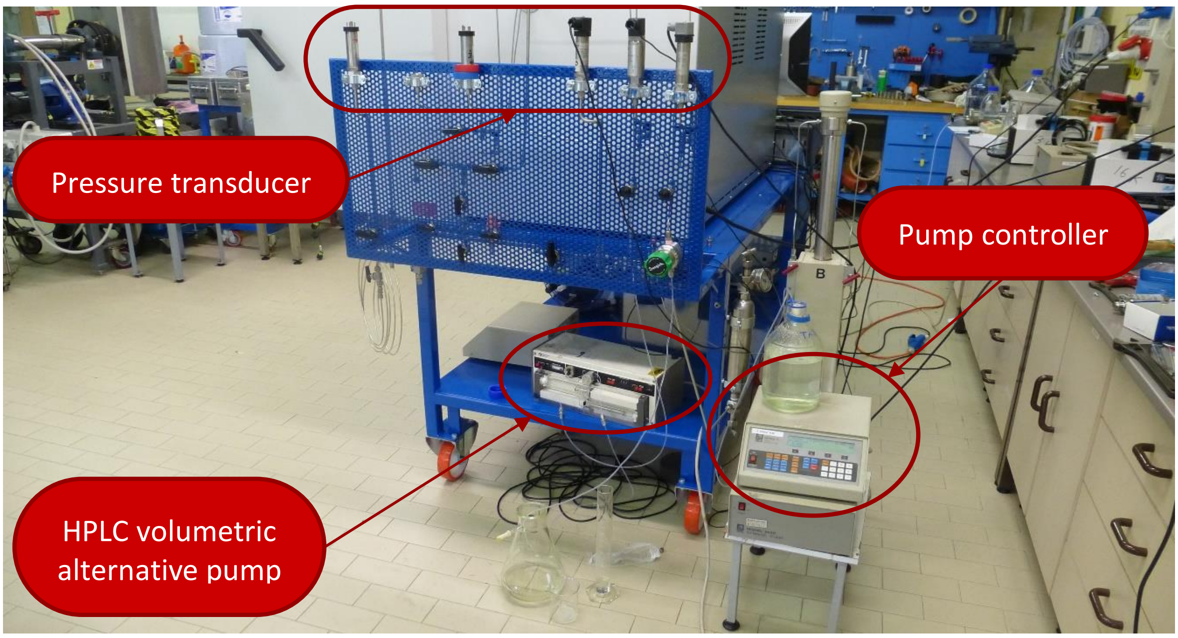

Figure 2-8: volumetric pump, pressure transducers and pump controller at ENI laboratory

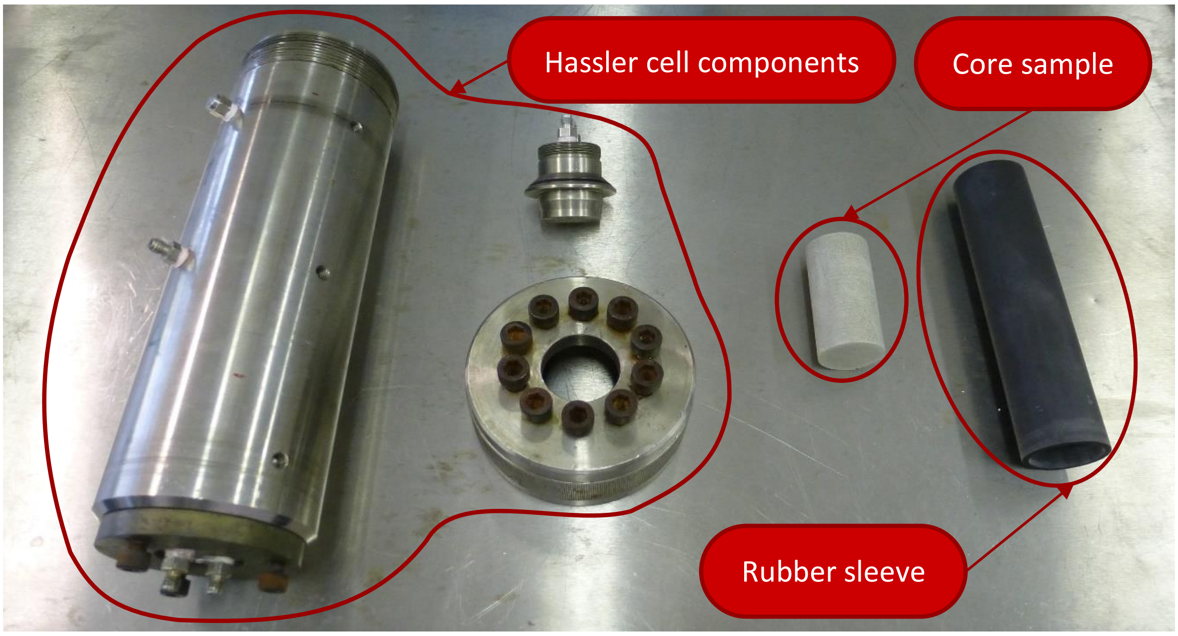

Figure 2-9: disassembled Hassler cell, core sample and rubber sheath

Coreflooding: equipment layout

The test has been performed on a plug from the core sample from Pozzo 1 C whose characteristics are outlined in Table 2-2:

Core sample characteristic	
$\boldsymbol{Length}\ [cm]$	7,90
$\boldsymbol{Diameter}\ [cm]$	3,81 (1,5'')
$\boldsymbol{Porosity}\ [\%]$	19,2
$\boldsymbol{Pore\ volume}\ [mL]$	17,3
$\boldsymbol{Average\ pore\ radius}\ [\mu m]$	2,9

Table 2-2: characteristic of the core sample from Pozzo 1C.

The plug, which from now on will be referred only as core sample or core for the sake of clarity, is an artificially compacted one. As a matter of fact plugs cores from sandstone reservoir tends to shatter due to the frailty nature of the rock, therefore they need to be reconstructed in laboratory so that their characteristics matches the one of the reservoir.

The Hassler cell and the other equipment parts have been set up as shown in the system diagram, Figure 2-10:

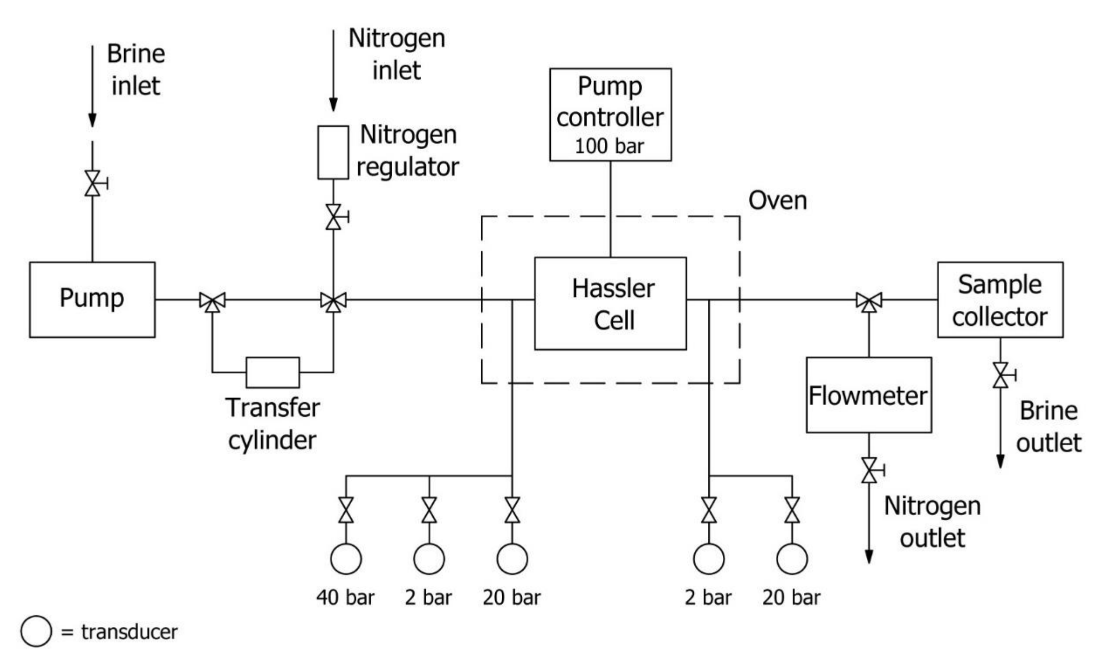

Figure 2-10: System schematic of the coreflooding equipment used in ENI laboratories for testing P100.

The core sample is jacketed within a thick rubber sleeve and positioned inside the Hassler cell. The pump controller applies a confining pressure of about $100\ [bar]$, which is high enough to guarantee a strong grip between the rubber and the core, so that no fluid will flows in the interstitial space, but not too high to cause any damage to the core. The top part of the cell, see Figure 2-7, is connected to the alternating volumetric pump and to a series of pressure transducers calibrated at $2\ [bar]$, $20\ [bar]$ and $40\ [bar]$. The bottom part of the cell is connected with one pipe, through a valve, to a sample collector, and with the other pipe, again, to a series of pressure transducers calibrated at $2\ ba$r and $20\ bar$. The pressure transducers can be switched between one and the other with relation to pressure level they are supposed to register. During gas injection the sample collector is exchanged with a flowmeter. During all the tests, the oven containing the Hassler cell is kept at reservoir temperature, around $43\ °C$.

Coreflooding: test overview

The test aims at providing, first thing first, the degree of permeability reduction to the water phase, then the quantity of adsorbed polymer, and also the mobility reduction during the polymer injection.

The 'Water residual resistance factor', defined as F_{rrw}, is probably the most important parameter that can be obtained since it provides a quantifiable value of the polymer-induced permeability reduction. This parameter is defined as in equation (2.1)

$$F_{rrw} = \frac{\left(k'_{r,w}\right)_{before}}{\left(k'_{r,w}\right)_{after}} \tag{2.1}$$

Where: $k'_{r,w}$ is the end-point permeability of water, and the subscription indicates whether the parameter is measured before, or a after, the polymer injection. The higher the value of this dimensionless parameter, and the less water the treated well is supposed to produce.

Of course it is also necessary to quantify the variation of the core relative permeability to oil, or gas in this case, with a very similar parameter defined as 'Gas residual resistance factor', F_{rrg}, in equation (2.2):

$$F_{rrg} = \frac{\left(k'_{r,g}\right)_{before}}{\left(k'_{r,g}\right)_{after}} \tag{2.2}$$

Where: $k'_{r,g}$ is the end-point permeability of gas, and once again the subscription indicates whether the parameter is measured before or a after the polymer injection. The value of F_{rrg} is expected to be around the unit since, theoretically, the process of disproportionate permeability reduction aims at leaving the hydrocarbons relative permeability unchanged.

The quantity of adsorbed polymer is evaluated through an experimental procedure: two successive slugs of polymer separated by brine are injected in the core. The delay between the first and the second polymer slugs, in terms of injected pore volumes, give the adsorption value. Anyway this test has not been performed in the ENI laboratory, and the values of the polymer adsorption is provided directly by the service company.

As for the injectivity of the RPM solution, the test aims at verifying that the polymer does not plug the core, thus the formation: during polymers injection a pressure increase is to be expected since the viscosity of the polymer solution is higher, and also because the process of adsorption begins immediately, posing higher attrition to further water-like fluids flow. Thus, during the injection of a non-plugging polymer, a plot of pressure versus time would show an initial growth followed by an inflexion and then a stabilization of the pressure. This trend is due to the fact that after the adsorption, which determines increasing pressure losses and thus the initial growth, the flow would reach a steady state, and further injected polymer wouldn’t interact with the pores surface and would flow through the core. Behaviours that differ from this one imply different interactions between the rock and the polymer, such as a surface plugging and thus an exponential trend in the pressure versus injected volume curve. So, the goal of the injectivity test is to confirm that after the injection of several pore volumes of RPM solution the pressure would stabilize around a fixed value, but most importantly that no damages occur to the core, thus the formation. During the coreflooding tests with water, the only parameters that can be measured are the pressure at both the inlet and the outlet of the Hassler cell, and the flow of the fluid through the cell itself, which is set by the pump. On the other hand, during the gas flooding, it is not possible to impose a steady flow since the gas cannot be assimilated to an incompressible fluid, as it happens for the water. This is the reason why a flowmeter is required. A pressure regulating valve, see Figure 2-10, imposes a stable pressure at the inlet of the cell, while the flowmeter registers the flow rate of the outlet gas. Considering the previous statements about brine, and given the values of its viscosity together with the viscosity of the RPM solution, it is possible to obtain the value of the various permeabilities with the Darcy’s law applied as in equation (2.3):

$$q = -A\frac{K}{\mu}\frac{\Delta P}{L} \tag{2.3}$$

Where: '*q*' is the volumetric fluid flow; '*A*' is the section area through which the flow occurs; 'μ' is the viscosity of the flowing fluid, 'L' is the length of the core, and '*ΔP*' is the pressure difference between the inlet and the outlet of the Hassler cell. Of course equation (2.3) is simplified by assuming that the flow is in a steady state, linear, horizontal, incompressible, and single phased. It is also possible to extend the formula for multi-phase flow, as in equation (2.4):

$$\frac{q_i}{A} = K\frac{k_{r,i}(S_w)}{\mu_i}\frac{\Delta P_i}{L} \tag{2.4}$$

The terms with the subscription '*i*' are referred to a specific phase that can be water, oil or gas. While the product '$K \cdot k_{r,i}(S_w)$' is the effective permeability of the inquired phase. The above equations considered the fluids to be incompressible, with a constant density in the flow system, which is not a bad assumption for water. However, gas is highly compressible. Thus, considering the last statement, an analytical solution to this problem can be obtained integrating Darcy's equation starting from equation (2.5):

$$q = -A\frac{k_g}{\mu_g}\frac{dp}{dx} \tag{2.5}$$

Introducing Boyle's law for real gasses under isothermal conditions, for volumetric flow rate, as in equation (2.6):

$$\left(\frac{pq}{zT}\right)_{res} = \left(\frac{pq}{zT}\right)_{sc} \tag{2.6}$$

Where: '*P*' is the absolute pressure, '*q*' is the volumetric flow rate, '*z*' is the compressibility factor, and '*T*' is the temperature. The subscription '*res*' indicate the reservoir condition, while the subscription '*sc*' indicates the standard conditions. Substituting (2.6) in equation (2.5), and separating the variables gives:

$$q_{sc}\int_0^L dx = -A\frac{k_g}{T_r}\left(\frac{zT}{P}\right)_{sc}\int_{P_1}^{P_2}\frac{p}{\mu_g(p)\,z_{res}(p)}dp \tag{2.7}$$

Where the viscosity and the compressibility factor changes with the pressure and should not be intended as constant. Anyhow, if the test is carried out at low pressure it is indeed possible to assume that their product, evaluated at an averaged squared pressure, is constant. Furthermore the ratio between the two compressibility factors will be very close to the unity, and the same goes for the temperatures. This hypothesis may appear very strong, and may also lead to notable errors, but it is necessary to remember that the goal of the coreflooding tests is to find the residual resistance factor, which is indeed a ratio between permeabilities. Therefore any error introduce by constants, during the elaboration of the data, is nullified during the computation of the aimed parameter. Anyway, introducing these hypothesis in equation (2.7) gives:

$$q_{sc} = -\frac{A\,k_g\,(P_{in}^2 - P_{out}^2)}{2\,P_{sc}\,\mu_g\,L} \tag{2.8}$$

Where the subscription ‘in’ and ‘out’ relatively stands for inlet position and outlet position in relation with the Hassler cell.

With this approximated analytical expression is possible to evaluate the permeabilities, absolute and relative, during any core flooding.

During these experiments, carried out at low pressure, it is common practice to use nitrogen instead of methane. This choice is mainly supported by safety issues, nonetheless the induced approximation are acceptable since at low pressure the solubility differences of the two gasses, meaning the Henry constants, especially in water, are very much similar. Additionally, always considering the low pressures, the considered gasses show properties alike perfect gasses ones.

Coreflooding: tests and results

The set of tests require to obtain all the information introduced in the previous subparagraph imply a series of eleven coreflooding.

Test 1: gas absolute permeability.

In the first experiment the dried core is flushed with nitrogen. Before starting this sequence, it is necessary to search the zeroes of the pressure transducers by flooding the core at a fixed inlet pressure until the registered pressure of both inlet and outlet transducer is stable. The value registered during this operation is taken into account during further data elaboration. Figure 2-11 illustrates the transducers response during their stabilization:

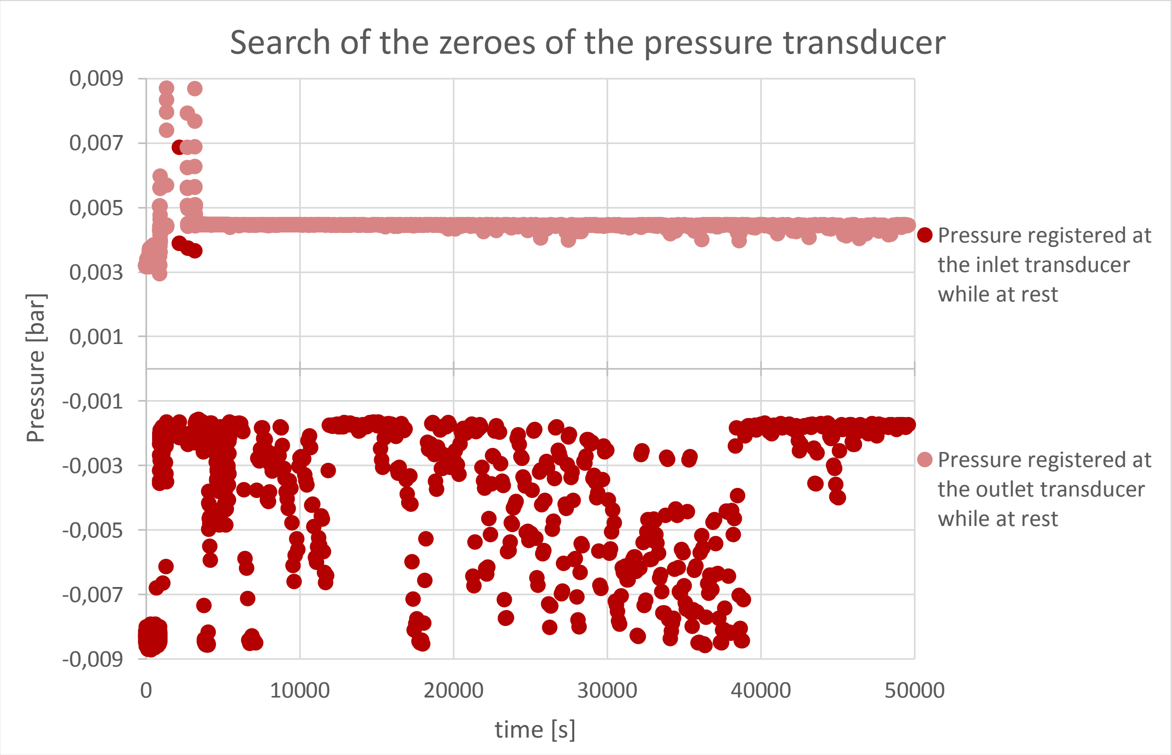

Figure 2-11: the plot illustrates the phase of stabilization of the pressure transducers necessary to find their zeroes.

The stabilization of the pressure transducer is the first operation to carry out in order to define their zeroes. Table 2-3 illustrates the value of pressure registered by the transducer while at rest:

$\boldsymbol{Transducers\ zeroes}\ [bar]$	
-0,0018	Inlet transducer
0,0044	Outlet tranducer

Table 2-3: zeroes of the pressure transducer during the test 1, gas coreflooding

The obtained values are to be removed from the registered pressure during the next flooding phase: the inlet pressure is measured by a 20 $[bar]$ pressure transducer while the pressure regulating valve keeps the gas flow rate constant first around 7 $[bar]$, then around 5 $[bar]$, and in the end around 3 $[bar]$. The outlet pressure of the cell is measure by a 2 $[bar]$ pressure transducers. The gas keeps flowing at a fixed pressure until the flowmeter at the outlet of the Hassler cell has collected enough gas to be sure that the steady state conditions are reached. Figure 2-12 shows the transducers pressure response during the core flooding.

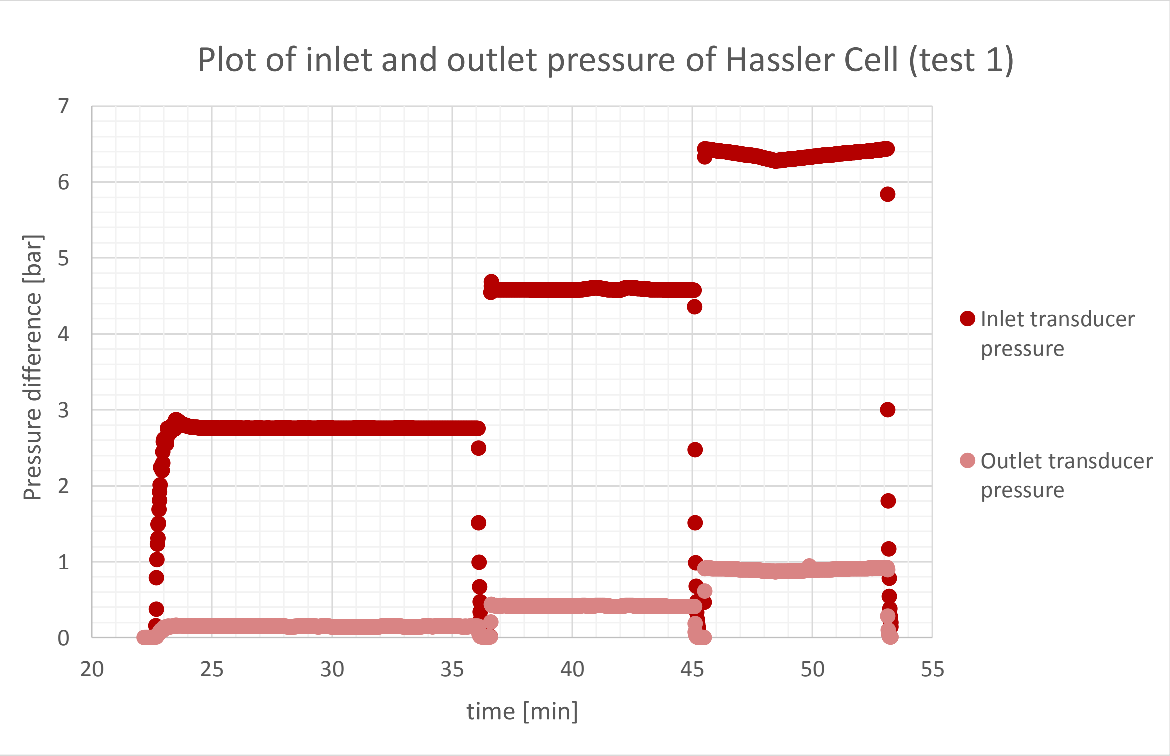

Figure 2-12: transducers pressure response during test 1, gas core flooding.

In Figure 2-12, the registered inlet pressure is not as high as the imposed one by the pump, due to some pressure losses along the injection tube. Even along the tubes that connect the pressure transducers to the cell there are pressure losses. Still, since the length of the tubes is equal and the aim of the test is to record a pressure difference, these losses can be neglected. The following table shows the average registered pressure during the flooding:

$P_{valve}\,[bar]$	$P_{in}[ata]$	$P_{out}[ata]$
3	3,75	1,15
5	5,57	1,41
7	7,36	1,9

Table 2-4: average registered pressure at the inlet and outlet transducers during test 1, gas flooding

While the flow rates reading given by the flowmeter, at different imposed inlet pressure, are illustrated in Table 2-5:

$P_{valve}\,[bar]$	$Displacement\ time\ [{}^{s}/_{L}]$	$Flow\ rate\ [{}^{mL}/_{min}]$
3	42,44	1413,87
5	19,47	3081,66
7	11,68	5139,19

Table 2-5: flow rates measured during test 1, gas flooding.

Using the Darcy's law introduced in the previous subparagraph and rearranging it so that the permeability term is explicit, gives:

$$K = -\frac{2\, q_{sc}\, P_{sc}\, \mu_g\, L}{\left(\frac{d}{2}\right)^2 \pi\, (P_{in}^2 - P_{out}^2)} \qquad (2.9)$$

Where: *'d'* is the core diameter, while all the other parameters have been previously explained: see pages 49 and 50. Equation (2.9) allow the computation of the permeability for each one of the three flooding at different pressure. Additionally, since the core contains only gas during the test, the obtained permeability, illustrated in Table 2-6, is the absolute permeability to gas.

$\boldsymbol{Absolute\ Permeability\ to\ gas\ \ [mD]}$	
$\boldsymbol{K_{g,1}\ \ at\ 3\ [bar]}$	46,89
$\boldsymbol{K_{g,2}\ \ at\ 5\ [bar]}$	44,88
$\boldsymbol{K_{g,3}\ \ at\ 7\ [bar]}$	42,99
$\boldsymbol{K\ (average\ permeability)}$	**44,92**

Table 2-6: the table illustrates the computed permeability after test 1, gas flooding, as K_1, K_2, and K_3. The last row contains the average absolute permeability to gas of the core sample.

Test 2: brine absolute permeability.

The second core flooding consist in flushing the core sample from Pozzo 1 C with the same brine, 2% KCl, used during the flocculation test. The test is repeat as previously done for the gas, with the only difference that the flowmeter is not required and it can be switched with a sample collector. Flushing the core at different flow rates, while measuring the inlet and the outlet pressure of the Hassler cell provides all the necessary parameters to compute the absolute permeability of brine. The equipment setup is, again, the same one as for the gas, and before the flooding the zero setting of the pressure transducers is acquired. The plot for this operation will no longer be shown in this document, neither for this test, nor for any other tests that follows, since the procedure has been satisfactorily argued for the first test. On the other hand, the plot of the recorded pressure at inlet transducer and outlet transducer is illustrated in the following graph, Figure 2-13:

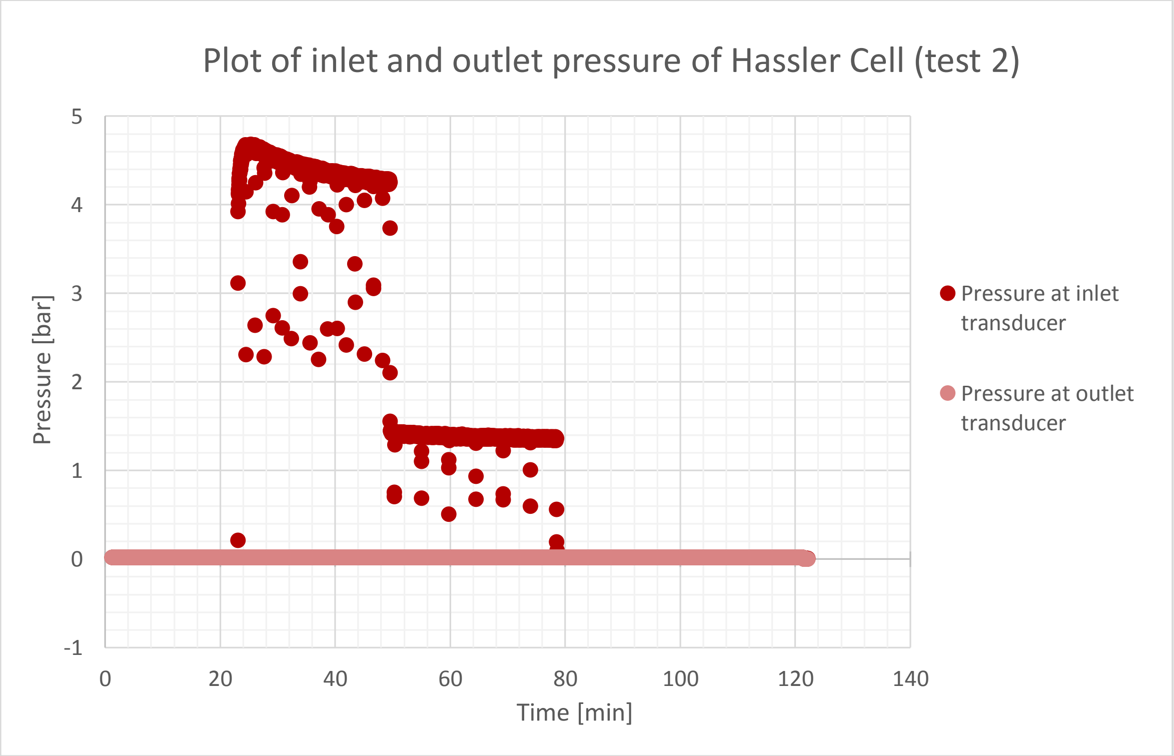

Figure 2-13: transducers pressure response during test 2, brine core flooding.

The scattered points that significantly detach from the quite constant trend of the pressure at the inlet transducer, in Figure 2-13, appear to repeat at constant intervals. They are due to the fact the pump used to impose a fixed brine flow rate, is a double acting volumetric pump. So, every time that the piston of the pump changes its direction, the inlet transducer measures a pressure loss. This effect does not occur at the outlet of the cell since the core sample acts a volumetric buffer capable of blocking the pressure loss propagation. During the test, the imposed flow rate are 360 $\left[{}^{mL}/_{h}\right]$ first, and 120 $\left[{}^{mL}/_{h}\right]$ after. During the flooding with 360 $\left[{}^{mL}/_{h}\right]$, the pressure requires a little more time to stabilize, thus the value of the registered pressure during this phase is evaluated on an average of the last part of this segment of curve. The following table, Table 2-7, illustrates the registered pressure already adjusted with transducers zeroes:

$\boldsymbol{Flow\ rate}\ \left[{}^{\boldsymbol{mL}}/_{\boldsymbol{h}}\right]$	$\boldsymbol{P_{in}}\ [\boldsymbol{bar}]$	$\boldsymbol{P_{out}}\ [\boldsymbol{bar}]$	$\boldsymbol{\Delta P}$
360	4,26	0,019	**4,241**
120	1,36	0,017	**1,343**

Table 2-7: average registered pressure at the inlet and outlet transducers during test 2, brine flooding, with the respective flow rate

These values can be used within the Darcy's law, equation (2.3), to obtain the core sample absolute permeability to brine, for each flow rate. Additionally it is possible to compute an average absolute permeability as it has been done for the previous test. Table 2-8 illustrates these values:

$\boldsymbol{Absolute\ permeability\ to\ brine}\ [\boldsymbol{mD}]$	
$\boldsymbol{K_{b,1}\ \ at\ 360}\ \left[{}^{\boldsymbol{mL}}/_{\boldsymbol{h}}\right]$	10,46
$\boldsymbol{K_{b,2}\ at\ 120}\ \left[{}^{\boldsymbol{mL}}/_{\boldsymbol{h}}\right]$	11,01
$\boldsymbol{K}\ (\boldsymbol{average\ permeability})$	**10,73**

Table 2-8: the table illustrates the computed permeability after test 2, brine flooding, as K_1 and K_2. The last row contains the average absolute permeability to brine of the core sample.

From a comparison of Table 2-6 with the results obtained in Table 2-8, it appears to be quite odd that the absolute permeability of the same rock computed at two different times are substantially so different. This anomaly is simply due to the presence of clay in the rock composition. In fact, during the brine flooding, when the water contacts the clay, tha latter swells diminishing the pores size, thus the permeability. This behaviour generally cause an absolute permeability reduction that can also be more than five time lower of the original one

Test 3: gas end-point effective permeability.

At the end of the second test the core is saturated with brine, and the brine itself become the wetting phase. The third test is a gas drainage[14] of the core that, at the end of the gas injection, provides the irreducible water saturation of the core and the gas end-point effective permeability. The equipment is again arranged as for the test one, and the pressure regulating valve imposes a fixed pressure that shift from 7 to 5, and then to 3 $[bar]$, each time for a period long enough for the flow to stabilize. The calibration of the pressure transducers precedes all. The results obtained are displayed in Figure 2-14:

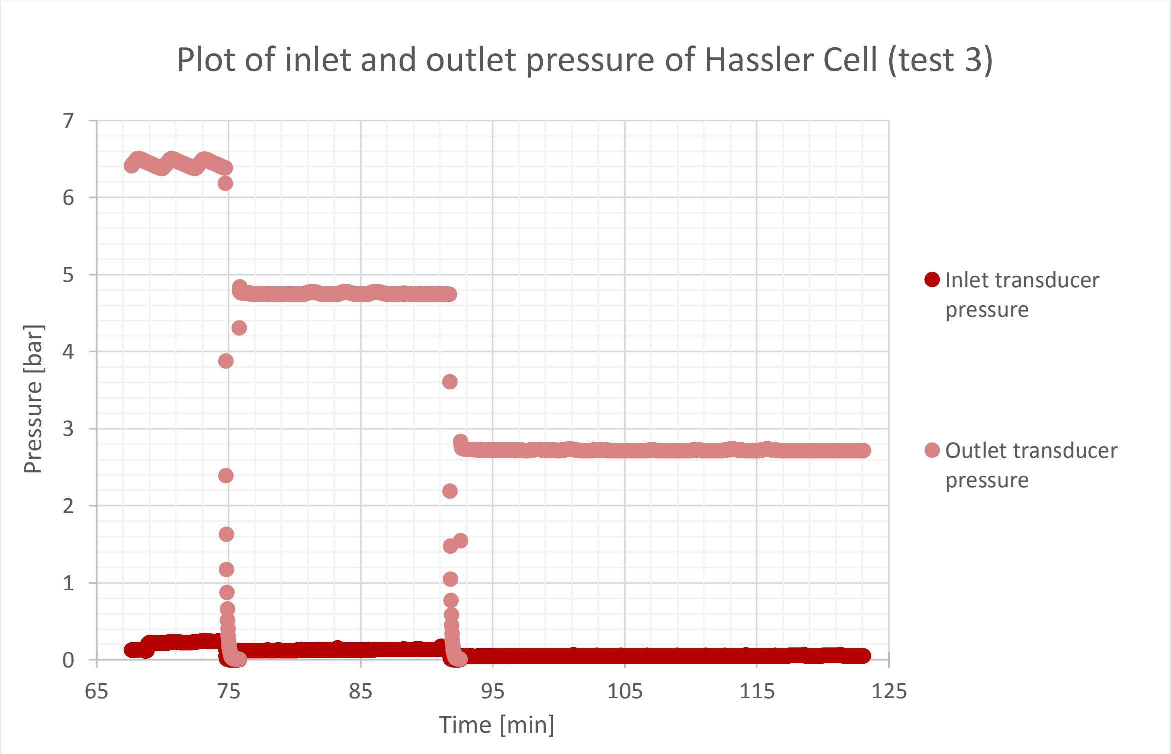

Figure 2-14: transducers pressure response during test 3, gas core flooding.

Aside from an anomaly pressure drop in the time intervals between the inlet pressure variations, the plot shows a very stable trend. It is quite simple to extrapolate and compute the average pressure for the inlet and the outlet pressure transducer in all three cases. The

---

[14] A drainage process consists in the reduction of the wetting phase through its displacement by another fluid.

following table, Table 2-9, illustrates such results, already cleared out from the transducers zeroes:

$P_{valve}\ [bar]$	$P_{in}[ata]$	$P_{out}[ata]$
3	3,72	1,05
5	5,74	1,13
7	7,42	1,23

Table 2-9: average registered pressures at the inlet and outlet transducers during test 3, gas drainage.

While the following table summarises the flow rate read on the flowmeter:

$P_{valve}\ [bar]$	$Displacement\ time\ [{}^{s}/_{L}]$	$Flow\ rate\ [{}^{mL}/_{min}]$
3	109,45	548,18
5	49,57	1210,33
7	33,21	1806,50

Table 2-10: flow rates measured during test 3, gas flooding

Comparing the displacement time reported in Table 2-10 to the displacement time obtained during the first test, illustrated in Table 2-5, considering that the flow rates in the third test are smaller, the gas appear to have more difficulties in flowing through the core. This is due to the fact that the presence of water diminishes the diameter of the pores enhancing the pressure losses during the flow. Therefore a substantial difference in the end-point permeability of gas, with respect to the absolute permeability of gas, is to be expected. Using equation (2.9) once more, gives the results of the gas effective permeability at irreducible water saturation.

Table 2-11 illustrates these results and their average:

$End - point\ gas\ effective\ permeability\ [mD]$	
$K_{g,1}$ $at\ 3\ [bar]$	14,89
$K_{g,2}$ $at\ 3\ [bar]$	16,87
$K_{g,3}$ $at\ 3\ [bar]$	19,04
$K\ (average\ permeability)$	**16,93**

Table 2-11: the table illustrate the computed permeability after test 3, gas flooding, as K_1, K_2, and K_3. The last row contains the average absolute permeability to gas of the core sample.

The obtained gas end-point permeability is accordance with the previous statements and with the theory, since its value is smaller than the absolute permeability of the rock, which was previously assessed around $45\ [mD]$.

Weighting the core after the gas displacement, and comparing the measured mass with the mass measured after the brine injection, when the core was fully saturated with brine, and the pore volume of the plug, gives an approximated value of the irreducible water saturation:

$Irriducible\ water\ saturation$	
$S_{w,irr}$ $[-]$	**0,29**

Table 2-12: irreducible water saturation of the sandstone core before the polymer injection.

Test 4: brine end-point effective permeability.

This is the last test prior the RPM solution injection, and it gives the last parameter necessary to assess the core sample behaviour: the end-point brine effective permeability. The experiment is carried out in the same way of the test number two. The only difference is that now the initial saturation in water of the core is equal to the irreducible water saturation, illustrated in Table 2-12. Additionally, at the end of the process of imbibition[15] performed in this test, the water does not fully saturate the core, since it is limited by the residual gas saturation. Before commencing the process, the pressure transducers are calibrated. The registered pressure during the water displacement at fixed flow rates are illustrated in Figure 2-15:

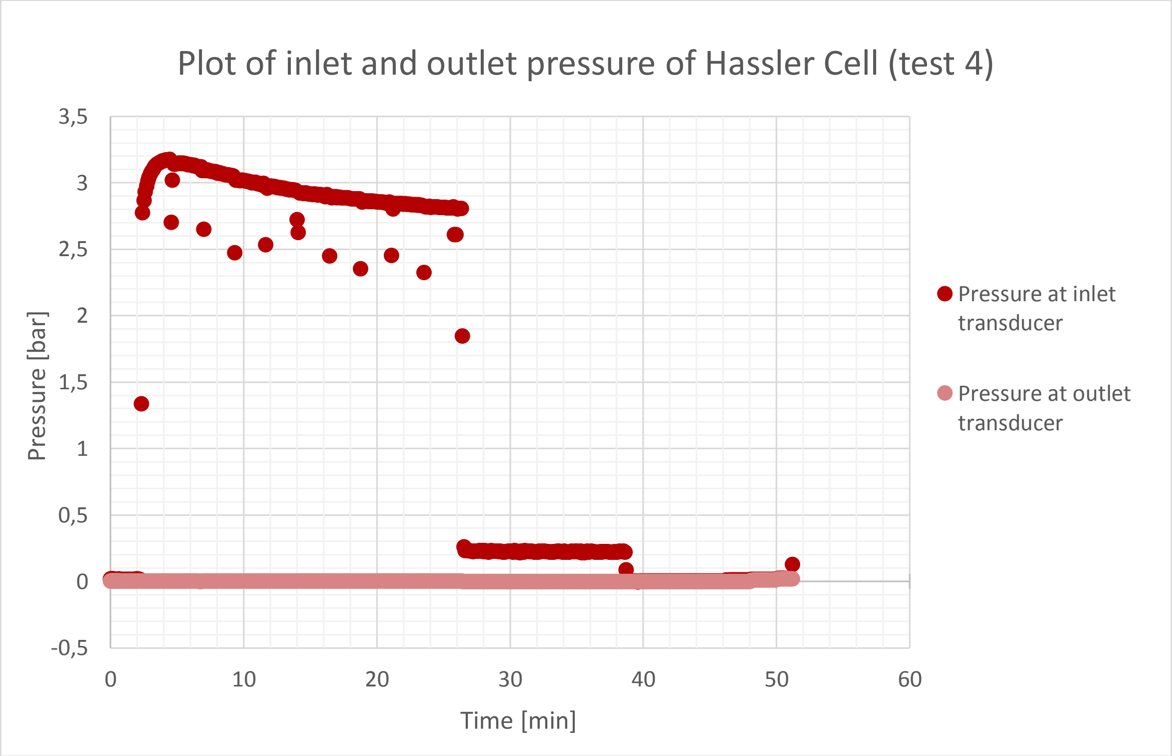

Figure 2-15: transducers pressure response during test 4, brine core flooding.

The recorded pressure in the plot shown above, has the same trend as the one in Figure 2-13: aside from some scattered points caused by the volumetric behaviour of the pump, and the initial adjustment of the flow, it is possible to extrapolate the two average pressures, at both the inlet and the outlet transducers, during the flow of two different fixed flow rates. The results are displayed in Table 2-13:

---

[15] During an imbibition process the saturation of the rock in its wetting phase increases, as the wetting phase fluid invades the rock pores and displaces any other fluids.

$Flow\ rate\ \left[{}^{mL}/_{h}\right]$	$P_{in}\ [bar]$	$P_{out}\ [bar]$	ΔP
240	2,81	0,001	2,809
20	0,241	0,001	0,24

Table 2-13: average registered pressure at the inlet and outlet transducers during test 4, brine flooding, with the respective flow rate.

The values of the pressure differences and the values of the flow rates can be used within Darcy's law, equation (2.4), to obtain the end-point effective permeability of the water. The results for such operation are illustrated in Table 2-14, below:

$End-point\ brine\ effective\ permeability\ [mD]$	
$K_{b,1}\ at\ 240\ \left[{}^{mL}/_{h}\right]$	10,53
$K_{b,2}\ at\ 20\ \left[{}^{mL}/_{h}\right]$	10,27
$K\ (average\ permeability)$	**10,40**

Table 2-14: the table illustrate the computed permeability after test 4, brine flooding, as K_1 and K_2. The last row contains the average absolute permeability to brine of the core sample.

A comparison between the results illustrated in Table 2-8 and in the one shown in Table 2-14, indicates the end-point permeability of brine and the absolute permeability of brine are extremely similar. This is due to the fact that residual gas saturation of the rock is very small, and even though little gas is still present within the core during the imbibition process, it poses very little, or no resistance to the flow of water, due to its compressibility and the fact that it is not the wetting phase. At this point is possible to evaluate the residual gas saturation. Anyway this operation is just an end in itself, thus it is not accomplished. Additionally it is possible to estimate that its value would be very small since, considering the previous statements, the brine flow is unaffected by it.

Test 5: P100 solution, at 500 ppm weight, injection.

During this coreflooding test the pump is used to squeeze the RPM solution out of a buffer volume, like a syringe, called transfer cylinder, see Figure 2-10, that contains about 200 $[mL]$ of solution, and into the core. The flow rate is set to be around 20 $\left[{}^{mL}/_{h}\right]$. Since the average pore radius, as reported in Table 2-2, is very close to the polymer particles diameter, see Figure 1-5, the pressure response during polymer flooding is expected to occur immediately.

Figure 2-16 illustrates such a plot, where the polymer injection is carried on for over than 6 pore volumes.

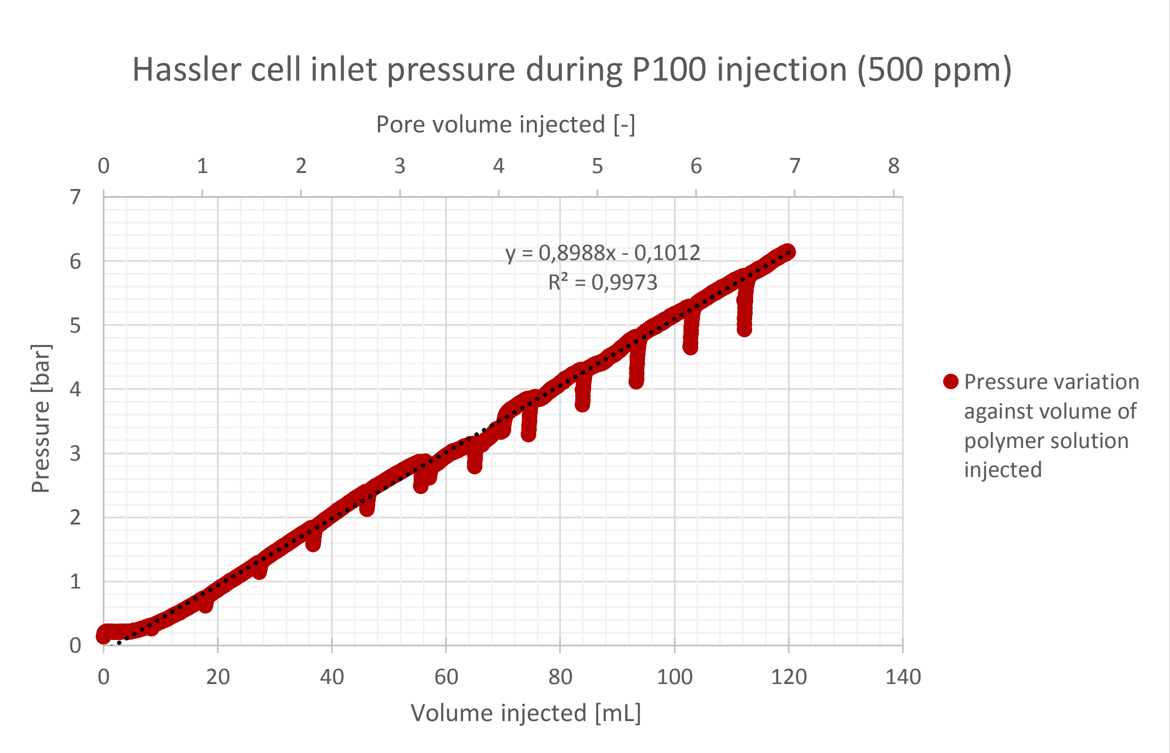

Figure 2-16: pressure response at the inlet pressure transducer during the injection of P100 at a concentration of 500 ppm w/w.

Aside from an initial step that might be due to the variation of the viscosity of the injected liquid, and looks like an entry pressure, the plot of Figure 2-16 shows a very clear linear trend. As a matter of fact the R-squared value is high enough to justify the previous statement. Its value would be even higher if it wasn't for the local minimum peaks due to the volumetric behaviour of the pump. This comportment differs very much from the expected one described in this paragraph, section ‘Coreflooding: test overview’. This suggest that a steady filtration is occurring and that the polymer is retaining within the pores with some other mechanism aside from adsorption. A multi-layered adsorption can be ruled out since the P100 is polyacrylamide based, which is apolar. There might be a surface plugging effect, but this would result in an exponential trend, anyway this hypothesis can be ruled out with the next test. A plausible cause of this trend might be the mechanical entanglement between polymers due to the low pore throat size. If this is the case, the injection of a more concentrated solution would cause a similar trend in the pressure response, but with a higher slope. Furthermore a mechanical entanglement would result in some outflow of the polymer during the post-treatment flushing of brine. As a matter of fact the process of adsorption can be somehow considered irreversible, while the mechanical bonds between polymers could be dissolved due to the attrition exerted by the brine flow. Anyway, a long term injection of the polymer is expected to cause a plugging in the core. This results do not necessarily imply that the RPM solution is not effective, as more test are required to asses such a statement, but simply that the polymer has a poor injectivity if used on sandstone with very small pore diameters.

Test 6: brine end-point effective permeability after polymer injection at 500 ppm weight.
The next step of the coreflooding sequence consist in injecting brine to evaluate the permeability reduction effect of the previous treatment, if such effect is noticed at all. The system layout is the same one as for test 4, therefore the only variation form the previous test is that the pump is directly connected to the cell instead of stepping through the buffer used to inject the polymer solution. Once more the pressure transducers calibrated before commencing any other injection operations.

Figure 2-17 illustrates the pressure response after test number 6:

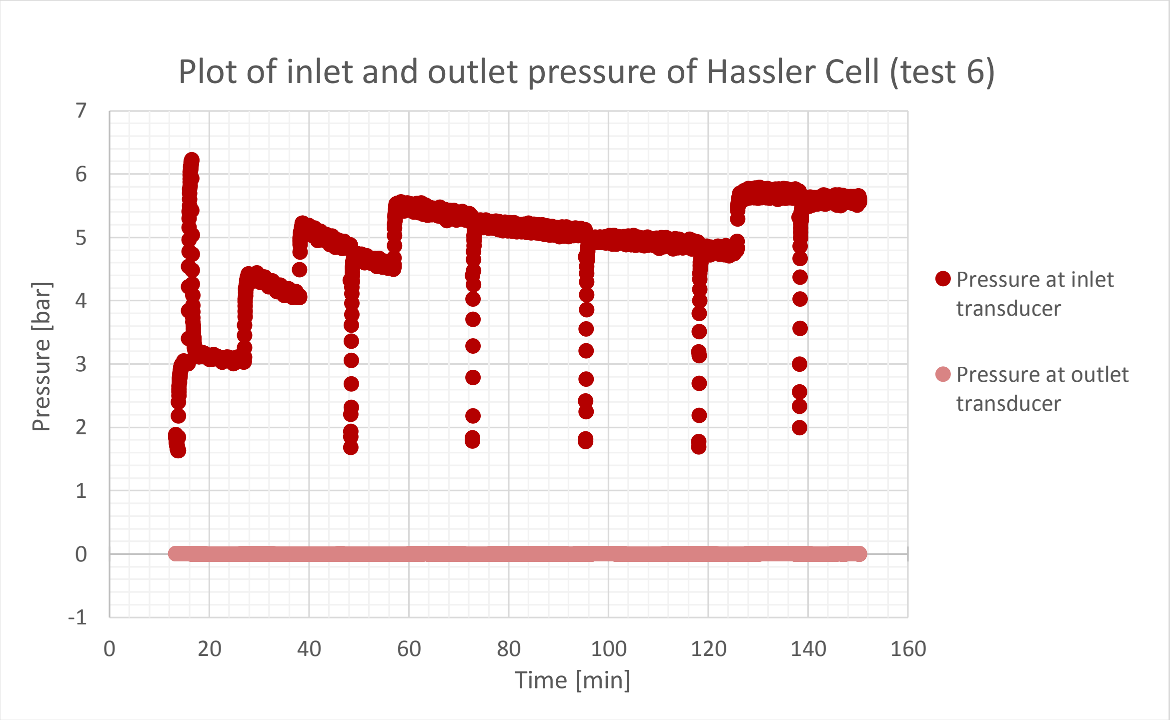

Figure 2-17: transducers pressure response during test 6, brine core flooding.

The plot shows once more the minimum peaks due to the volumetric pump behaviour. Additionally the flow rates steps do not seems to be stable around a fixed value of pressure, and this could indicate an out flow of some of the product, especially during the initial stages. Still, the real difference between this plot and the plots of both Figure 2-15 and Figure 2-13 can be appreciated observing Table 2-15:

$\boldsymbol{Flow\ rate}\ \left[{}^{mL}/_{h}\right]$	$P_{in}\ [bar]$	$P_{out}\ [bar]$	ΔP
5	1,63	0	1,63
10	3,01	0	3,01
15	4,05	0	4,05
20	4,5	0	4,5
25	4,74	0	4,74
30	5,57	0	5,57

Table 2-15: average registered pressure at the inlet and outlet transducers during test 6, brine flooding, with the respective flow rate.

The pressure difference, while flushing a few tens of millilitres every hour, is the same one as it was before the polymer injection while flushing a few hundreds of millilitres every hours. This behaviour may be due to two different causes: the first cause is that the polymer adsorbed onto the pores surface and it is operating its permeability reduction effect; the second cause is that the polymer did not enter the rock pores and plugged the inlet surface of the core. A third scenario may be due to the fact that the polymer plugged some pore channels inside the core and this would result in a permeability reduction of both the water and the gas. This scenario can only be excluded by computing the new end-point water effective permeability, and comparing it with the new end-point gas effective permeability. This operation is carried out in the next test. Anyhow, if the first scenario is the real one, then it is possible to use Darcy's law to compute the new permeability after the treatment, which is displayed in Table 2-16:

$End - point\ brine\ effective\ permeability\ after\ P100\ at\ 500\ ppm\ [mD]$	
$K_{b,1}\ at\ 5\ \left[{mL}/{h}\right]$	0,38
$K_{b,2}\ at\ 10\ \left[{mL}/{h}\right]$	0,41
$K_{b,3}\ at\ 15\ \left[{mL}/{h}\right]$	0,46
$K_{b,4}\ at\ 20\ \left[{mL}/{h}\right]$	0,55
$K_{b,5}\ at\ 25\ \left[{mL}/{h}\right]$	0,65
$K_{b,6}\ at\ 30\ \left[{mL}/{h}\right]$	0,66
$K\ (average\ permeability)$	**0,52**

Table 2-16: the table illustrates the computed permeability after test 6, brine flooding, as K_1, K_2…K_6. The last raw contains the average absolute permeability to gas of the core sample.

On the other hand it is necessary to rule out any possibility that a surface plugging effect of the polymer is occurring. In order to do this the direction of the flow is inverted so that surface supposed to be plugged becomes the outlet one. With this new layout, if this case scenario is plausible, the inlet pressure transducer should register a much lower pressure difference. Before flooding the core it is also necessary to switch the new inlet pressure transducer from the previous 2 $[bar]$ to the 20 $[bar]$ one, while for the new outlet transducer it is the opposite. Of course it is also necessary to exchange the pump with the sample collector and vice versa. Once the new equipment setup is arranged, and the pressure transducers are calibrated, is possible to begin the backflow test. The pressure response on this second part of the experiment is illustrated in the following picture:

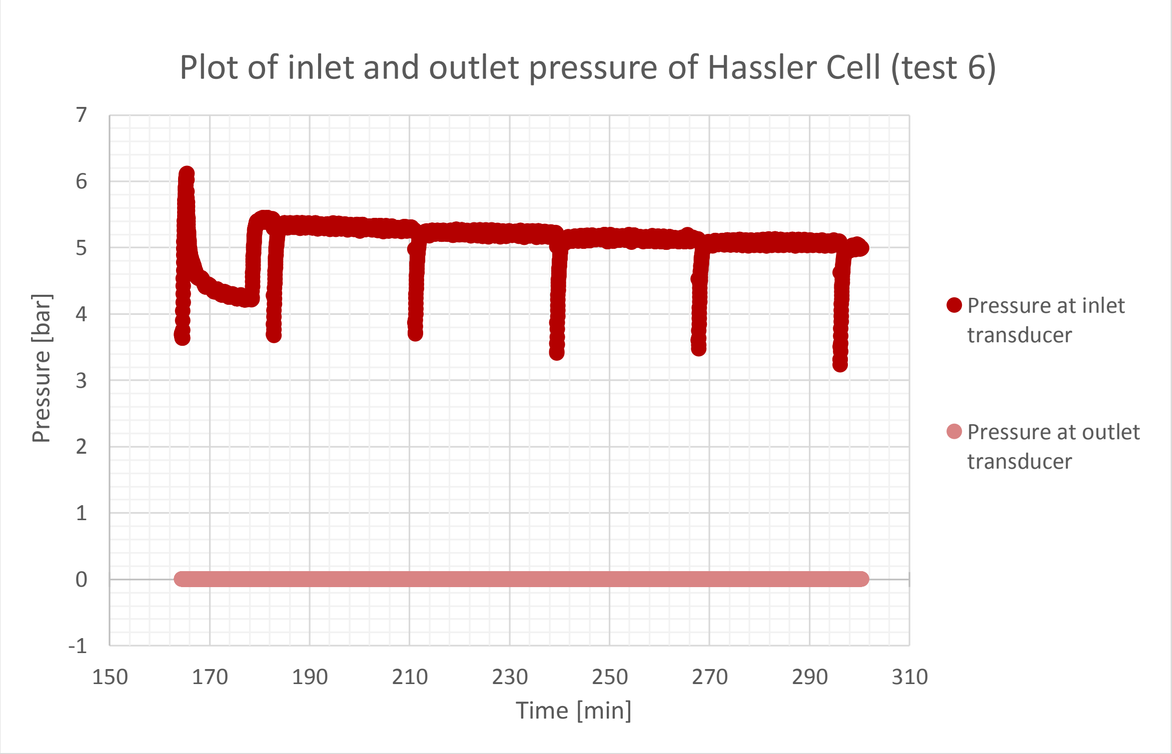

Figure 2-18: transducers pressure response during test 6, backflow brine core flooding.

This time it was only necessary to flood with two different flow rate to verify the previous result: 15 $\left[{}^{mL}/_{h}\right]$ and 20 $\left[{}^{mL}/_{h}\right]$. The plot still shows a very high pressure difference if compared with the one obtained during test 4. This preliminary statement suggests the surface plugging effect could be ruled out, while the inside plugging of the core is still a possibility. Furthermore the pressure seems to slightly drop as the brine is flowing through the core, this is another hint of the possible outflow of some of the non-adsorbed polymer.

Nevertheless the following table, Table 2-17, show the obtained results:

$\boldsymbol{Flow\ rate\ [^{mL}/_{h}]}$	$\boldsymbol{P_{in}\ [bar]}$	$\boldsymbol{P_{out}\ [bar]}$	$\boldsymbol{\Delta P}$
15	3,63	0	3,63
20	4,99	0	4,99

Table 2-17: average registered pressure at the inlet and outlet transducers during test 6, backflow brine flooding, with the respective flow rate.

With this data is once again possible to evaluate the permeability of the core sample, after the polymer injection, using the Darcy’s law. Table 2-18 shows the backflow permeability of the core sample:

$\boldsymbol{Backflow\ end-point\ brine\ effective\ permeability\ after\ P100\ at\ 500ppm[mD]}$	
$\boldsymbol{K_{b,1}\ (backflow) at\ 20\ [^{mL}/_{h}]}$	0,51
$\boldsymbol{K_{b,2} (backflow) at\ 20\ [^{mL}/_{h}]}$	0,58
$\boldsymbol{K\ (average\ \ backflow\ permeability)}$	**0,53**

Table 2-18: the table illustrate the computed permeability after test 6, brine flooding, as K_1, K_2. The last raw contains the average absolute permeability to brine of the core sample.

The permeability obtained during the backflow core flooding is in accordance with the previous one, Table 2-16, thus it indicates that there is no surface plugging effect and that the polymer treatment may have actually caused an effective water permeability reduction, or the plugging is simply not situated on the surface but inside the core.

Test 7: gas end-point effective permeability after polymer injection at 500 ppm weight. This test aims at establishing if P100 operated, during the previous test, a disproportionate permeability reduction to water, or it has simply in-depth plugged the core, eventually reducing the overall permeability. This can be simply verified by evaluating, once more, the end-point effective permeability of the gas and comparing it with the one obtained during test number three, prior the RPM treatment. So, this phase is therefore a simple gas drainage, which can be carried out by setting the equipment with the same layout as during test 3. The imposed pressures at the inlet side of the Hassler cell are always 3 $[bar]$, followed by 5 $[bar]$, and in the end 7 $[bar]$. The pressure response obtained after calibrating the pressure transducers and flushing the gas through the core is depicted in Figure 2-19:

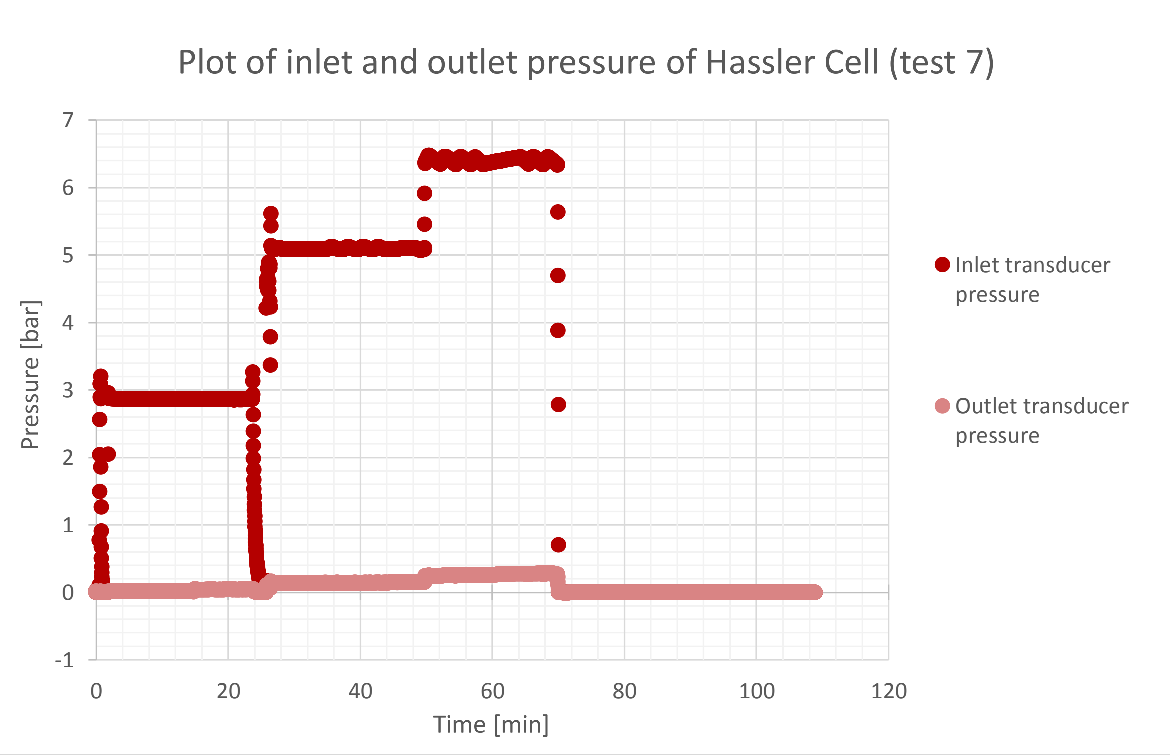

Figure 2-19: transducers pressure response during test 7, gas core flooding.

The plot above shows that the recorded value of the outlet pressure during test 7 are very much alike as the ones registered during test number three.

This consideration is quite unuseful if not supported by the value of the registered flow rate illustrated in the following table:

$P_{valve}\ [bar]$	$P_{in}[ata]$	$P_{out}[ata]$	$Displacement\ time\ [{}^{s}/_{L}]$	$Flow\ rate\ [{}^{mL}/_{min}]$
3	2,86	0,03	106,40	551,69
5	5,09	0,12	37,32	1622,35
7	6,35	0,26	22,90	2601,91

Table 2-19: flow rates measured during test 7, gas flooding

A comparison between these results and the ones obtained during the third test, reported in Table 2-10, shows similar flow rates with similar pressure differences. This means that the gas end-point effective permeability value shouldn't have changed much. Implementing Darcy's law, as in Table 2-20, confirm such a result:

$End-point\ gas\ effective\ permeability\ after\ P100\ at\ 500\ ppm\ [mD]$	
$K_{g,1}\ at\ 3\ [bar]$	17,58
$K_{g,2}\ at\ 5\ [bar]$	19,99
$K_{g,3}\ at\ 7\ [bar]$	21,91
$K\ (average\ permeability)$	**19,83**

Table 2-20: the table illustrate the computed permeability after test 7, gas flooding, as K_1, K_2, and K_3. The last row contains the average absolute permeability to gas of the core sample.

This result confirms that the third case scenario opened up after the polymer injection, suggesting an in-depth core plugging, can be ruled out since the original end-point effective gas permeability is left unchanged. Therefore the only reasonable explanation for the steady growing pressure response during the polymer injection is a mechanical entanglement of the polymers chains that block the pore channels. Anyway, these blocks, as explained in Chapter 1, can be temporarily undone by the gas flow.

Test 8: brine end-point effective permeability after polymer injection at 500 ppm weight. This test is a repetition of test number 6 and it is necessary to establish if the channels exposed by the flow of gas are just temporary or can also be used by water. The equipment layout and the testing procedure have already been explained. Eventually there's no need in showing the plot of the transducers pressure response, while a table containing the results is due:

$\boldsymbol{Flow\,rate}\left[{}^{\boldsymbol{mL}}/_{\boldsymbol{h}}\right]$	$\boldsymbol{P_{in}}\,[\boldsymbol{bar}]$	$\boldsymbol{P_{out}}\,[\boldsymbol{bar}]$	$\boldsymbol{\Delta P}$
60	1,42	0	**1,42**
120	3,21	0	**3,21**
180	5,4	0	**5,4**

Table 2-21: average registered pressure at the inlet and outlet transducers during test 8, brine flooding, with the respective flow rate.

Table 2-21 shows that for the same pressure difference obtained in test 6, see Table 2-15, the flow rates are higher. This imply that some of the original permeability to water may have been re-established. Using Darcy's law once more gives:

$\boldsymbol{End-point\ brine\ effective\ permeability\ after\ P100\ at\ 500\ ppm}\,[\boldsymbol{mD}]$	
$\boldsymbol{K_{b,1}\ \ at\ 60}\left[{}^{\boldsymbol{mL}}/_{\boldsymbol{h}}\right]$	5,22
$\boldsymbol{K_{b,2}\ at\ 120}\left[{}^{\boldsymbol{mL}}/_{\boldsymbol{h}}\right]$	4,60
$\boldsymbol{K_{b,3}\ at\ 180}\left[{}^{\boldsymbol{mL}}/_{\boldsymbol{h}}\right]$	4,11
$\boldsymbol{K}\ (\boldsymbol{average\ permeability})$	**4,64**

Table 2-22: the table illustrates the computed permeability after test 6, brine flooding, as K_1, K_2 and K_3. The last raw contains the average absolute permeability to brine of the core sample.

The end-point water permeability significantly rose with respect the one evaluated right after the polymer injection, see Table 2-18. This may be due to the fact that the mechanical interaction between polymers have been, in some way, weakened during the gas flooding, and could not be restored during the second flush with brine. To overcome this problem there may be two solutions:

1. Trying to flood the core with a higher concentration of polymer solution may form a larger quantity of knotted polymers. This effect could be observed in a higher slope of the curve pressure against injected pore volume during the injection of a more concentrated polymer solution.
2. Using a weakly crosslinked polymer that guarantees a stronger bond between polymer chains, but presents more difficulties during the injection phase since it is necessary to keep the gelling process under control.

Test 9: P100 solution, at 1500 ppm weight, injection; followed by P100X100, at 4000 ppm weight, injection.

The aim of this phase of the coreflooding tests, is to assess whether the injection of a solution with higher concentration of polymer, or the injection of a crosslinked polymer, may or may not help enhancing the permeability reduction effect, with respect to the previous treatment, after the creation of pathways through the polymer/gel matrix by gas displacement. The equipment setup for both cases is the same used for the test number three and it won't be further discussed. The first step in this direction is to flush the core with P100 solution at $1500\ ppm$ weight. The starting point is manually set so that the pressure response curve starts from the origin. The pressure response measured by the pressure transducers, at a flow rate of $20\ \left[{}^{mL}\!/_{h}\right]$, is the following:

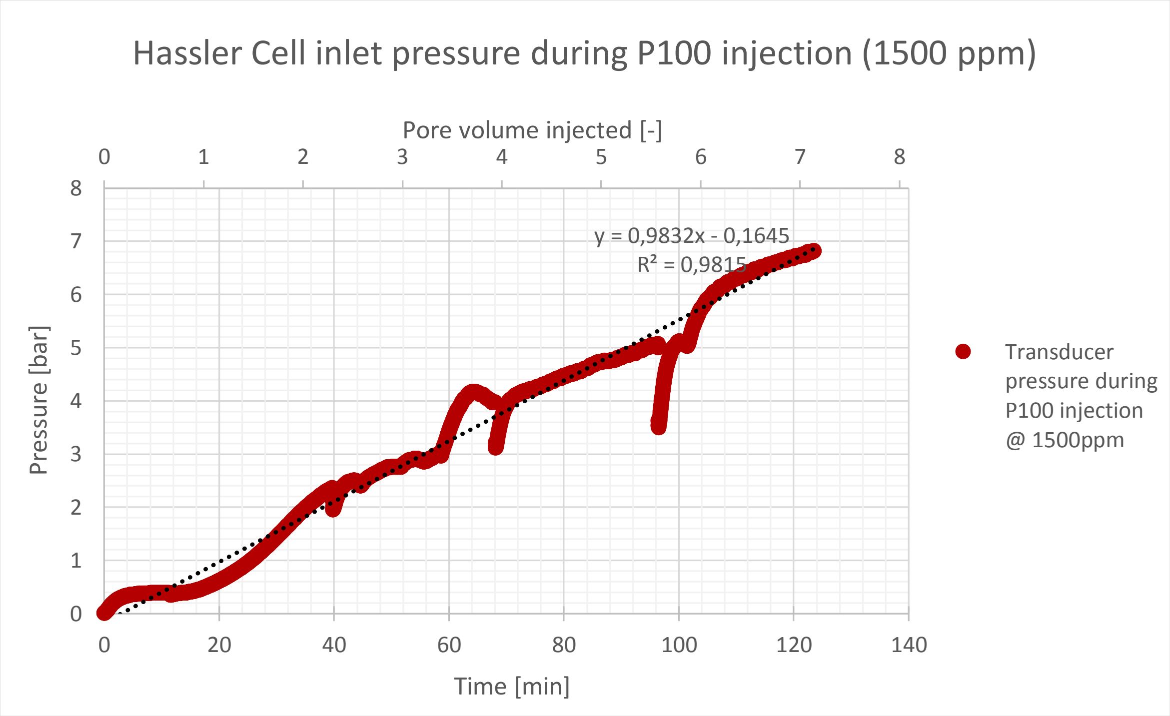

Figure 2-20: pressure response at the inlet pressure transducer during the injection of P100 at a concentration of 1500 ppm w/w.

The pressure response in Figure 2-20 appear to be quite unsteady, but such a behaviour is caused by the polymer transfer cylinder: the latter is a simple cylinder divided into two parts by a rubber diaphragm, which can slide along the axis of the cylinder; when the water, driven by the pump, enters one side, it moves the separator and pushes out, and into the core, the solution contained in the other half of the cylinder. This system may sometime show and elastic response when the diaphragm movement is shortly prevented or fastened. The result of this can be observed at the minute 64 and at the minute 96 after the polymer injection started: two maximum pressure peaks, caused by a diaphragm acceleration, are followed by two minimum pressure peaks caused by a sudden lack of pressure to support the dislocation of the fluids. Such an erratic behaviour can be caused by the presence of little bubble of air. Given this fact, it is possible to observe, comparing this result with the one obtained in test number 5, that the pressure responses are quite similar with the exception that in this case the slope of the curve is slightly higher due to the higher concentration of the polymer. This little variation justify the injection of a gel solution with the aim of creating a thicker and stronger matrix inside the pores. The product that is used to achieve this objective is the P100X100, which is a polyacrylamide based RPM that uses an organic crosslinker, X100, to form a gel. The minimum required concentration of P100, to obtain a gel, is of 4000 ppm. The sequence operated for the injection of this polymer is the one adopted the two previous time and the gel pressure response can be appreciated in Figure 2-21, where the starting point is once more forced to start from a pressure equal to zero. Since we expect a strong pressure growth during the injection of this last solution, a pressure transducer of 40 $[bar]$ is used to replace the previous 20 $[bar]$ transducer at the inlet of the Hassler cell.

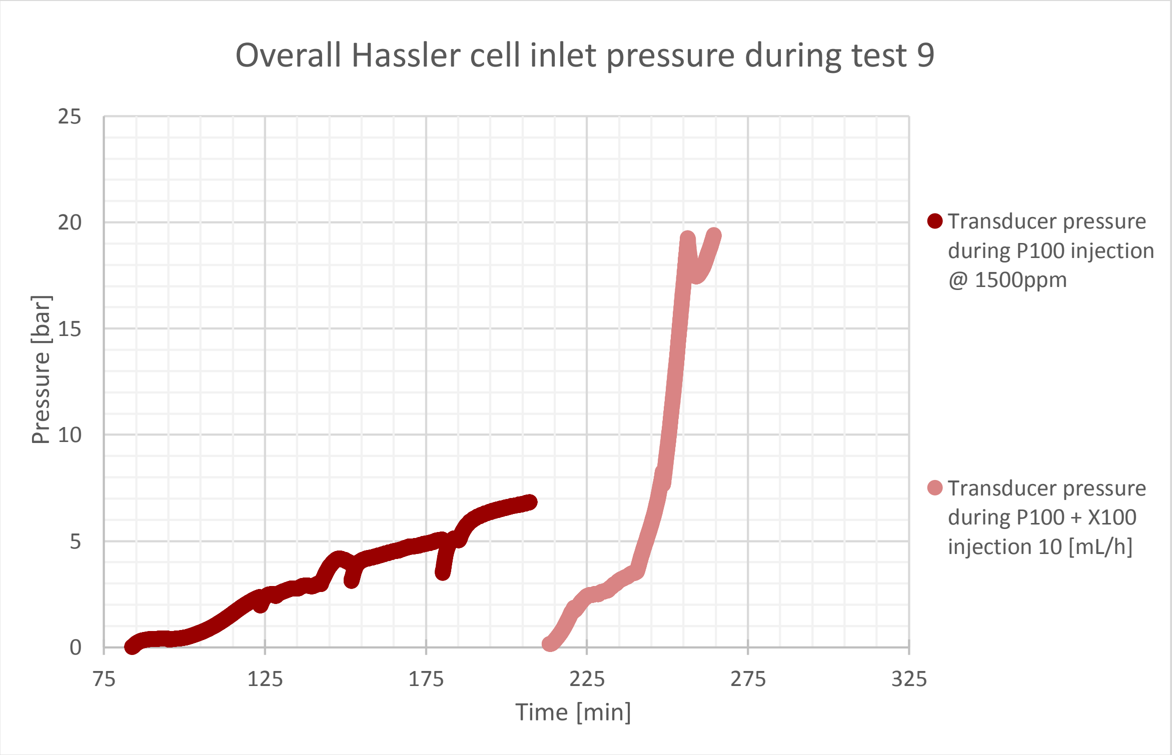

Figure 2-21: pressure response at the inlet pressure transducer during the injection of P100, first, at a concentration of 1500 ppm w/w, then, at a concentration of 4000 ppm w/w with an organic crosslinker called X100, in the end, the same as the latter but with reduced flow rate.

Figure 2-21 shows a collapsed plot of the RPM solution injection: the first curve, up to 205 minutes is the same as show in Figure 2-20, and illustrates the injection of the simple polymer at a concentration of 1500 ppm at a flow rate of 20 $\left[{}^{mL}/_{h}\right]$, while the second curve represents the injection of the crosslinked polymer at a flow rate of 10 $\left[{}^{mL}/_{h}\right]$. The second curve shows an initial, quite steep, but almost linear trend. This indicates that the polymer is flowing within the core and it is not plugging the surface, but it is indeed being retained inside the pores. About 25 minutes after the beginning of the second polymer injection there is a sudden change of the curve slope and this may be due to the gelling reaction or to a steady filtration completed plug. Either cases the crosslinked polymer is confirmed to have a stronger filling capability, and what remains to be verified is the possibility of re-establishing a certain permeability for the gas to flow, and also the degree of water permeability reduction, after this second treatment.

Test 10: gas end-point effective permeability after gel injection.

This coreflooding is necessary to test and eventually to restore, the gas permeability after the core has been plugged with a low crosslinked polymer gel. The gas injection sequence always includes three phases at different pressure, that are the ones already used in test number 1, test number 3 and test number 7. The equipment layout is, once more, the one which has always been used during gas injection (see previous gas test for a description). The elaborated data coming from the test are summarised in the following table:

$P_{pump}\ [bar]$	$P_{in}[ata]$	$P_{out}[ata]$	$Displacement\ time\ [s/L]$	$Flow\ rate\ [mL/min]$
3	2,93	0,04	106,43	567,30
5	5,02	0,1	46,1	1309,57
7	6,4	0,18	31,59	1932,99

Table 2-23: flow rates measured during test 10, gas flooding

The results illustrated in Table 2-23 suggest that the value of the gas permeability should have been left untouched. As a matter of fact the latter obtained results are very similar to the one previously obtained (see Table 2-11 and Table 2-20). Anyway the computed end-point gas permeability is the one depicted in the following table:

$End - point\ gas\ effective\ permeability\ after\ gel\ [mD]$	
$K_{g,1}\ at\ 3\ [bar]$	15,99
$K_{g,2}\ at\ 5\ [bar]$	16,50
$K_{g,3}\ at\ 7\ [bar]$	17,44
$K\ (average\ permeability)$	**16,64**

Table 2-24: the table illustrates the computed permeability after test 10, gas flooding, as K_1, K_2, and K_3. The last row contains the average absolute permeability to gas of the core sample

Table 2-24 confirms that the gas end-point effective permeability is unchanged after the gel treatment, meaning the gas is still able to create channels, within the gel matrix, that allow the formerly gas flow.

As after test number 3, weighting the core after this gas displacement, and comparing the measure mass with the mass measured after the brine injection, when the core was fully saturated with brine, gives an approximated value of the irreducible water saturation:

$Irriducible\ water\ saturation$	
$S_{w,irr}\ [-]$	**0,41**

Table 2-25: irreducible water saturation of the sandstone core before the polymer injection.

The value of the irreducible water saturation illustrated in Table 2-12, that is 0,29, and in Table 2-25 are just rough measures, but they clearly shows that RPM treatment, as thoroughly explained in chapter 1, increases their values. This is another confirmation that the polymer and the gel are, somehow, modifying the physical properties of the formation.

Test 11: brine end-point effective permeability after gel injection.

A further brine coreflooding is necessary to assess whether the injection of a gelling RPM instead of a simple polymer RPM, considering this core sample, can maintain a lower water permeability even after the gas channelled through the RPM matrix. Without further description of how this test is carried out, since it has been extensively discussed in the previous subparagraph, the data elaborated from the experiment are the following:

$Flow\ rate\ \left[{}^{mL}/_{h}\right]$	$P_{in}\ [bar]$	$P_{out}\ [bar]$	ΔP
20	2,06	0,041	2,019
30	3,25	0,041	3,209
40	4,43	0,041	4,389

Table 2-26: average registered pressure at the inlet and outlet transducers during test 11, brine flooding, with the respective flow rate.

Comparing these data with the ones obtained after test number 6 and after test number 8, see Table 2-17 and Table 2-21, it is clear that the water permeability value should be lower with respect to the one obtained after the first polymer injection, at 500 ppm, followed by gas displacement.

Table 2-27 show the new water end-point effective permeability evaluated with Darcy's law:

$End-point\ brine\ effective\ permeability\ after\ gel\ [mD]$	
$K_{b,1}\ at\ 20\ \left[{}^{mL}/_{h}\right]$	1,22
$K_{b,2}\ \ at\ 30\ \left[{}^{mL}/_{h}\right]$	1,15
$K_{b,3}\ \ at\ 40\ \left[{}^{mL}/_{h}\right]$	1,12
$K\ (average\ permeability)$	**1,16**

Table 2-27: the table illustrates the computed permeability after test 11, brine flooding, as K_1, K_2 and K_3. The last raw contains the average absolute permeability to brine of the core sample.

The value of this last water end-point effective permeability is three times lower than the one obtained after the injection of P100 solution at 500 ppm. This means that the matrix created by the gel is capable of reconditioning the permeability reduction effect, after the gas flooding, better than matrix created by polymer entanglement.

Coreflooding: Test overview and inference

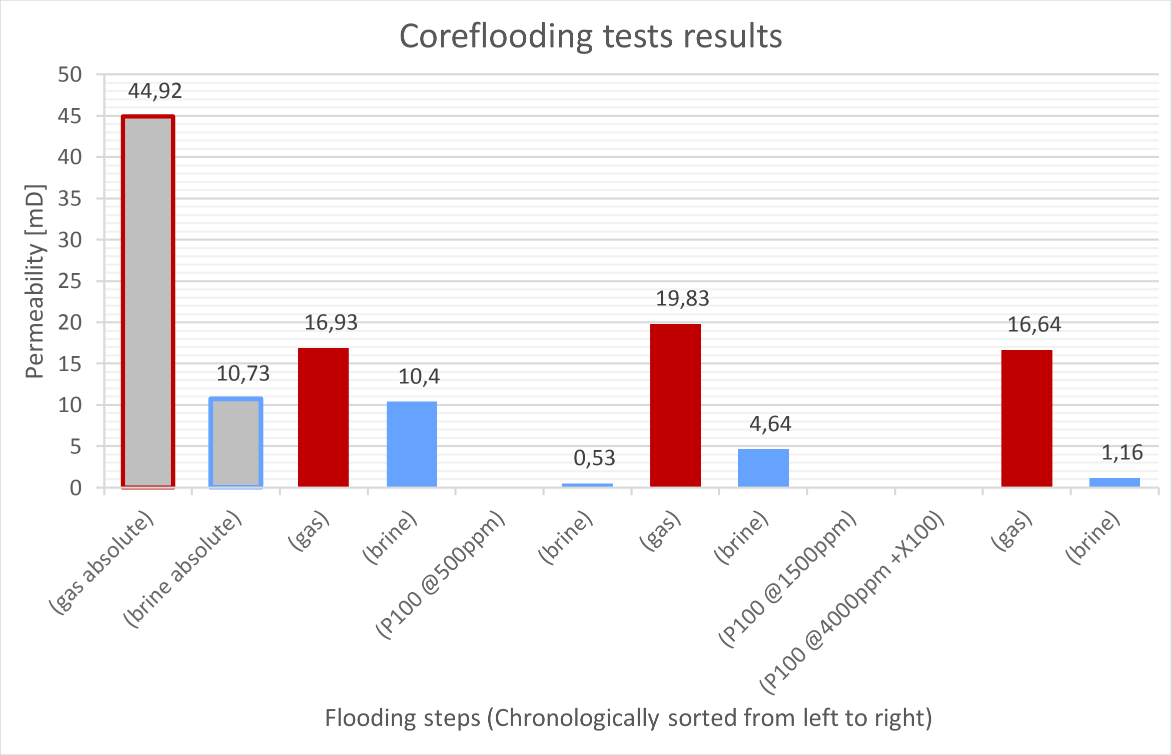

Figure 2-22 overview of the coreflooding tests results

The sequence of eleven coreflooding gives a clear overview of the core sample permeability behaviour: the following plot, Figure 2-22, summarises all the result obtained during the experiments. Each column in the graph represent the average permeability measure during a single coreflooding test. The first two columns, with grey filling, respectively indicate the absolute permeability to gas and two water. The red columns show the gas end-point effective permeability, while the blue columns show the water end-point relative permeability. It is evident that the gas permeability is pretty much left untouched by the RPM treatments. On the other hand the water effective permeability is drastically reduced when tested immediately after the polymer injection, while it appears to be only moderately reduced if measured after the gas flowed through the core. This performance has already been largely discussed in the previous subparagraph, but it is necessary to highlight that the gel can better withstand the gas flow, and later restore the water permeability reduction effect, rather than the simple polymer. This may be due to the fact that the gel matrix created by the crosslinkers is stronger, or has better elastic properties, than the matrix created by the mechanical entanglement of the polymer chains; meaning that once the gas is flushed and creates a preferential path to flow, when the water starts to flow back again, the gel matrix undergoes some sort of expansion, due to its hydrophilic properties, that is more extended than the one obtained with the simple polymer. As a matter of fact the crosslinkers create a solid-like structure that is more rigid, while the structure created by the mechanical entanglement of the polymer can be modified, for example compressed, more easily during the gas flow. This would also explain the higher value of the effective gas permeability after the injection of the first polymer solution with low concentration.

Given these statement it is finally possible to evaluate the residual resistance factor for the water and for the gas, computed with equation (2.1) and equation (2.2). The following tables, Table 2-28 and Table 2-29, illustrates their values:

$\boldsymbol{Gas\ residual\ resistance\ factor}\ [-]$	
$\boldsymbol{F_{rrg}\ (after\ polymer\ injection)}$	0,85
$\boldsymbol{F_{rrg}\ (after\ gel\ injection)}$	1,02

Table 2-28: Gas residual resistance factor evaluated both after the polymer injection, at 500 ppm, and after the gel injection

$\boldsymbol{Water\ residual\ resistance\ factor}\ [-]$	
$\boldsymbol{F_{rrw}\ (after\ polymer\ injection)}$	2,24
$\boldsymbol{F_{rrw}\ (after\ gel\ injection)}$	8,96

Table 2-29: Water residual resistance factor evaluated both after the polymer injection, at 500 ppm, and after the gel injection

It is obvious that the permeability reduction effect of the crosslinked polymer, gel, is much higher than one obtained with the simple polymer. As for the permeability of the gas the residual resistance factors indicates that it doesn't change much. The problem is that the injectivity of the gelling solution is very low, as can be seen from the high slope of the second curve in Figure 2-21. A solution with such a low injectivity is difficult to pump downhole if the target radius of the treatment is extended. The risk associated with this operation is to damage the formation: fracturing. Therefore the practice of gel injection, during the treatment of the wells in the Adriatic see, is only advisable when the pressure response during the polymer injection is very low.

The last note regards the value of polymer adsorption during the polymer and the gel injection, which is assessed around $200\ \left[{}^{\mu g}/_{g}\right]$, expressed as mass of gel adsorbed on a mass of rock with the same properties as the core samples from the wells in the Adriatic sea [24].

CHAPTER 3

ANALYSIS OF ENI TREATED WELLS

Once the behaviour of the RPM polymer solutions have been assessed, it is possible to better comprehend the effect that they may have when used within a real reservoir. Indeed this chapter argues about four ENI wells that have been treated with the RPM. The structure of the description is the following. First, the characteristic of each one of them, such as the formation and the completion specific, will be largely discussed. Then the data collected during the polymer injection will be presented and argued using a collapsed plot showing the registered well head pressure against time, the injection rate against time, and also their ratio versus time. The last information that will be debated is the production history of gas and water both before and after the RPM treatment to understand the outcome of the latter. Anyway it is important to notice, once again, that all the treated wells are exclusively gas producing wells. Following this introduction of the above, a broad discussion and calculation are due to introduce and debate the conclusion presented in the following chapter.

Moving from the analysis of a laboratory core to the analysis of a real formation, it is inevitable to introduce many variables and even more approximations. The main hypothesis used during the following analysis are:

- The reservoir layers are homogeneous, meaning that they are characterized by a uniform distribution of the permeability. This is a somehow good hypothesis, since the Adriatic Sea wells generally consist of a series of thin layers, which is also the reason why a bullhead treatment is required to achieve a water mitigation treatment.

- The polymer adsorption is ideal, and all the injected polymer is adsorbed in the near wellbore area in accordance to the adsorption level indicated in the previous chapter: $200\ [{}^{\mu g}/_{g}]$.
- The polymer solution that lingers in the string, in the casing below the packer, and the already treated formation, after the polymer injection I completed, is displaced by nitrogen injection and is completely adsorbed. Where the nitrogen pumped downhole after the polymer injection is necessary to reconnect the well to the gas within the formation.
- The well produces in a steady state condition. A condition of pseudo steady state is generally assumed, but since the time interval before and after the treatment is very limited if compared to the life of a well, this hypothesis appears to be reasonable.

Additionally it is required to take into account that all the gathered data may suffer from a certain degree of errors since, from time to time, they can be overseen. This is the reason why the author, when it is appropriate, and has the means to do it, would re-evaluate certain characterizing parameters of the formations. For example the value of the water effective permeability of the formation will be evaluated in accordance with the hypothesis previously presented.

The RPM treatments performed on the four different well, always follow the same procedure that was suggested by the service company and includes:

- The pickling[16] of the string to remove rust and other particle from the string itself.

---

[16] The pickling process uses a relatively weak, inhibited acid to remove scale, rust and similar deposits from the internal surfaces of equipment such as treating lines, pumping equipment or the tubing string through which an acid or chemical treatment is to be pumped. The pickling process removes materials that may react with the main treatment fluid to create undesirable secondary reactions or precipitates damaging to the near-wellbore reservoir formation [34].

- An injection test, performed with the RPM solution at a very low concentration of polymer $(200\ ppm)$, to verify the well capability of undergoing the RPM treatment within a reasonable period of time, and without any risk of premature plugging.
- An eventual acid injection to be performed if the injection test revealed a poor injectivity.
- An injection phase of the polymer solution to be executed with increasing polymer concentration over time, with the aim of quickly reaching the maximum achievable pressure drop, thus the maximum disproportionate permeability reduction effect.
- A nitrogen displacement of the liquid in the string and in the near-wellbore formation, as previously stated, to reconnect the gas zone of the formation with the well.

The quantity of polymer solution injected, both during the injection test and the treatment itself, and the quantity of acid, when it is necessary, varies from well to well with respect to the height of the pay zone.

3.1 - CASE 1: POZZO 1 C

In this first case the considered well is Pozzo 1 C, which is the same well the core sample used in the laboratory tests came from, see chapter 2. It is located off-shore in the Adriatic Sea and it has been perforated and completed, as a short side-track of a main well, between June and September 2010. The perforated interval of the well has been producing without any problem until July 2011 when sand started flowing along the gas and the water. To mitigate the problem of sand production, the top-head well components and the well-sand separator were reinforced. Anyway the increasing water production, thus the sand production that comes with it, led to the choice of performing an RPM treatment in order to mitigate the water production and consolidate the near-wellbore sand. The treatment was performed at the end of February 2014.

The procedure followed during the injection is the one explained in the introduction of chapter 3 and, since the injection test proved a slightly poor injectivity of the polymer solution, an acid treatment was performed to restore the well, gas and water, permeability. The acid used to restore the formation was formic acid, which is the only one compatible with the Adriatic Sea formation. Additionally, before starting the polymer injection, a sand cleansing was done by coil tubing.

Preliminary data from the well indicates properties very similar to the ones reproduced in laboratory, even though there are slight variation to them. The following table, Table 3-1, summarizes these parameters and will be presented for every study case that follows this one:

Pozzo 1 C, properties	
Water permeability $[mD]$	2,1
Temperature $[°C]$	43
Salinity $\left[{}^{g}/_{L}\right]$	3
Static top head pressure $[bar]$	169,2
Reservoir pressure $[bar]$	200,5
Perforated casing lenght $[m]$	6,5
Top vertical height of the perforation $[m]$	6,1
Numbers of separated layer $[-]$	2

Table 3-1: Pozzo 1 C preliminary properties.

To have a complete set of information regarding the well, Figure 3-1 illustrates a seismic log of the formation giving an insight on the pay zone, thus the perforated depth:

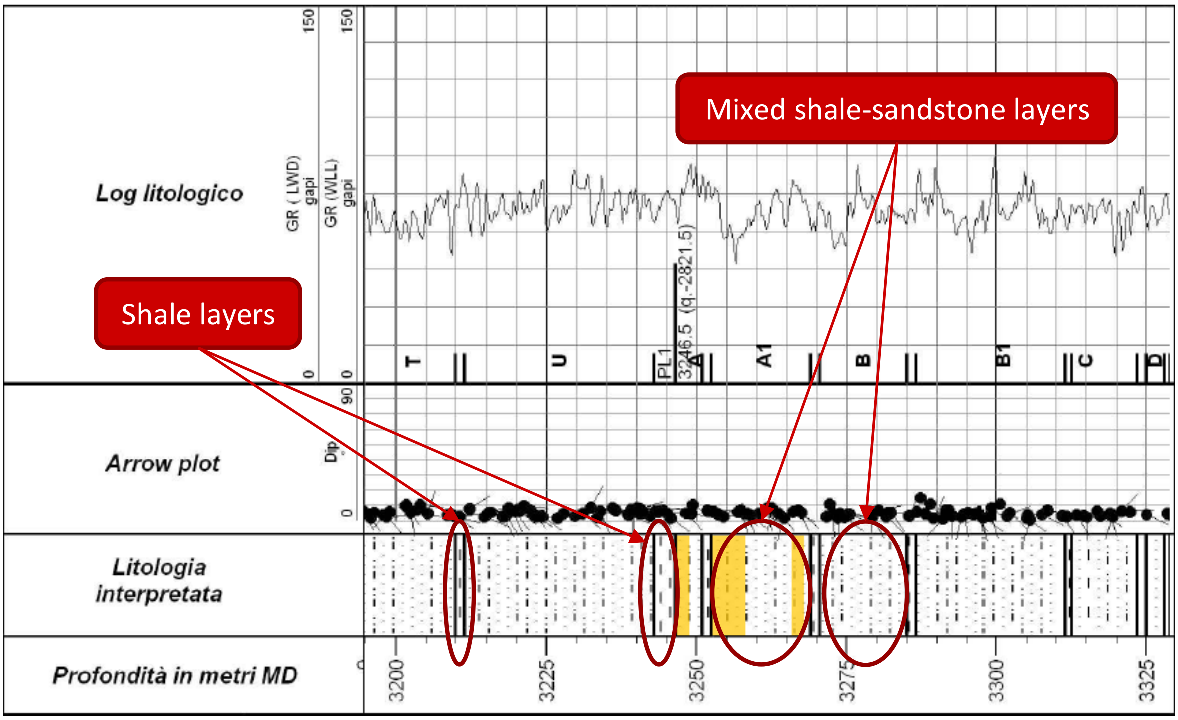

Figure 3-1: Pozzo 1 C seismic log schematic, the orange highlighted areas indicates the perforated interval. Image from ENI archives.

From the data illustrated above it is possible to notice that the salinity of the formation is a bit higher than expected, about 33 %, while the permeability is 5 times lower than the one calculated from the core used for the laboratory tests. As stated in chapter 2, it is necessary to take into account that the core form Pozzo 1 C are artificially reproduced in laboratory in order to have a properties similar to the reservoir one, still such a big difference justify a second evaluation of the reservoir average permeability. This operation is carried out, once more, using the Darcy's law, and will be illustrated further in this paragraph. Furthermore, when it is possible, the evaluation of the permeability will be repeated for each well to acknowledge and verify the provided data. On the other hand, from the seismic log, it is possible to see that the formation was perforate in three different zones of mixed shale and sandstone, where two of them may be vertically connected, while the third one, situated on top of them, is certainly isolated from the others by a shale layer. Isolated layers might be a hint of different permeability, still, in accordance with the hypothesis presented in the introduction and for the sake of simplicity, they are considered homogenous. These consideration will be useful further in the paragraph during the evaluation of the treatment.

In light of the previous statements it possible to proceed and introduce the data collected during the main treatment phase, which included the injection of 5 tanks, each one with a volume of 8 $[m^3]$, of polymer solution at different polymer concentration. The polymer used for the treatment was different with respect to the one used in the laboratory tests and more adapt to a lower permeability to water but, accordingly to the service company, with the same behavior.

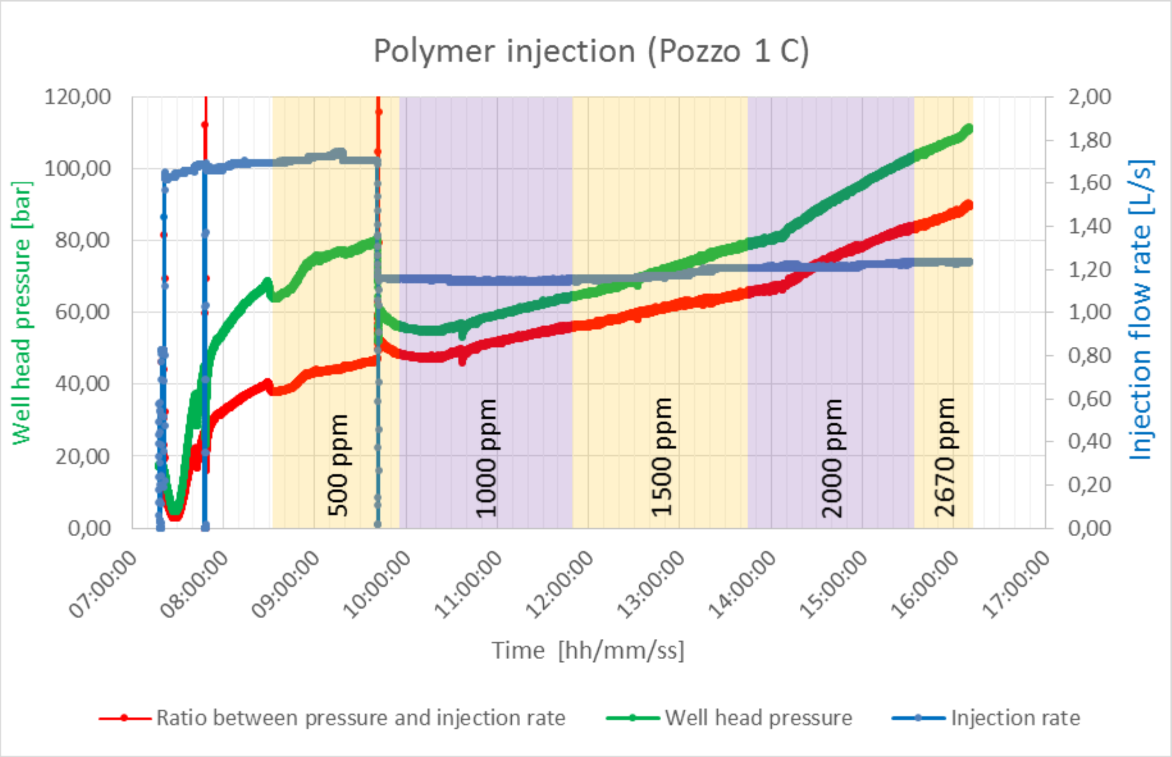

Figure 3-2: Injection rate, well head pressure and their ratio during the polymer injection phase of Pozzo 1 C. Data provided by ENI.

Figure 3-2 illustrates the registered well head pressure, green, and the injection rate, blue, versus time, during the polymer injection phase. The red curve is obtained as a punctual ratio between the pressure and the flow rate during the injection, and it is an easy-to-read curve which can be quickly compared with the one obtained during the test, since the injection rate used in laboratory was constant. The shaded orange and purple areas indicates the time interval at which the polymer solution, at a certain concentration, first reaches the formation. The border between one shaded area and the other indicates when one slug of polymer has completely entered the formation, and the following slug is about to enter it: since the polymer slugs are injected one after the other, the shaded areas are consecutives. From Figure 3-2 is possible to see that the treatment consisted of five different steps, each one of them is characterized by an increase of $500\ ppm$ of polymer in the polymer solution. If the normalized red curve is taken into account, it is possible to see that the pressure profile is quite linear aside from an initial rump-up, due to the string being filled with liquid, and a slope variation around $14:10:00$. This unexpected change of trend doesn’t seem to be connected to any operations performed on the platform, thus it may only be due to some heterogeneity within the reservoir. The still linear trend that follow this variation suggests that whatever occurred didn’t affect the polymer solution behavior, but it only changed its effectiveness. From Figure 3-2 can be inferred that the polymer treatment produced a pressure response very similar to the one obtained in laboratory, with the only difference that the change in polymer concentration didn’t really affect the pressure against time slope. The only change of slope in the curve happened at a random time, aside from the transitory occurred when the polymer reached the formation and when the injection rate was diminished, and not at the border between shaded areas.

The polymer treatment is therefore expected to have worked properly as can be seen from the following figure that illustrates the production history before and after the treatment:

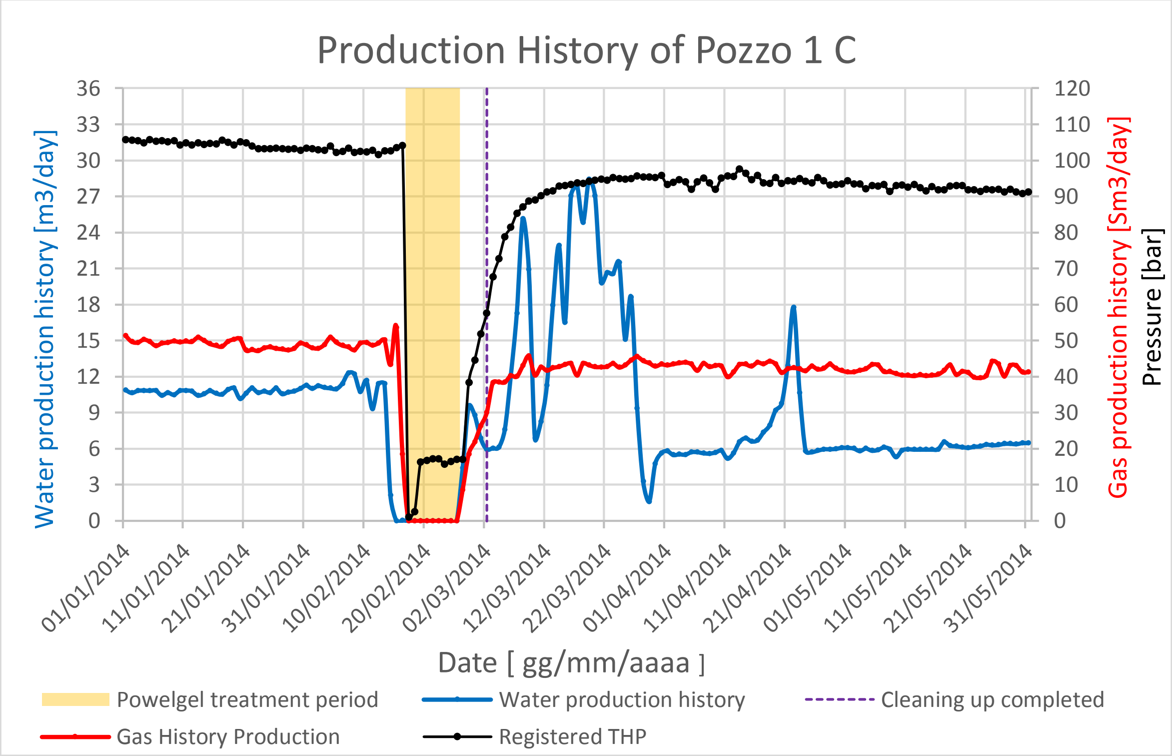

Figure 3-3: Pozzo 1 C production history. The blue line refers to water, the red line refers to gas, while the black line indicates the top well head pressure. The yellow shaded area indicated the treatment period. The dotted vertical line indicates the backflow of all the injected water from the polymer solution. Data provided by ENI.

Figure 3-3 clearly shows that the water production rate after the treatment is halved. The anomalous trend of the water production rate right after the treatment, is connected with a malfunctioning of the water-gas separator, due to an accumulation of gasoline in it. Therefore the value of the water flow rate to be considered is the stabilized one obtained around the month of May. The overall pressure drop may be linked to the permeability reduction effect operated by the adsorbed polymer, thus the increase of pressure losses across the near-wellbore area of the reservoir. The following table illustrates the average production parameters of the well before and after the treatment:

$\boldsymbol{Pre - treament\ data}$			$\boldsymbol{Post - treatment\ data}$		
$\boldsymbol{Q_g\left[{Sm^3}/{day}\right]}$	$Q_w\left[{m^3}/{day}\right]$	$FTHP\ [bar]$	$Q_g\left[{Sm^3}/{day}\right]$	$Q_w\left[{m^3}/{day}\right]$	$FTHP\ [bar]$
50 000	11	102	45 000	6	95

Table 3-2: Pozzo 1 C production parameters before and after the RPM treatment.

At this point it would be interesting to evaluate the permeability value before and after the treatment, and subsequently calculate the residual resistance factor, thus the permeability reduction. The integration of Darcy's law for a radial geometry and for a steady state flow gives:

$$k_{eff,w} = \frac{q_w\, B_w\, \mu_w}{(P_r - P_w)\, 2\, \pi\, h} \ln \frac{r_r}{r_w} \tag{3.1}$$

Where the unknown parameter is $k_{eff,w}$, the effective permeability of the formation to water. While q_w is the water flow rate, B_w is the water formation volume factor, μ_w is the viscosity of the formation water at reservoir condition, P is the pressure, r is the radius and h is the height of the pay zone. The subscripts r and w, respectively stand for reservoir and well. Before the polymer treatment all the parameters are known, or can be easily obtained, so the permeability can be computed. After the treatment it is always possible to evaluate the new permeability using Darcy's law, but it is required an iterative calculation that keeps adjusting the permeability until the well pressure reaches its real value after the treatment. Furthermore it is necessary to consider that the treatment does not extend through all the reservoir, but it only affect a limited radius around the wellbore. The equation necessary to carry out this iteration is the following:

$$P_w = P_r - \frac{q_w\, B_w\, \mu_w}{2\, \pi\, k_{eff,w}\, h} \ln \frac{r_r}{r_m} - \frac{q_w'\, B_w\, \mu_w}{2\, \pi\, k_{eff,w}'\, h} \ln \frac{r_m}{r_w} \tag{3.2}$$

Where the apex indicates that the marked parameter refers to its value after the treatment, while the subscription *'m'* denotes the radial extension of the polymer treatment. Equation (3.1) has two unknown parameters: $k'_{eff,w}$ and r_m. To obtain the latter it is necessary to use the hypothesis introduced at the beginning of this chapter, stating that the polymer is completely adsorbed on the surface of the rock pores, and that the adsorption degree is $A_d = 200\ \left[{}^{\mu g}/_{g}\right]$. So, given the quantity of the injected polymer, it is possible to evaluate the invasion radius of it:

$$r_m = \sqrt{\frac{\frac{m_p}{A_d}\ 10^6}{\rho_s\ (1-\phi)\ \pi\ h} + \left(\frac{OD_c}{2}\right)^2} - \left(\frac{OD_c}{2}\right) \tag{3.3}$$

In equation (3.3) the term r_m is the invasion radius, m_p is the mass of injected polymer, A_d is the adsorption degree in terms of adsorbed mass over the rock effective mass, ρ_s is the solid sandstone average density, ϕ is the porosity of the formation, while OD_c is the outside diameter of the casing and h is the thickness of the pay completed zone. The above equation implies that all the polymer is adsorbed on a continuous monolayer surface of the rock.

The values of the parameter calculated with equations (3.1), (3.3), and then (3.2) are displayed in Table 3-3, along with the residual resistance factor, evaluated accordingly with equation (2.1):

$\boldsymbol{Pozzo\ 1\ C, treatment\ data}$	
$\boldsymbol{Water\ effective\ permeability\ before\ RPM[mD]}$	4,52
$\boldsymbol{Water\ effective\ permeability\ after\ RPM[mD]}$	0,87
$\boldsymbol{Invasion\ radius\ [m]}$	2,2
$\boldsymbol{Water\ residual\ resistance\ factor\ [-]}$	5,2

Table 3-3: Pozzo 1 C computed parameters before and after the polymer treatment.

The average water effective permeability before the treatment appears to be quite different from the provided one, $2{,}2\ [mD]$, and closer to the one obtained in the laboratory for the sample core, $10{,}4\ [mD]$. The interesting parameter is the residual resistance factor, which indicates that the adsorbed polymer decreased of about 5 times the water effective permeability in the near wellbore area that extends for $2\ [m]$ around the casing. It must be noted that in these calculations the effect of the acid is not considered. The following plot gives an interesting overview of the pressure drop across the reservoir:

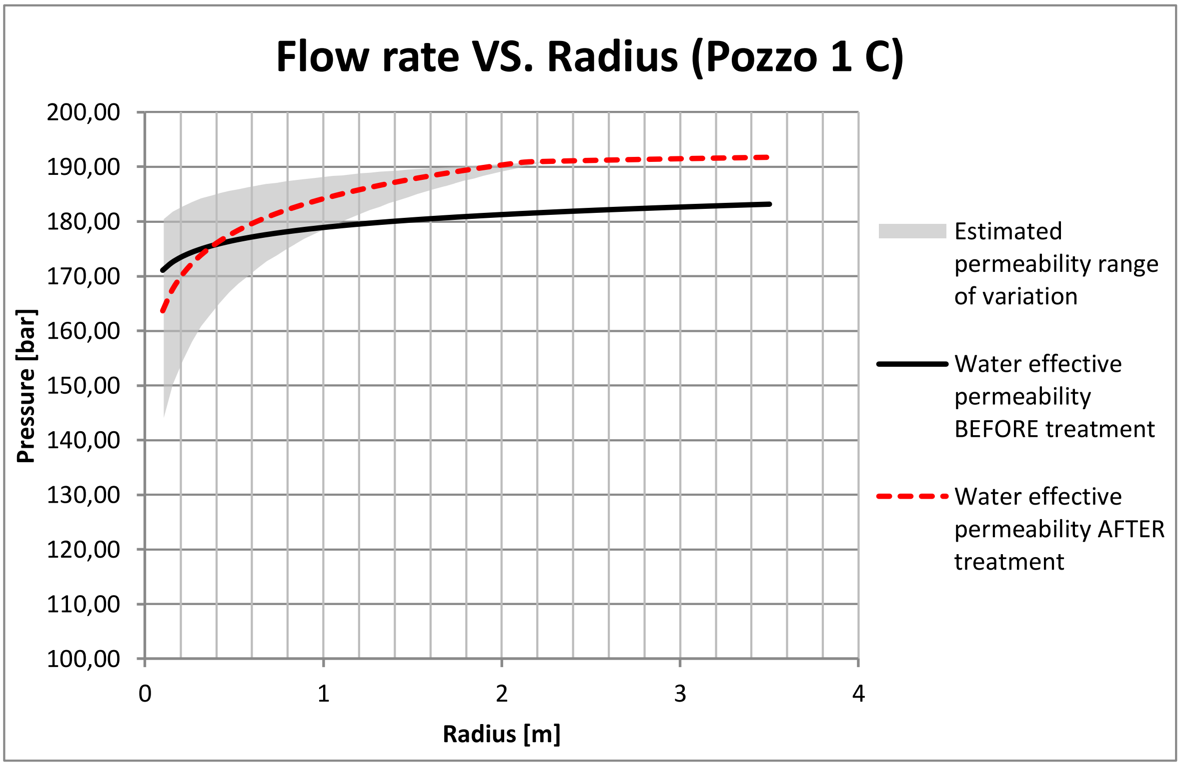

Figure 3-4: Pozzo 1 C pressure drop across the near wellbore reservoir before and after the treatment. The Shaded area indicates the expected pressure drop range.

Figure 3-4 shows the pressure drops only in a limited radius across the reservoir, in the near wellbore area, so that it is possible to appreciate the induced skin factor to water. The solid black line shows the pressure trend before the treatment is performed, while the red dashed line shows the pressure drop after it. At an infinite distance from the well, the reservoir radius, the two line would collide, still, the reduced water production caused fewer pressure losses that justify the position of the red line above the black one. This tendency changes in the modified permeability zone, where the loss of pressure that the water flow sustain are far greater than before. This is the evidence that the treatment effectively reduced the water effective permeability around the well. The gray shaded area highlight the expected pressure drop in the near wellbore area, with the well post treatment production parameters, if the permeability reduction effect would be the one obtained in the laboratory tests. The upper limit of the gray shaded area refers to a water residual resistance factor of $2{,}24$, while the lower border of it refers to a water residual resistance factor of $8{,}96$. The post treatment data, thus the red dashed line in Figure 3-4, and the F_{rrw} of Pozzo 1 C confirms not only the success of the treatment, but also the experimental data obtained in laboratory.

3.2 - CASE 2: POZZO 2 C

Pozzo 2 C is also located off-shore in the Adriatic Sea and it has been perforated and completed, as a short side-track of a main well, Pozzo 2 between November 2009 and February 2010. On July 2011 the well was set to produce from the levels it is still producing from, with a constant gas and water flow rate. Anyway the increasing in water production and the decreasing in gas production over time, led to the choice of performing an RPM treatment, in order find a solution to the continuous malfunctioning and damages to the top head separator caused by the sand hauled to the surface. The treatment was performed in July 2013, and it is chronologically the first performed RPM treatment out of the four analyzed in this chapter.

The procedure followed during the injection is the same one used for Pozzo 1 C, explained in the introduction of chapter 3, and, since the injection test proved a poor injectivity of the polymer solution, an acid treatment was performed to restore the well, gas and water, permeability. The acid used to restore the formation, just like in the previous case, was formic acid, which is the only one compatible with the Adriatic Sea formation.

Data available for Pozzo 2 C are illustrated in the following table, Table 3-4:

Pozzo 2 C, properties	
Water permeability [*mD*]	14
Temperature [°*C*]	46
Salinity $\left[{}^{g}/_{L}\right]$	3
Static top head pressure [*bar*]	158,5
Reservoir pressure [*bar*]	160
Perforated casing lenght [*m*]	51,5
Top vertical height of the perforation [*m*]	51,5
Numbers of separated layer [−]	7

Table 3-4: Pozzo 2 C preliminary properties.

To have a complete set of information regarding the well, Figure 3-5, just like for the previous case, illustrates a seismic log of the formation giving an insight of the pay zone, thus the perforated depth:

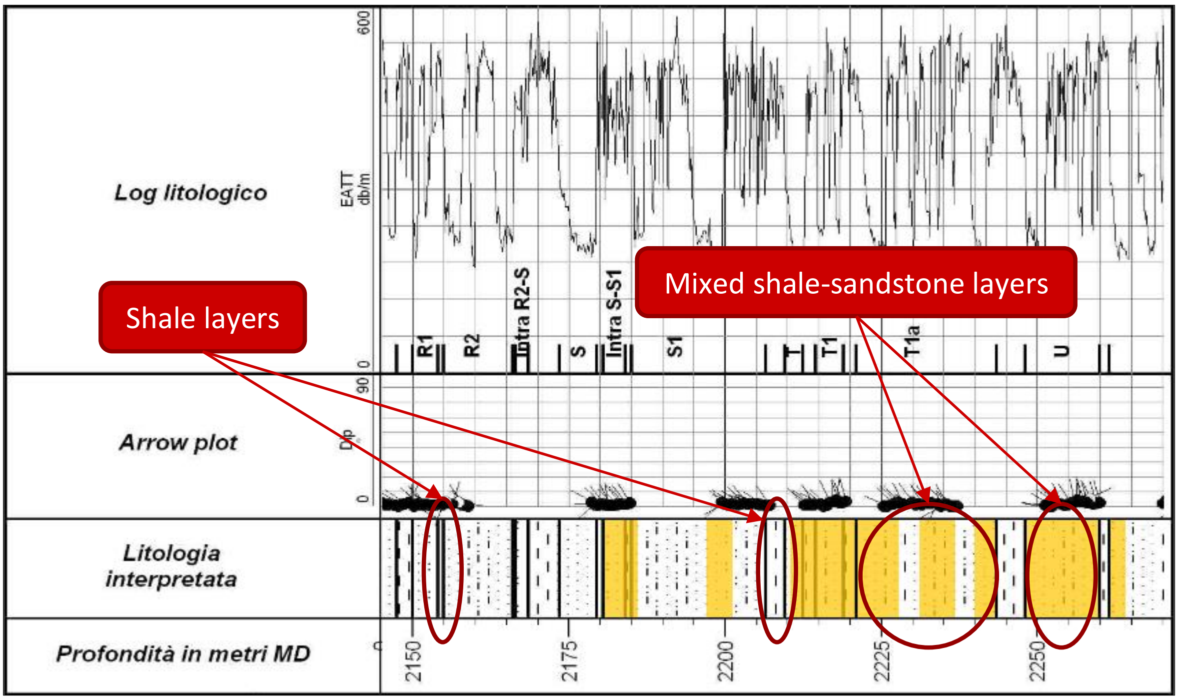

Figure 3-5: Pozzo 2 C seismic log schematic; orange highlighted areas indicates perforated interval. Image from ENI.

From the data illustrated above it is possible to notice that the salinity of the formation is a bit higher, about $33\ \%$, than the one used for the tests, as well as the permeability which is the $40\ \%$ higher than the one of the test core. Nevertheless, as for the previous case, the permeability of the reservoir is re-evaluated further in this paragraph, and once more this operation is carried out using the Darcy's law.

From the seismic log, it is possible to see the formation has been perforated in seven different zones of mixed shale and sandstone, where two of them may be vertically connected, while the others are certainly isolated from the firsts by shale layers. This is the well with the highest number of layers, due to the extension of the perforations, thus it is the one which might be more heterogeneous. Still, in accordance with the hypothesis presented in the introduction, as for the previous well, the pay zone is considered homogenous.

As for Case 1, after a brief description of Pozzo 2 C, it is possible present the data collected during the main treatment phase, which included the injection of 3 tanks of polymer solution at different polymer concentration that consisted of: a first $9\ [m^3]$ tank, at $500\ ppm$ of polymer, a second $18{,}8\ [m^3]$ tank, at $1000\ ppm$ of polymer, and a last $9\ [m^3]$ tank, at $1500\ ppm$ of polymer. The service company was planning a further injection of a gel slug, but since the maximum well head pressure was rapidly reached, the polymer injection was stopped. No gel solution was used. The polymer used in this case is the same one used for the laboratory test since the permeability is around the same value, or a little higher.

Figure 3-6 illustrates the registered well head pressure, green, and the injection rate, blue, versus time, during the polymer injection phase. The red curve is obtained as a punctual ratio between the pressure and the flow rate during the injection, and it is an easy-to-read curve which can be quickly compared with the one obtained during the test, since the injection rate used in laboratory was constant. The shaded orange and purple areas indicates the time interval at which the polymer solution, at a certain concentration, first reaches the formation. The border between one shaded area and the other indicates when one slug of polymer has completely entered the formation, and the following slug is about

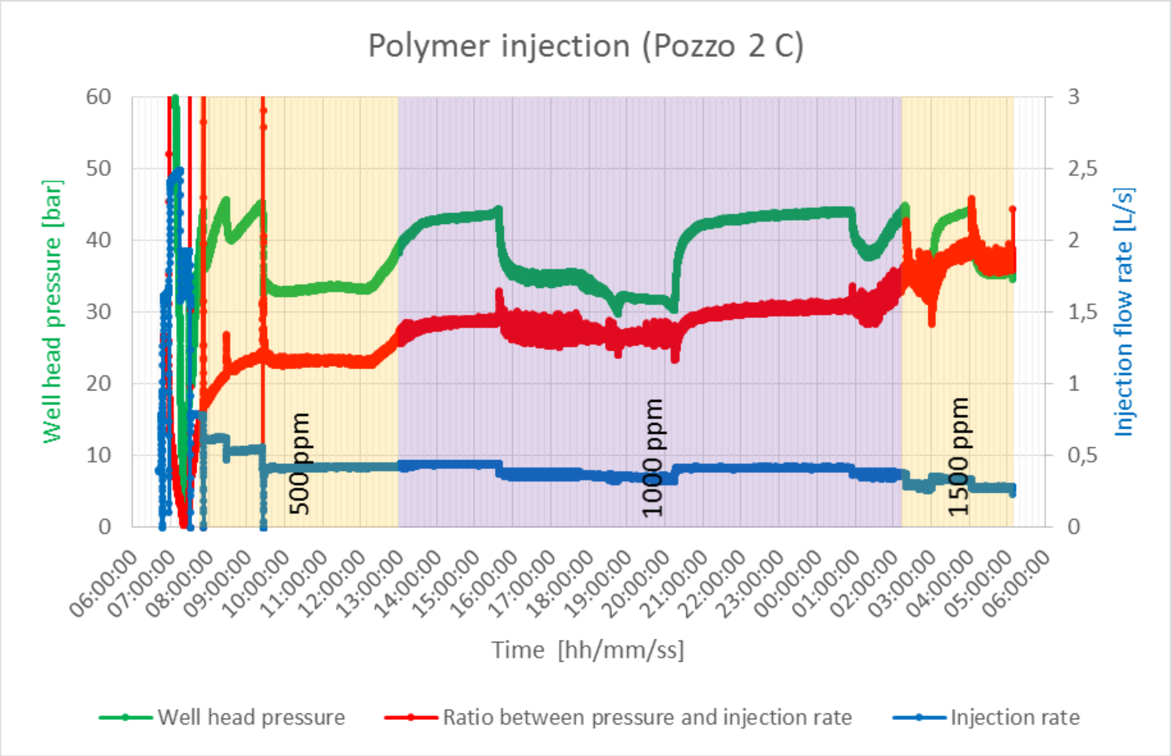

Figure 3-6: Injection rate, well head pressure and their ratio during the polymer injection phase of Pozzo 2 C. Data provided by ENI.

to enter it: since the polymer slugs are injected one after the other, the shaded areas are consecutives. From Figure 3-6 is possible to see that the treatment consisted of three different steps, each one of them is characterized by an increase of $500\ ppm$ of polymer in the polymer solution. If the normalized red curve is taken into account, the expected linear growing trend cannot be appreciated anywhere along it. Additionally the curve appears to have a very low slope, if not flatness, all along the purple shaded area. This could be due to a strong heterogeneity of the reservoir: one or more layers with a much higher permeability than expected could accept the most part of the injected solution with a slight variation of its permeability value, i.e. the very low slope. On one hand this might lead to think of a treatment failure, while on the other hand, considering that watered out layers are usually the most permeable, this could be an advantage, since the polymer solution would be more eager to invade these layers, thus to selectively extend the radius of the treatment in the water producing zones. The strong oscillation between $4\ pm$ to $8\ pm$

o'clock, and from 1 am till the end of the treatment are due to some problem with the injection pumps.

The polymer treatment results are hard to predict from such an injection test, and the only way to evaluate it, is to analyze the production history illustrated in following figure:

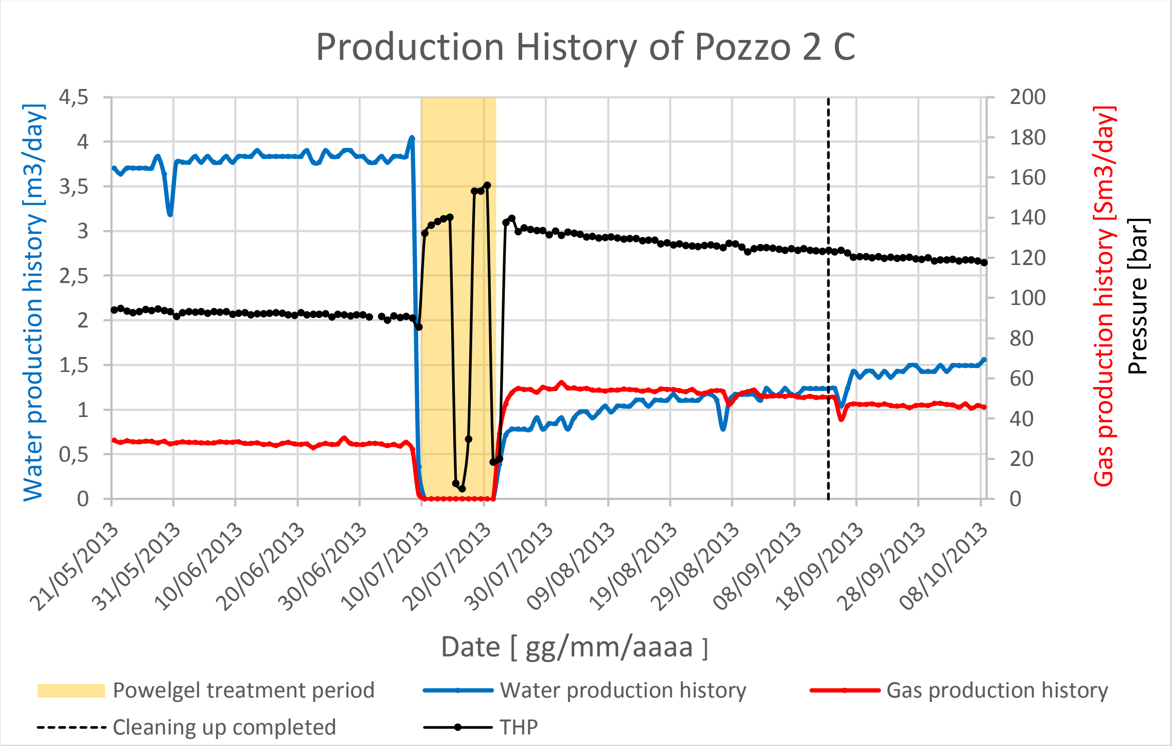

Figure 3-7: Pozzo 2 C production history. The blue line refers to water, the red line refers to gas, while the black line indicates the top well head pressure. The yellow shaded area indicated the treatment period. The dotted vertical line indicates the backflow of all the injected water from the polymer solution. Data provided by ENI.

Figure 3-7 clearly shows that the water production rate after the treatment is much lower, even though it shows a growing trend that is a bit higher than how it was before the treatment. The overall pressure rise may be linked to the effect of the acid treatment, which also led to an increased gas production, but it is probably due to the string cleaning operations since the pressure drop across the reservoir, in this case, is moderate. Anyway, it is possible to state that even this treatment was successful since the water flow rate has significantly decreased. The pressure trend in the yellow shaded area represent an error of reading, as a matter of fact the pressure in this time period should be nihil. The following table illustrates the average production parameters of the well before and after the treatment:

$\boldsymbol{Pre - treament\ data}$			$\boldsymbol{Post - treatment\ data}$		
$\boldsymbol{Q_g\ [Sm^3/day]}$	$Q_w\ [m^3/day]$	$FTHP\ [bar]$	$Q_g\ [Sm^3/day]$	$Q_w\ [m^3/day]$	$FTHP\ [bar]$
27 000	3,7	95	46 000	1	130

Table 3-5: Pozzo 2 C production parameters before and after the RPM treatment.

As conducted in the previous paragraph, it is once again possible, with the aid of equations (3.1), (3.3), (3.2), and then (2.1), to evaluate the water effective permeability, before and after the treatment, thus the water residual resistance factor. The only problem is that the flowing bottom-hole pressure after the treatment is unknown, so it is not thinkable to precisely evaluate the new near wellbore permeability. Anyway, the only conceivable way to proceed with the calculation is to hypothesize that the bottom-hole pressure remains constant after the polymer injection. These results are displayed in Table 3-6:

$\boldsymbol{Pozzo\ 2\ C, treatment\ data}$	
$\boldsymbol{Water\ effective\ permeability\ before\ RPM [mD]}$	12,04
$\boldsymbol{Water\ effective\ permeability\ after\ RPM [mD]}$	0,89
$\boldsymbol{Invasion\ radius\ [m]}$	0,64
$\boldsymbol{Water\ residual\ resistance\ factor\ [-]}$	13,5

Table 3-6: Pozzo 2 C computed parameters before and after the polymer treatment.

The average water effective permeability before the treatment appears to be lower than the provided one, 14 $[mD]$, but very close to it. More interesting is the reduction of residual resistance factor of about 13 times in the near wellbore area that extends for $0{,}64\ [m]$ around the casing. This reduction is higher that the once obtained in the laboratory tests, and even higher than the one obtained in the previous case. This could be due to the hypothesized constant bottom-hole pressure that might actually be a bit higher than expected. The following plot, similar to the one presented in the previous case, gives an interesting overview of the pressure drop across the reservoir and helps to clear the last statement:

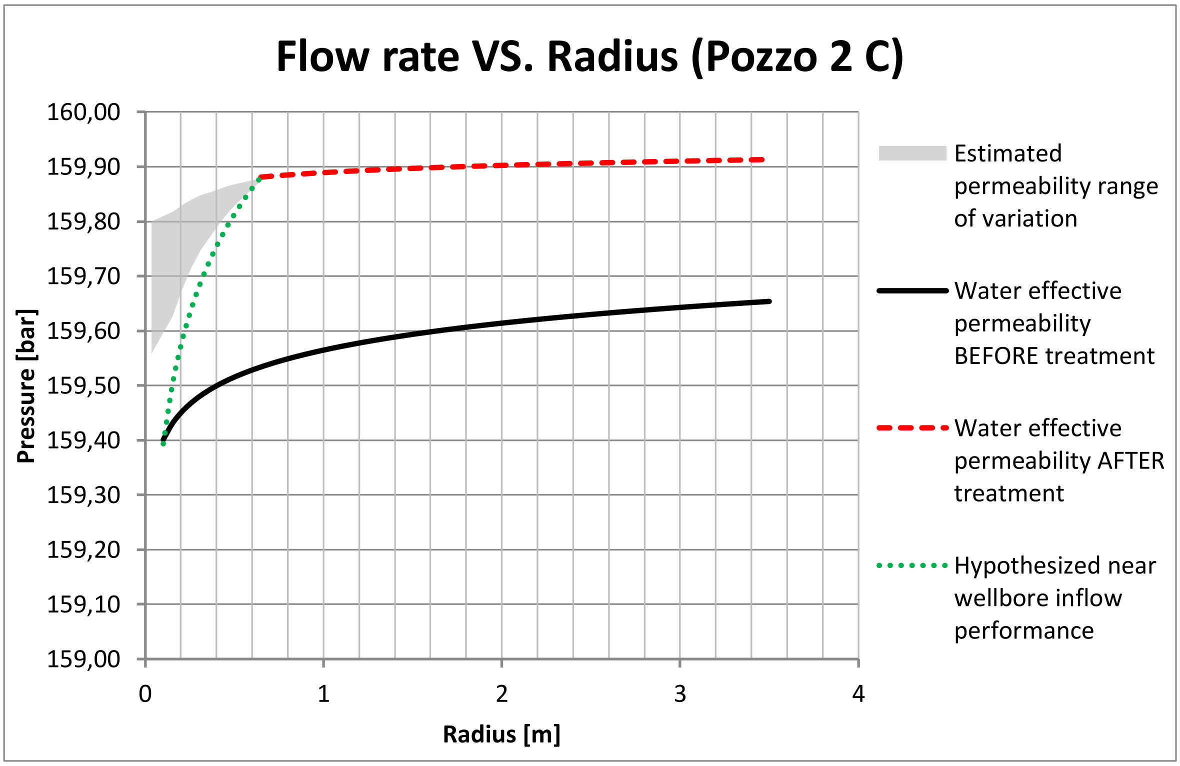

Figure 3-8: Pozzo 2 C pressure drop across the near wellbore reservoir before and after the treatment. The Shaded area indicates the expected pressure drop range.

Figure 3-8 shows the pressure drop only in a limited radius across the reservoir, in the near wellbore area, so that it is possible to appreciate the induced skin factor to water. The solid black line shows the pressure trend before the treatment is performed, while the red dashed line shows the pressure drop after it. At an infinite distance from the well, the reservoir radius, the two line would collide, still, the reduced water production caused fewer pressure losses that justify the position of the red line above the black one. The gray shaded area highlight the expected pressure drop in the near wellbore area, with the well post treatment production parameters, if the permeability reduction effect would be the one obtained in the laboratory tests. The upper limit of the gray shaded area refers to a water residual resistance factor of $2{,}24$, while the lower border of it refers to a water residual resistance factor of $8{,}96$. In this case the red dashed lines stop when it reaches the radius of the treated zone since the unknown bottom-hole pressure does not allow to compute the near wellbore pressure drop. Anyway, since the treatment appeared to be successful, the pressure drop in the near wellbore area is very likely to be situated in the gray shaded area, just like the previous case, and not below it, as the approximated F_{rrw} indicates with the green dotted line in Figure 3-8.

3.3 - CASE 3: POZZO 3 L

Pozzo 3 L, as for all the others well, is located off-shore in the Adriatic Sea and it was completed, as a short side-track after the main well, Pozzo 3, between November 2009 and February 2010, the same period of the well in the previous case. Starting from the beginning of 2011 the well registered a decline of its performance and a constant increase of the water production. This condition lasted for one year, until the well completed levels were shut and others were perforates. These new levels produced without any problem up to July-August 2013 when the gas flow rate had to be decreased to $20\ \left[{kSm^3}/{day}\right]$ to reduce the water and sand production. The value of the flow rate was decided so that the superficial velocity of the gas inside the string would not be high enough to lift and carry liquid to the surface, justifying, as it is further illustrated, the extremely low water flow rate: $0{,}13\ \left[{m^3}/{day}\right]$.

The RPM treatment performed on this well had the goal of allowing higher gas production without the associated water and sand problems previously encountered. Unluckily the operating conditions of the well before the treatment do not consent an effective evaluation of the water effective permeability, since the water production rate is affected by the gas flow rate regulation. The treatment was performed between January and February 2014, and it is chronologically the third one, after Pozzo 2 C, and Pozzo 1 C.

The procedure followed during the injection is the same one used for the other wells, explained in the introduction of chapter 3, but this time the injection test proved a good injectivity of the polymer solution, thus no acid was used to clean the formation. Nevertheless a cleansing of the borehole was performed with simple brine. This operation, can operate a fines displacement from the completed formation and it can restore the permeability of the well, even though the washing effect is not as high as the one obtained with the acid.

Data available for Pozzo 3 L are illustrated in the following table, Table 3-7:

Pozzo 3 L, properties	
Water permeability $[mD]$	3,5
Temperature $[°C]$	45
Salinity $\left[{}^{g}/_{L}\right]$	3
Static top head pressure $[bar]$	174,5
Reservoir pressure $[bar]$	175,5
Perforated casing lenght $[m]$	18
Top vertical height of the perforation $[m]$	18
Numbers of separated layer $[-]$	2

Table 3-7: Pozzo 3 L preliminary properties.

To have a complete set of information regarding the well, Figure 3-9, just like for the previous cases, illustrates a seismic log of the formation giving an insight on the pay zone, thus the perforated depth.

From the data illustrated in the following figure it is possible to notice that the salinity of the formation is once again higher, about 33 %, than the one used for the laboratory tests, while the water effective permeability is 3 times lower than the one of the test core. In

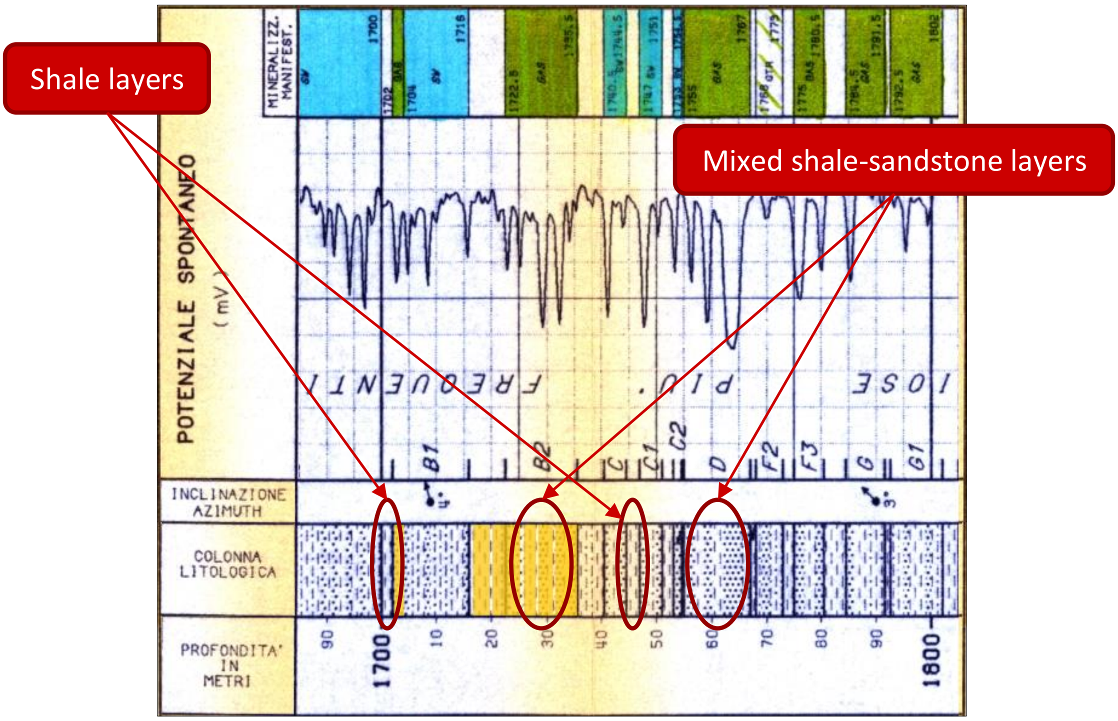

Figure 3-9: Pozzo 3 L seismic log schematic, the orange highlighted areas indicates the perforated interval. Image from ENI archives.

this case the average permeability of the completed zone is not revaluated due the inconsistence of the available data.

From the seismic log, it is possible to see that the formation has been perforate in six different zones of mixed shale and sandstone, where four of them may be vertically connected, while the other two are certainly isolated from the first ones by a shale layer. The considerations about the heterogeneity of the pay made for the previous wells can be extended to this one too, still, in accordance with the hypothesis presented in the introduction, if they subsist, they are neglected and the formation is considered homogenous.

Once more it is possible present the data collected during the main treatment phase, which included the injection of 5 tanks of polymer solution with rising concentration (from 500 ppm in the first to 2500 ppm in the last, with steps of 500 ppm), each one with a volume of 9,3 $[m^3]$, exception made for the third one which was of 10 $[m^3]$. The polymer used for the treatment was the same one used for Pozzo 1 C, which is more adapt to lower permeability.

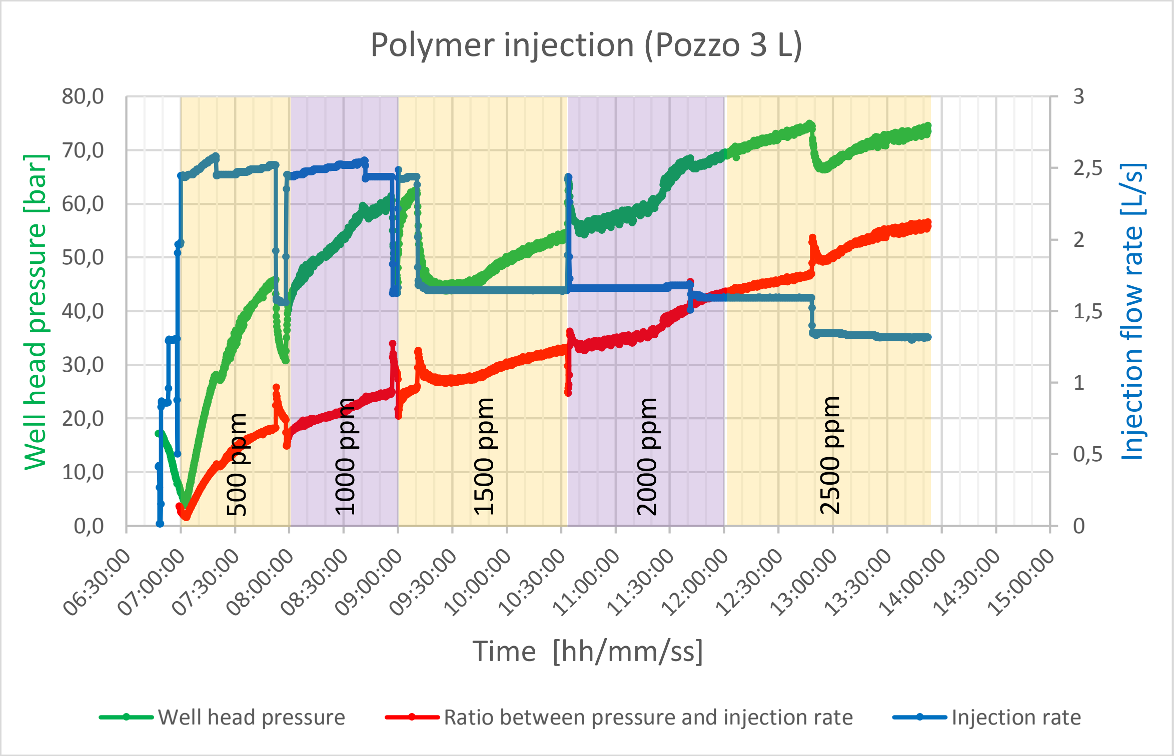

Figure 3-10: Injection rate, well head pressure and their ratio during the polymer injection phase of Pozzo 3 L. Data provided by ENI.

Figure 3-10 illustrates the registered well head pressure, green, and the injection rate, blue, versus time, during the polymer injection phase. The red curve is obtained as a punctual ratio between the pressure and the flow rate during the injection, and it is an easy-to-read curve which can be quickly compared with the one obtained during the test, since the injection rate used in laboratory was constant. The shaded orange and purple areas indicates the time interval at which the polymer solution, at a certain concentration, first reaches the formation. The border between one shaded area and the other indicates when one slug of polymer has completely entered the formation, and the following slug is about to enter it: since the polymer slugs are injected one after the other, the shaded areas are consecutives. From Figure 3-2, considering the normalized red curve, it is possible to see that the pressure profile is quite linear, aside from the transitory occurred when the polymer reached the formation and when the injection rate was diminished. Just like in the first case study it can be inferred that the polymer treatment produced a pressure response very similar to the one obtained in laboratory, and once more the only difference is that the change in polymer concentration didn't really affect the curve slope. The only non-linear trait of the curve, the first yellow shaded area on the left, may be attributed to a transient phase at the beginning of the polymer injection. Given the behavior of the pressure response during the injection, it would be very like to state that the treatment was a success. Still, for the reasons illustrated in the introduction of this paragraph, this statement may be hard to prove, especially by looking at the following figure:

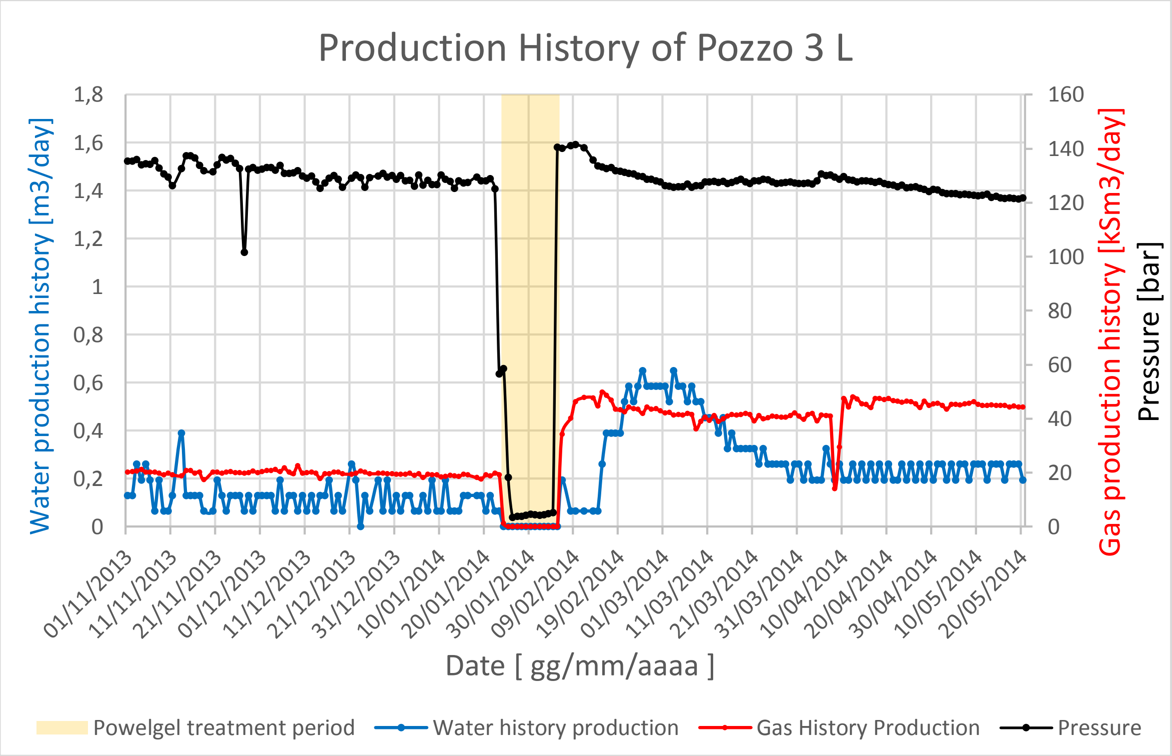

Figure 3-11: Pozzo 3 L production history. The blue line refers to water, the red line refers to gas, while the black line indicates the top well head pressure. The yellow shaded area indicated the treatment period. The dotted vertical line indicates the backflow of all the injected water from the polymer solution. Data provided by ENI.

Figure 3-7 clearly depicts a raise of water production, almost doubled, right after the treatment, which is to opposite of what should have happened. Anyway it must also be noted that the gas production is two times and a half more than it was before the treatment, while the pressure, aside from an initial peak, is following the same trend. The scenario would be easier to understand with more reliable production data in the period of time prior the polymer injection, but it is still possible to glimpse the effect of the permeability reduction: the well is capable of sustaining a much higher gas flow rate without suffering from high level of water, thus sand, production that caused the former gas flow rate control. This result was nothing less but what was expected from the treatment that, despite the increase of water flow rate, was a success.

The following table illustrates the average production parameters of the well before and after the treatment:

$\boldsymbol{Pre-treament\ data}$			$\boldsymbol{Post-treatment\ data}$		
$\boldsymbol{Q_g\left[{Sm^3}/{day}\right]}$	$Q_w\left[{m^3}/{day}\right]$	$FTHP\ [bar]$	$Q_g\left[{Sm^3}/{day}\right]$	$Q_w\left[{m^3}/{day}\right]$	$FTHP\ [bar]$
20 000	128	95	45 000	0,2	128

Table 3-8: Pozzo 3 L production parameters before and after the RPM treatment.

In this case it is not possible to verify the permeability before the treatment, so the reference value will be take into account. The only way to compute the water effective permeability after the treatment, as there is no sign of variation of the bottom-hole pressure after the treatment, is to hypothesize that the latter is constant. Using equations (3.3), (3.2), and then (2.1), leads to the value of the new water effective permeability, and to the water residual resistance factor. These results are displayed in Table 3-6:

$\boldsymbol{Pozzo\ 3\ L, treatment\ data}$	
$\boldsymbol{Water\ effective\ permeability\ before\ RPM[mD]}$	3,58
$\boldsymbol{Water\ effective\ permeability\ after\ RPM[mD]}$	12,84
$\boldsymbol{Invasion\ radius\ [m]}$	1,67
$\boldsymbol{Water\ residual\ resistance\ factor}\ [-]$	0,28

Table 3-9: Pozzo 3 L computed parameters before and after the polymer treatment.

The value of the residual resistance factor indicates, given the validity of steadiness of the bottom-hole pressure, that the treatment increased the water effective permeability instead of decreasing it. This conclusion is hardly true, especially considering the facts the no acid was injected in the formation, and the brine cleansing of the bottom hole could not cause such a gain of permeability. The only explanation to this phenomena is that the pressure at the bottom of the well is lower that the hypothesized one. The following plot, similar to the one presented in the previous case, clarifies the inflow performance in each of the depicted case scenarios:

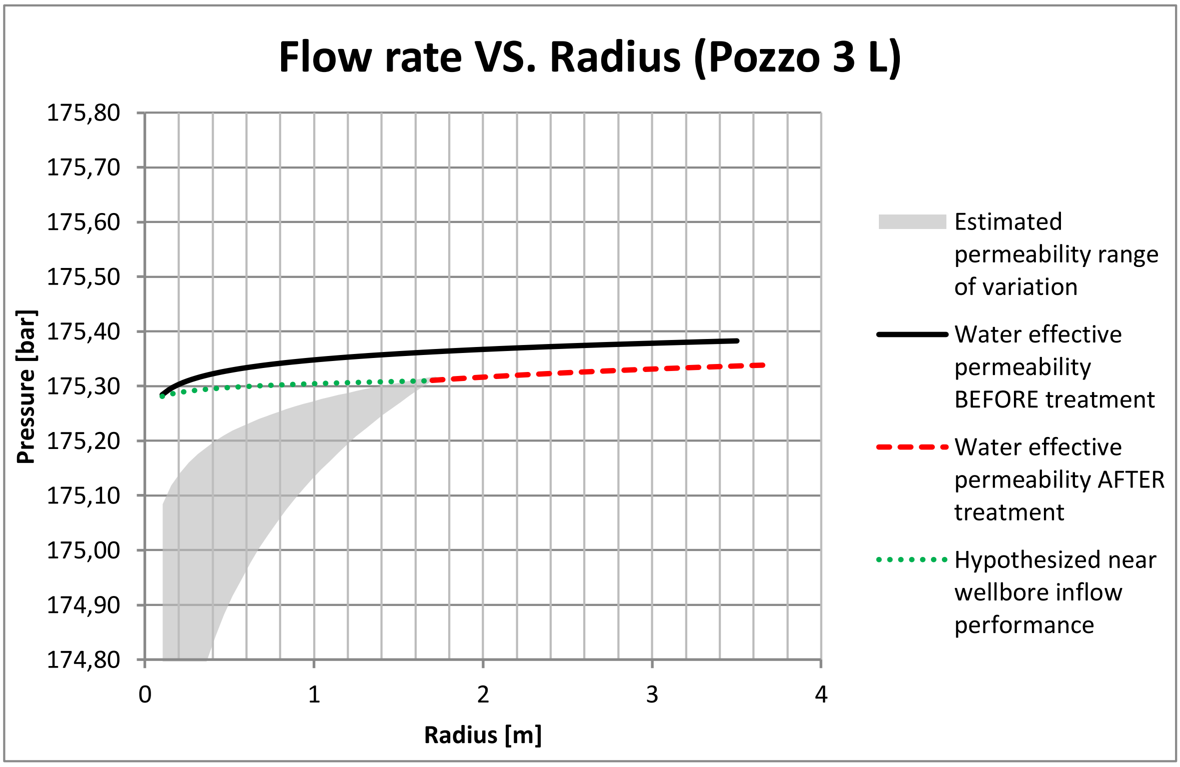

Figure 3-12: Pozzo 3 L inflow performance near wellbore before and after the treatment. The Shaded area indicates the expected pressure drop range.

In the figure above the solid black line shows the pressure trend before the treatment is performed, while the red dashed line shows the pressure drop after it. As in the previous similar plots, at an infinite distance from the well, the two line would collide, still, the increased water production caused higher pressure losses that justify the position of the red line below the black one. The green dote line is obtained continuing the red dashed one when the previously stated hypothesis is applied. What is relevant, is that Figure 3-8 shows that a variation of tenths of pressure could cause significant variation of the computed permeability. This is due to the fact that the pressure drop from the outer boundary of the reservoir and the well is very low, only few bars, thus is very difficult to predict the real trend of the inflow performance after the treatment. A plausible situation, given the good results of the first two treatment, would place the inflow performance curve somewhere in the gray shaded area, as the latter highlight the expected pressure drop in the near wellbore area, with the well post treatment production parameters, if the permeability reduction effect would be the one obtained in the laboratory tests. The upper limit of the gray shaded area refers to a water residual resistance factor of $2{,}24$, while the lower border of it refers to a water residual resistance factor of $8{,}96$.

3.4 - CASE 4: POZZO 4 L

Pozzo 4 L, located off-shore in the Adriatic Sea, was completed as a side-track of the main well, Pozzo 4, between February 2006, the same period of the well in the previous case. At the well start-up it produced $75\ \left[{kSm^3}/_{day}\right]$ of gas, but the production performance declined over time, and now the well water production reached $10\ \left[{m^3}/_{day}\right]$, while the gas production dropped to $43\ \left[{kSm^3}/_{day}\right]$. The well is not affected by high quantity of produced sand, but the high level of water flow rate decreases the well performances, and significantly contributes to saturate the water treatment-and-disposal offshore authorized limits. These are the two reasons behind the RPM treatment performed during March 2014, which is the latest one performed.

As for all the other wells, the procedure followed during the polymer injection is the one explained in the introduction of chapter 3. In this case the injection test proved a poor injectivity of the polymer solution, thus an acid cleansing was executed.

Data available for Pozzo 4 L are illustrated in the following table, Table 3-10:

$\text{Pozzo 4 L}, properties$	
$Water\ permeability\ [mD]$	2
$Temperature\ [°C]$	44
$Salinity\ \left[{}^{g}/_{L}\right]$	3
$Static\ top\ head\ pressure\ [bar]$	127
$Reservoir\ pressure\ [bar]$	215
$Perforated\ casing\ lenght\ [m]$	6,5
$Top\ vertical\ height\ of\ the\ perforation\ [m]$	6,1
$Numbers\ of\ separated\ layer\ [-]$	1

Table 3-10: Pozzo 4 L preliminary properties.

To have a complete set of information regarding the well, Figure 3-9, just like for the previous case, illustrates a seismic log of the formation giving an insight on the pay zone, thus the perforated depth:

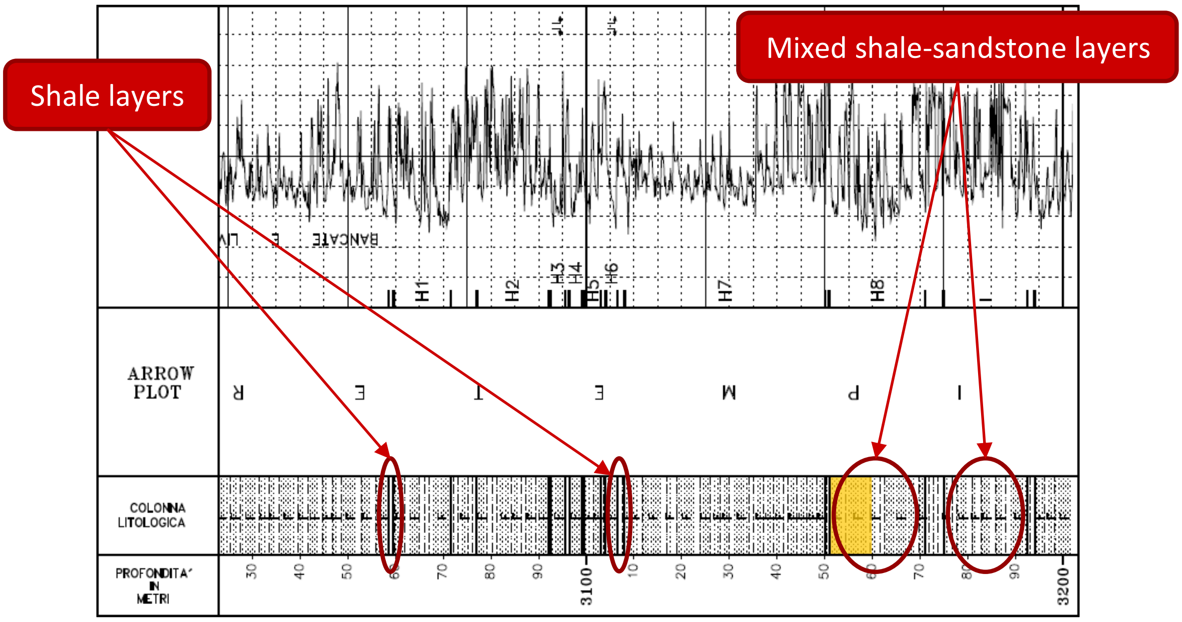

Figure 3-13: Pozzo 4 L seismic log schematic, the orange highlighted areas indicates the perforated interval. Image from ENI archives.

From the data illustrated in the following figure it is possible to notice that the salinity of the formation is, as for all the other cases, about $33\ \%$ higher than the one used for the laboratory tests, while the water effective permeability is the lowest yet encountered, 5 times lower than the one of the test core. Its value will be verified further in this chapter.

The main difference from all the other analyzed well, is that, as illustrated in the seismic log, the formation has been completed in just one layer. Then it is plausible to expect that the properties of the pay are homogeneous, accordingly to the hypothesis presented in the introduction. Another important aspect is that this is the well that was treated with the highest quantity of acid if related to the length of the completion zone: $4\ [m^3]$ distributed over a $6{,}1\ [m]$ perforated zone. Since it is very likely that the near wellbore area is damaged, as the injection test proved poor injectivity, this operation could lead to significant gain in the near wellbore permeability due to the removal of high skin factor, thus an increased gas and water production.

Even in this last case it is possible present the data collected during the main treatment phase, which consisted of an injection of 5 tanks of polymer solution with rising concentration (from $500\ ppm$ in the first to $2500\ ppm$ in the last, with steps of $500\ ppm$), each one with a volume of $8\ [m^3]$. The polymer used for the treatment was the same one used for Pozzo 2 C, and also for the laboratory test, and it has never been used or tested on a reservoir with such a low expected permeability.

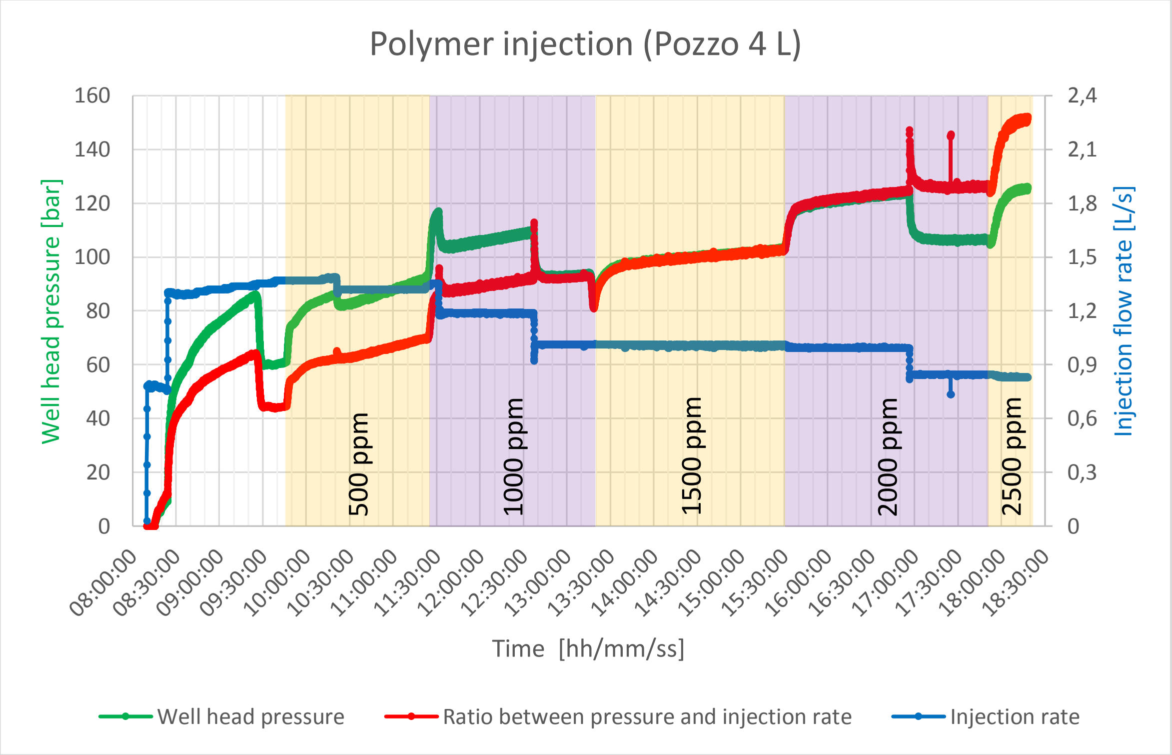

Figure 3-14: Injection rate, well head pressure and their ratio during the polymer injection phase of Pozzo 4 L. Data provided by ENI.

Figure 3-10 illustrates the registered well head pressure, green, and the injection rate, blue, versus time, during the polymer injection phase. The red curve is obtained as a punctual ratio between the pressure and the flow rate during the injection, and it is an easy-to-read curve which can be quickly compared with the one obtained during the test, since the injection rate used in laboratory was constant. The shaded orange and purple areas indicates the time interval at which the polymer solution, at a certain concentration, first reaches the formation. The border between one shaded area and the other indicates when one slug of polymer has completely entered the formation, and the following slug is about to enter it: since the polymer slugs are injected one after the other, the shaded areas are consecutives. From Figure 3-2, considering the normalized red curve, it is possible to see that the pressure profile is characterized by a repetitive pattern in each one of the shaded area: an initial pressure step followed by a linear pressure growth. The interesting fact is that the pressure steps always occur at the interface of the shaded areas, that is when a polymer solution with an increased concentration reach the formation. This behavior may be due to the interaction of the polymer type and the low permeability of the formation: a polymer more adapt to lower permeability should have been used. As a matter of fact these sudden rises of pressure resemble a surface plugging effect, thus a difficult dispersion of the RPM within the formation. Anyway the overall pressure rise indicates a possible reduction of the permeability to water.

As for the previous cases, the history production illustrate in the following figure clears the effect of the treatment:

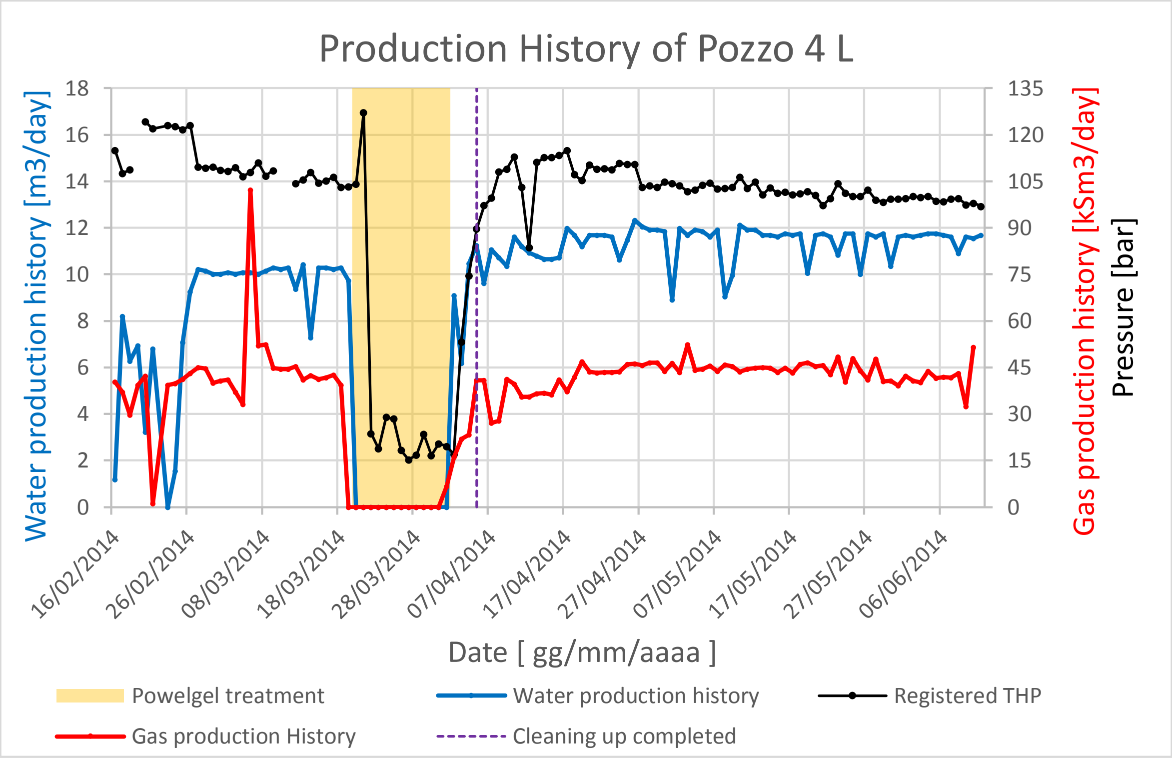

Figure 3-15: Pozzo 4 L production history. The blue line refers to water, the red line refers to gas, while the black line indicates the top well head pressure. The yellow shaded area indicated the treatment period. The dotted vertical line indicates the backflow of all the injected water from the polymer solution. Data provided by ENI.

Figure 3-7 shows a fairly raise of both water and gas production after the treatment, while the pressure kept following the same trend. This behavior clearly point to a failure of the failure of the water mitigation process. Still, the polymer injection may have actually decreased the water effective permeability: On one hand, as previously stated, the cleansing with acid performed on this well was heavier than in the other cases, and this could have significantly restore, thus increased, the permeability of the area around the wellbore; On the other hand the RPM treatment worked on the opposite way reducing the water effective permeability. Still, the higher increase of water production with respect to the really moderate increase in gas production, cannot be explained only by these effect. An important aspect that justifies the treatment response may have been played by the mono-layer nature of the pay zone. This trait will be further discussed in the following chapter, where the conclusion of this document are extrapolated. Anyway the target of the treatment was not accomplished.

The following table illustrates the average production parameters of the well before and after the treatment:

$\boldsymbol{Pre - treament\ data}$			$\boldsymbol{Post - treatment\ data}$		
$\boldsymbol{Q_g\left[{}^{Sm^3}/_{day}\right]}$	$Q_w\left[{}^{m^3}/_{day}\right]$	$FTHP\ [bar]$	$Q_g\left[{}^{Sm^3}/_{day}\right]$	$Q_w\left[{}^{m^3}/_{day}\right]$	$FTHP\ [bar]$
41 000	10	103	43 000	12	103

Table 3-11: Pozzo 4 L production parameters before and after the RPM treatment.

As conducted in the previous paragraph, it is once again possible, with the aid of equations (3.1), (3.3), (3.2), and then (2.1), to evaluate the water effective permeability, before and after the treatment, thus the water residual resistance factor. The only problem is that the flowing bottom-hole pressure after the treatment is unknown, so it is not thinkable to precisely evaluate the new near wellbore permeability. Anyway, the only conceivable way to proceed with the calculation, as in the previous cases, is to hypothesize that the bottom-hole pressure remains constant after the polymer injection.

These results are displayed in Table 3-6:

$\boldsymbol{Pozzo\ 4\ L, treatment\ data}$	
$\boldsymbol{Water\ effective\ permeability\ before\ RPM}[\boldsymbol{mD}]$	1,81
$\boldsymbol{Water\ effective\ permeability\ after\ RPM}[\boldsymbol{mD}]$	2,93
$\boldsymbol{Invasion\ radius}\ [\boldsymbol{m}]$	3,11
$\boldsymbol{Water\ residual\ resistance\ factor}\ [-]$	0,62

Table 3-12: Pozzo 4 L computed parameters before and after the polymer treatment.

The value of the residual resistance factor indicates, given the validity of steadiness of the bottom-hole pressure, that the treatment increased the water effective permeability, confirming the data in the history production plot. The following plot, similar to the one presented in the previous case, clarifies the inflow performance:

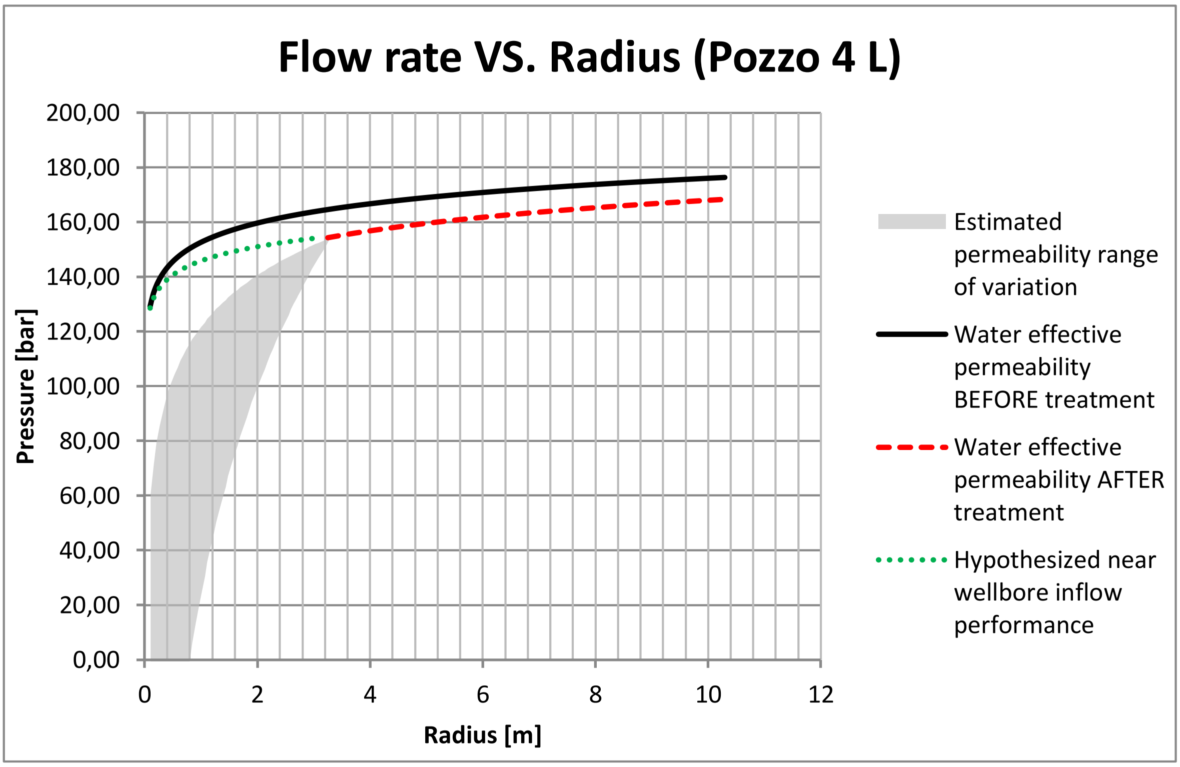

Figure 3-16: Pozzo 4 L inflow performance near wellbore before and after the treatment. The Shaded area indicates the expected pressure drop range.

In the figure above the solid black line shows the pressure trend before the treatment is performed, while the red dashed line shows the pressure drop after it. As in the previous similar plots, at an infinite distance from the well, the two line would collide, still, the increased water production caused higher pressure losses that justify the position of the red line below the black one. The green dote line is obtained continuing the red dashed one when the previously stated hypothesis is applied. Differently from the previous case, Figure 3-16 shows that the computed permeability value can be affected only by substantial variation of registered pressure, thus the hypothesis of constant bottom-hole pressure may actually be plausible. This implies that the positive variation of the water effective permeability may be true. On the other hand, another explanation of this phenomena, is that the joined action of the acid and the polymer, together with the fact that the pay zone is a single layer, may have created the condition for such behavior. As already said this aspect will be discussed in the following chapter, together with the conclusion. Therefore, in this case, the inflow performance curve does not definitely lay in the gray shaded area, which highlight the expected pressure drop in the near wellbore area, with the well post treatment production parameters, if the permeability reduction effect would be the one obtained in the laboratory tests.

CHAPTER 4

RPM USAGE GUIDELINES

In the first part of this chapter, based on the information provided in the preceding chapters, it is possible to draw some inferences concerning the selection of the best candidate for a water mitigation treatment with RPM, such as the water soluble polymers or relatively weak crosslinked gels. In the second part, is outlined the best practice to perform the treatment. These indications are mainly deduced from chapter 3, where four ENI water mitigation treatment, based on RPM, are discussed and analyzed. Despite the fact that chapter 3 is specifically targeted at gas-producing wells, the same general arguments, also hold for oil-producing wells, thus for all hydrocarbons-producing wells.

Furthermore it is important to highlight that a successful RPM treatment provides a long-term decrease in water production. Where by “long-term” it is meant that the target longevity of the treatment must be greater than the payoff time of the treatment itself, including the production loss related to the treatment operations.

4.1 - CANDIDATE SELECTION

The aspect of paramount important for a RPM treatment that aims at being successful, is the selection of the right candidate. This process requires the knowledge of the reservoir characteristic under a lithological point of view. As a matter of fact the blind usage of this technology could lead to ineffective, underperforming or disappointing water mitigation treatment.

As described in the previous chapter, a well could be completed in a pay zone characterized by a single or by multiple hydrocarbons producing intervals of the reservoir. In the latter case the multiple intervals may, or may not, be connected to each other depending on the vertical permeability, k_v, of the separating layers, which may allow a certain degree of crossflow, i.e. k_v is not too little. Even the extend of these layers around the wellbore is very important: for the selection of the right candidate, it is important to distinguish impermeable layers that extend for a radius smaller than the well drainage radius, from layers who extend for a greater distance.

Anyway, before introducing the above arguments, for the sake of clarity, it is useful to list all the prerequisite of any candidate well:

- The reservoir must not be either a naturally fractured or a hydraulically fractured reservoir.
- All the analyzed wells are completed in a sandstone reservoir and the interaction between the polymers, or the weakly crosslinked gels, with different kind of rocks cannot be predicted with the information contained in this document.
- The hydrocarbons flow toward the well is considered radial. No considerations can be inferred regarding partially completed wells whose inflow characteristics are difficult to predict.
- The completed zones of the analyzed wells are vertical or slightly deviated, up to 20° from the azimuth. Completed zones of horizontal wells or highly deviated wells could behave differently.

Given this information it is possible to introduce and analyze the remaining lithological characteristic with the aim of selecting the most suitable well for a treatment.

Single hydrocarbon producing zone.

This configuration can be related to Pozzo 4 L and the RPM treatment are not applicable. RPM treatments are not very useful when applied to a single zone reservoir. This is because after the treated well is put back on production, a relative permeability water block will form just beyond the outermost penetration of the treatment. The relative-permeability water block occurs because after the RPM treatment, water and hydrocarbons in the far wellbore region continue to flow to the well at the originally produced water to oil, or gas, ratio. When this oil, or gas, and water fluid stream reaches the outer radial penetration of the treatment, the water flow is impeded, whereas no permeability reduction and impediment is encountered by the hydrocarbons flow. Thus, with time, the water saturation builds up just beyond the treatment material. As the water saturation builds up, the relative permeability to oil flow is reduced. As a result, the hydrocarbons permeability is also reduced in this volume. The best that anyone can do in this single hydrocarbons-producing-zone situation over the long term is to end up with the final equilibrium water cut being the same as the pre-treatment water cut, but the well producing at lower production rate. This is a lose-lose result. WOR or WGR is not reduced, and the hydrocarbons production rate is reduced. From a practical point of view, this argument normally still holds if the single hydrocarbons-producing zone is mildly or somewhat heterogeneous. Stated another way, RPM treatments are of no value for promoting long-term WSO within any single, isolated hydrocarbons-producing zone that is nearly watered out [1].

Multiple producing intervals when crossflow exist.

RPM treatment could be applicable. First thing first it is necessary to explain that reservoir with ‘multiple producing intervals when crossflow exist’, are those reservoir characterized by pseudo-layers originated by slabs of shale rock, practically impermeable, whose radius of extension is smaller than the well drainage radius. Additionally it is necessary to distinguish the situation in which the water producing layer are fully drawn down, and the situation where is not fully drawn down. In the first case the relative permeability water block alts the production of water in the pseudo-layers with higher water cut, but due to existence of a certain degree of connection between pseudo-layers, the blocked water flows across and into the low water cut producing layers. This increases the water saturation of the latters, and the final layout is the one presented in the previous subparagraph, single hydrocarbon producing zone, where WOR, or WGR, is unaffected, while the oil-production rate is reduced.

The second situation, not fully drawn down layers, differs from the first one since the build-up of the water saturation just beyond the outermost penetration of the treatment requires a certain amount of time. In this period of time, the pseudo-layers with higher water cut would have a reduced production rate, whilst the higher hydrocarbons cut pseudo-layers would be unaffected, since the crossflow is not yet occurring. This, results in a temporary situation of reduced water production. Still, this behaviour is quite unpredictable since it is difficult to establish not only the number of layers with higher water cut, but also the degree of their water cut. The RPM treatment on these wells would be advisable only when the well is close to the end of its production lifetime.

Multiple producing intervals without crossflow.

RPM treatment is applicable. Differently from the last case, the reservoir with 'multiple producing intervals without crossflow', are those reservoir characterized by pseudo-layers originated by slab of shale rock, practically impermeable, whose radius of extension is greater than the well drainage radius. In this category are also included those wells who cut across multiple isolated reservoir at the same pressure level. This situation is a favourable one because no water block problem forms in the hydrocarbons-producing zones. This is a type of excessive water production problem that is amenable to successful RPM treatments. To maintain this favourable result, the hydrocarbons-producing zones must continue to produce dry oil or dry gas for the economic life of the treatment, or longer. Otherwise, if the oil zones produce at a finite intermediate water cut, this situation degenerates to the problem of a series of isolated oil/gas-producing zones producing at a finite water cut and the associated polymer, or weak gel treatment, induced water-block problem, as discussed previously.

Anyway is quite difficult, if not impossible, to predict whether the layers of a reservoir are completely isolated, or not, from one another. The best practice would be to perform a water mitigation procedure with RPM polymers only on wells with a high number of layers, particularly, the more layer it has and the higher the chances of a successful treatment. Pozzo 1 C, Pozzo 2 C and Pozzo 3 L all belong to a multilayered reservoir configuration, either with crossflow or without: based on the results presented in the last chapter and on the considerations above, it is very likely that Pozzo 1 C does not have crossflow, while little can be said for the other two wells.

Other aspects regarding multi-layered reservoir

It is very important to highlight that information provided in the previous section are appropriate for those wells whose layers, or pseudo layers, cannot be characterized in terms of permeability, meaning that it is only possible to evaluate an average permeability of the pay zone. As a matter of fact, if it is possible to evaluate the permeability of the layers of a reservoir, and they show an evident heterogeneity, the situation differs. Indeed in this cases the injection of a polymer, or gel, solution is always advisable, if a bullheadable treatment is the only feasible one. This consideration is justified by the fact that an evident contrast of permeability among different layers indicates that some of these layers experienced a water breakthrough, while some other, the less permeable one, are still producing hydrocarbons. This is the most suitable situation in which a disproportionate permeability reduction treatment can be performed, since the polymer solution would only invade the more permeable layers, where the water is produced, without affecting the hydrocarbons producing layers.

The thickness of the layers, or pseudo-layers, of a possible candidate well is another parameter that need consideration. Actually, the height of a layer itself is not very important as long as the condition of diffuse flow are dominant. To be more specific the fluids, gas, or oil, and water, during their flow toward the production well, do not separate accordingly to density, meaning that the dynamic pressure gradient dominate the flow:

$$\frac{\partial P}{\partial x} \gg g\ \Delta\rho \qquad (4.1)$$

Where $\frac{\partial P}{\partial x}$ is the pressure gradient along the direction of the radial flow toward the well, $\Delta\rho$ is the difference of density of the flowing fluids, and g is the gravity acceleration.
If the conditions of this equation are met, the vertical saturation of fluids are uniform, as depicted in the following figure:

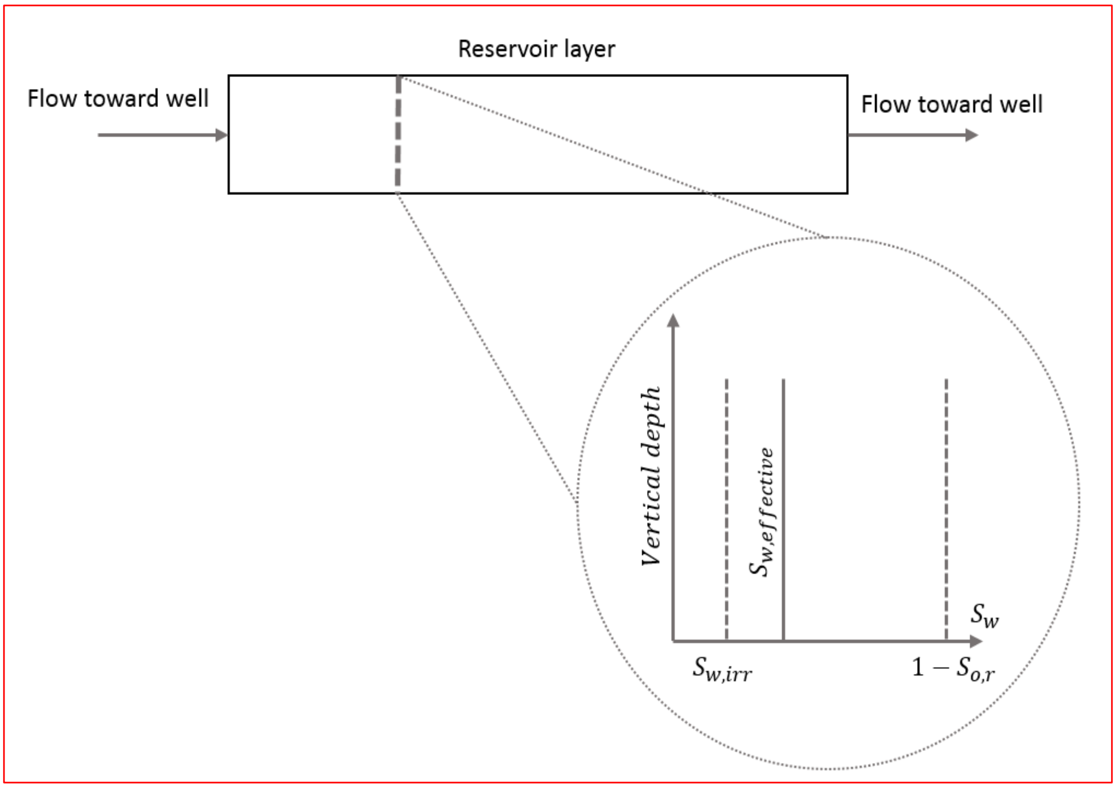

Figure 4-1: Illustration of the conditions of diffuse flow in a single layer of a reservoir, where the water vertical saturation is uniform.

In this case, the transition between gas and water production from the layer is quick, just like in a piston-like displacement. So once the saturation of the water in the layers reaches a level for which the production is no longer economical, an RPM treatment would stop the production of water without trapping valuable hydrocarbons in the formation. This condition is generally met where the height of the layer is small, in the order of magnitude of decameters. On the other hand, if the thickness of the layer grows in the order of magnitude of meters, it is very likely that the gravity forces would become dominant. Higher gravity forces cause the instauration of a segregated flow and an earlier and higher water production. An RPM treatment performed in this case, causes the two different stream of oil, or gas, and water to reach the outer radial penetration of the treatment, where the water flow is impeded, whereas no permeability reduction and impediment is encountered by the hydrocarbons flow. Thus, with time, the water saturation builds up just beyond the treatment material. As the water saturation builds up and creates a water block, the hydrocarbons are trapped. The outcome of this is a halt of the production and an economic loss.

Thus, it is possible to state that the thinner the layers, the higher the chances of success of a treatment.

Water coning

RPM treatment could be applicable. RPM treatments can only delay the water from coning around the emplaced treatment. The extent of the period of time the water can be delayed depends on the characteristic of the reservoir and the degree on the coning effect. The higher the coning effect, the less effective the treatment.

4.2 - RPM TREATMENT PROCEDURE AND EVALUATION

A RPM treatment must be correctly performed and evaluated to assess its effectiveness and performance. In fact, after the selection of the right candidate, it is necessary to establish a well treatment procedure, and, once the latter is accomplished and the production is restored, a correct evaluation of the result must follow.

RPM treatment procedure

A correct RPM treatment in the considered reservoir, see the description at the beginning of this chapter, requires the execution of different operations before the polymer, or weakly crosslinked gel, is injected.

First of all it is necessary to perform a string pickling not only to eliminate rust and other particles from the string itself, to avoid any reaction between the latters and the RPM solution, but also to remove sand lingering in the tubing so that the pumped solution reaches the formation more easily.

The first operation must be followed by an injection test, with the aim of establishing the average water effective permeability of the near wellbore area. This is necessary to evaluate the condition of the well in terms of inflow limitations due to skin factor. If the permeability of the near wellbore area appears to be reduced with respect to the expected one, meaning that the well is partially clogged with particles carried by the produced fluids, an acid treatment, should be performed in order to restore the original hydrocarbons and water permeability. This operation leaves the WOR or the GOR intact, but increases the overall hydrocarbon flow rate.

After this it would be advisable to perform an additional injectivity test, and then to return the well to production, in order to evaluate the effectiveness of the acid treatment and to gather additional data, extremely important to correctly evaluate the outcome of the RPM treatment.

Once this last operation is accomplished and the water effective permeability of the well is correctly evaluated, it is possible to select the adequate polymer or gel for the treatment: a polymer solution characterized by short polymer chains, such as the one used in Pozzo 1 C or Pozzo 3 L, would be optimal for a well that registered a very low injectivity, i.e. a low permeability to water, while a low-concentration-weakly crosslinked gel solution would be optimal for a well that registered a very high injectivity, i.e. a high water permeability. It must be noted that the permeability tested until now, whether in laboratory experiments, or in field application, ranges from $2\ [mD]$ to $15\ [mD]$. The successful application of polymers outside these range of permeability cannot be guaranteed. Anyway, further laboratory tests are required to assess the size and the nature of the RPM that best suits certain ranges of permeability, and what is the permeability limits for a RPM water mitigation treatments.

Once the right polymer has been selected, it is possible to start its injection in the reservoir. The concentration of the polymer solution and the amount of injected volume depends on the thickness of the completed layer, and on the aimed depth of the near wellbore treatment: in oil industry a near wellbore treatment can extend up to $10\ [ft]$ from the well outer boundary, and it is defined with relation to the fact that the higher pressure drop in a reservoir is in the near wellbore area, since the pressure is regulated by a logarithmic law with distance from the well. Anyway much depends on the heterogeneity of the reservoir itself: a very low permeability layer deviates the polymer solution to a more permeable one so that the polymer distribution around the wellbore would not be uniform. This effect makes the estimation of the right quantity of polymer solution very difficult. Still it must be noted, as described in the previous chapter and paragraph, that in a multilayered reservoir, the most permeable layers are usually the watered out ones. Thus, if the polymer solution were to enter only these layers, the outcome of the treatment could still be positive. So, a good practice is to design the polymer amount, given the knowledge of the near wellbore area and the adsorption characteristic of the polymer, in order that its radial penetration ranges from $2\ [ft]$ to $10\ [ft]$ from the well outer boundary. Concerning this fact, all the wells analyzed in the previous chapter meet this specification, which, for future treatment, can be correctly evaluated with the following equation:

$$m_p = \left[\left(r_m + \frac{OD_c}{2}\right)^2 - \left(\frac{OD_c}{2}\right)^2\right] \pi\ h\ \rho_s\ (1-\phi)\ A_d \qquad (4.2)$$

The term r_m is the invasion radius (ranges from $2\ [ft]$ to $10\ [ft]$), m_p is the mass of injected polymer, A_d is the adsorption degree in terms of adsorbed mass over the rock effective mass, ρ_s is the solid sandstone average density, ϕ is the porosity of the formation, while OD_c is the outside diameter of the casing and h is the thickness of the pay completed zone. Equation (4.2) gives the mass of the dry polymer, or gel, necessary for the treatment. The concentration of the polymer solution, based on the procedure followed for the cases studied in the previous chapter, should be increased in step of $500\ ppm$ starting from an initial concentration of $500\ ppm$. This step procedure is necessary to avoid sudden pressure peaks, which may damage the well. The volume of each tank batch with different concentration should be maintained constant, and it should be defined so that the treatment can be carried out in the least time possible, based on the result of the injectivity test. Following this procedure, the polymer injection phase should be considered completed only when the maximum allowed well head pressure is reached. This goal should be achieved either all the polymer has been injected or not: if the maximum allowed well head pressure is reached before all the polymer is injected, the injection process must be interrupted to avoid damages to the formation, on the other hand, if the injection does not cause the expected pressure response, once all the previously evaluate mass of polymer has been injected, this phase should be prolonged until the maximum well head pressure is reached. Anyway, if the maximum well head pressure can be hardly reached even with a polymer solution with $3000-4000\ ppm$ of polymer, it would be advisable to switch to a weakly-crosslinked gel solution.

The polymer, or gel, injection sequence should be followed by a nitrogen displacement procedure. This is necessary to reconnect the formation with the well, by sweeping the RPM solution, lingering in the tubing and in the near wellbore reservoir, deeper into the formation.

RPM post treatment evaluation

To correctly evaluate the success or the failure of a water mitigation treatment it is necessary to compute the water residual resistance factor, see Coreflooding: test overview page 47. This parameter can be suitably evaluated only if the variation of the well production parameter are due to the treatment itself, and they are not attributable to some regulation occurred at the wellhead, Christmas tree. Thus, the two fundamental operations are:

- Establishing the well production parameter before the RPM treatment, but after both the pickling and the acid cleaning.
- Restoring the well production, after the treatment, without changing any well regulation.

Additionally it would be advisable to sample the produced water after the treatment to gauge the presence of the backflow of the polymer, or gel, solution, and its proportion. Thus this operation should be conducted immediately after the treatment, and also sometime after it, i.e. a few weeks, so that it could provide information about the efficacy of the adsorption and the effective stability of the polymer.

CHAPTER 5

CONCLUSION

Throughout this document both experimental and field data have been obtained, analyzed and elaborated, to get a better understanding of which parameters make a disproportionate permeability reduction treatment, to mitigate water production in sandstone gas field, successful. These treatments are performed with aqueous solution of polymers, or weakly crosslinked gels, whose operating principles, as outlined in chapter one, are still being debated in the scientific community. Thus, a series of viscosity tests, flocculation test, and coreflooding tests provided the basic and necessary information to assess the behavior and the effectiveness of these chemicals, to confirm the data provided by the service company, and to gather information necessary to comprehend the production data from the gas wells. Consequently, with the production history of four different gas wells, it was possible to grasp the main variables that affect the effectiveness of a treatment, hence to formulate some rough guidelines that increase the chances of success for such a procedure: ranging from the selection of the most suitable candidate well, to the planning of the procedure for the treatment itself.

With a complete set of data it has been deduced that the increase of polymer concentration, during the field treatment, does not cause any variation in the injectivity pressure response, while during laboratory experiments, it evidently origins a rise of the slope of the injectivity curve. This effect may be related to the heterogeneity of the reservoir formation, in opposition with the homogeneity of the core plug used for tests.

Another note of interest regards the evident sand consolidation effect of the polymers, which could be exploited in those wells whose production is greatly affected and diminished by fine debris.

Additionally it has been noted that the acid treatment, performed before any polymer injection, does not affect the polymer behavior itself, but it could be of great use to remove any skin factor and obtain a higher production post job.

Anyway, aside from these considerations, and despite the many uncertain variables that regulate the behavior of a gas well, with which the oil industry is accustomed, it has been possible to understand that the key for the success of a disproportionate permeability reduction treatment, lays in a correct selection of both the candidate well, in relation with the lithology of the reservoir, and the relative permeability modifier product, in relation with the permeability of the reservoir. Additionally it has been deduced that a correct procedure to perform the treatment itself, as described in the previous chapter, is of a paramount importance not only to increase the chances of success, but also to correctly evaluate its outcome.

Therefore the know-how included in this dissertation, highlighted in the fourth chapter, can contribute to solve one of the major problem in oil and gas industry, that is the excessive water production from both oil and gas fields.

Besides it must also be considered that there are various limitations that were confronted, and that the guidelines provided in chapter four could be further perfected in the future. One of the main development could be achieved with a series of laboratory tests aimed at providing precise information about the correlation between the rock permeability, and the type polymer, or gels, and its concentration, with the goal of creating a set of rules describing which chemical should be used for a given rock permeability. Moreover, with the aid of the recommendations suggested in the previous chapter, it would be possible to gauge the effective response of the gas, or oil, wells to the treatment, ruling out redundant variables. Finally, if all this information were collected, it would be possible to implement a numerical procedure to predict the response of a well after the injection of a relative permeability modifier solution.

APPENDIXES

Appendix A - RESERVOIR CONFORMANCE

The term conformance in its truest and original form is defined as the measure of the volumetric sweep efficiency during and oil-recovery flood or process being conducted in an oil reservoir [3]. The Figure A-1, below, can be used to clarify the meaning of conformance and what conformance problems are:

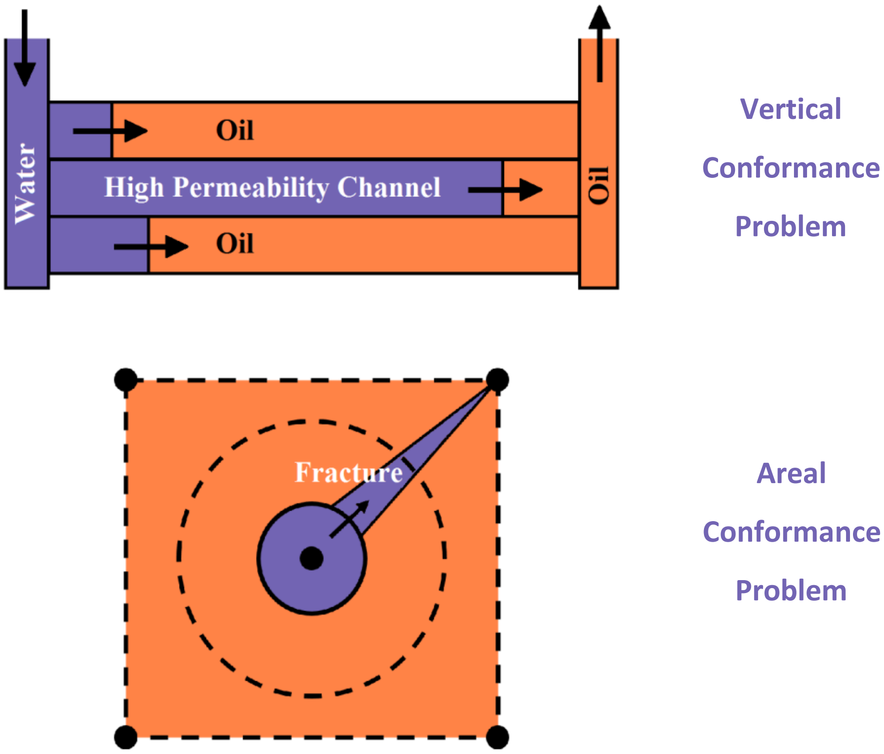

Figure A-1: Generalized matrix-rock and high-permeability anomaly conformance problem. Sydansk, Robert D. e Romero-Zeron, Laura. Reservoir Conformance Improvement.

In the upper part of Figure A-1, it is possible to see a vertical plane of the reservoir laying on the axis of both the water injection well and the production well. In this case the conformance problem is caused by a higher permeability of the middle layer which causes an inadequate vertical sweep efficiency, early displacement fluid breakthrough, and delayed oil production from the other oil-saturated rock layers. This is a typical *vertical conformance problem*. The lower part of the Figure A-1, shows a horizontal plane, normal to the injector well axis, with an *areal conformance problem*. In this second case it is possible to notice a bumpy advancing front of the displacement fluid caused by a very high-permeability irregularity of the rock. This rock fracture, which resemble a quite common problem in 5-spot vertical well pattern, would lead to the same problems associated with a vertical conformance problem. The following figure, Figure A-2, shows a typical waterflooding operation in a 5-spot vertical well pattern in which both vertical and areal conformance problem can be noted.

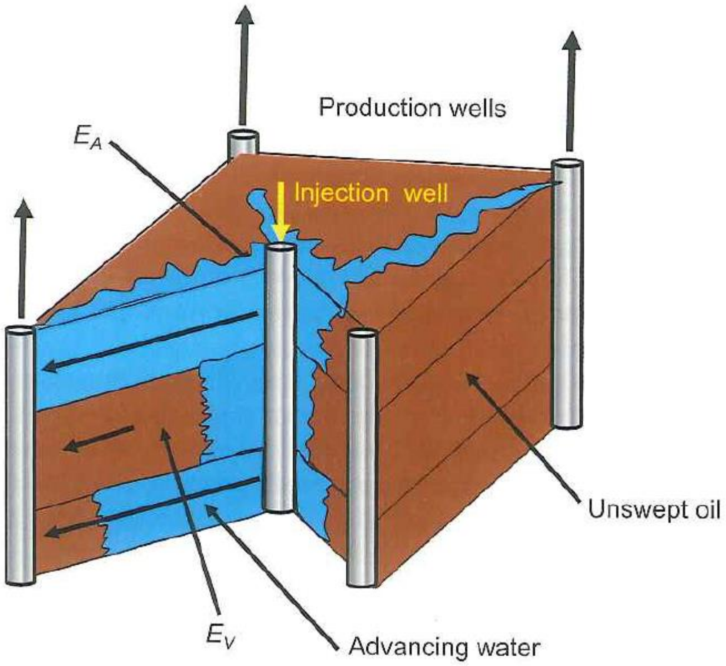

Figure A-2: A Waterflood in a 5-spot well pattern displaying both poor vertical and areal sweep efficiency. Sydansk, Robert D. e Romero-Zeron, Laura. Reservoir Conformance Improvement.

Appendix B - FOCUS ON CHEMICAL ASPECTS OF POLYMERS GELS

As already reported in Chapter 1, organic RPM can be classified mainly in synthetic polymers and biopolymers. Both of them need crosslinkers. The latter may be either of metallic nature, thus they create ionic bond with vinyl polymers, or of organic nature, thus they create covalent bond with polymers. Previous studies, conducted by Conway et al. [25], demonstrated that at least 22 metallic elements can be used as crosslinkers, amidst which the most important ones are: Chromium, Aluminum, Zirconium and Titanium [4]. While some organic crosslinkers can be either phenolic or aldehydes. Some phenolic crosslinkers are phenol, hydroquinone, resorcinol, phenyl acetate, etc. [4]. While some aldehydes ones are formaldehyde, paraformaldehyde, etc. [4].

Focus on synthetic polymers

The most common synthetic polymers that can be used to disproportionate reduce permeability are PAM, polyacrylamide, and HPAM, Hydrolyzed polyacrylamide. Polyacrylamide in its pure state is electrically neutral (non-ionic), seeming to preclude any cross-linking through ionic bonding. However, when mixed with a little alkaline solution, such as sodium hydroxide, or when subjected to elevated temperature, some of the amide groups convert to carboxylate groups. Each of these new groupscarries a negative charge. The proportion of amide groups that convert to carboxylate is called the degree of hydrolysis and typically varies from 0 to 60 per cent. In this form, the polymer is called partially hydrolyzed polyacrylamide, PHPAM or HPAM, and with its negatively charged carboxylate groups becomes susceptible to ionic cross-linking [4]. PAM is generally not referred as HPAM until the carboxylate content of the molecule exceed the 2% molar weight [3]. Because the low degree of cross-linked molecules in standard polyacrylamide, its hydrolyzed version is much more widely employed. The Figure B-1, gives the reader an illustration of a small section of both these two different molecules:

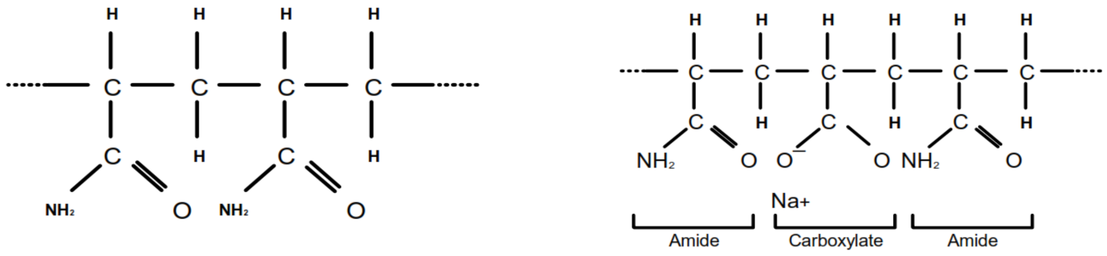

Polyacrylamide, PAM

Hydrolyzed Polyacrylamide, HPAM

Figure B-1: Illustration of two polymer molecules: Polyacrylamide and Hydrolyzed Polyacrylamide. Images taken from A.H. Kabir, SPE 72119, Chemical Water and Gas shutoff Technology – An Overview, 2001.

Though, the synthetizing process of Polyacrylamide, or its hydrolyzed form, are beyond the goal of this document, thus they won't be further discussed.

A polymer that became very popular and extensively applied is Chromium(III)-Carboxylate/Acrylamide-polymer, where the carboxylate group, in several cases, is an acetate. This molecule, aside from practical advantages, represents an evolution with respect to the use of other metals like Aluminum(III), whose crosslinking reaction cannot be controlled or delayed [26], and Chromium(VI), which is cancerous [4]. Furthermore Chromium(III)-Carboxylate/Acrylamide-polymer gelation time can be retarded with three methods: the use of gelation retardants agents such as strong carboxylate ligands, i.e. lactate, the use of ultra-low-hydrolysis polyacrylamide within the gel formulation, i.e. PAM, and the use of low molecular weight acrylamide polymers [3].

Focus on Biopolymers

Bio-polymers can also be cross-linked in the same way as synthetic ones. The most common Bio-polymers used for conformance controls are:

- xanthan
- polysaccharide (nonionic scleroglucan)
- lignosulfonates cross-linked with Cr
- Sodium carboxymethyl cellulose

- Guar Derivatives
- Hydroxyethylcellulose, HEC

The first two polymers are the most common ones. Xanthan gum is a polysaccharide secreted by the bacterium Xanthomonas Campestris. It is composed of pentasaccharide repeated units, comprising glucose, mannose, and glucuronic acid in the molar ratio 2:2:1. It is produced by the fermentation of glucose, sucrose, or lactose. After a fermentation period, the polysaccharide is precipitated from a growth medium with isopropyl alcohol, dried, and ground into a fine powder. Later, it is added to a liquid medium to form the gum or gel [27]. Scleroglucan is a water soluble, nature-derived polysaccharide produced by fermentation of the filamentous fungus Sclerotium Rolfsii. Scleroglucan has rheological properties, and unlike most natural and synthetic gums, has high thermal stability [28]. Thanks to its property it finds applications as water control gel.

Other kind of synthetic polymers

Further chemicals that have been either mentioned or tested, whether in laboratory on in real applications, can be grouped in the following four categories:

- Copolymers containing AMPS[17] monomers and acrylamide monomers.
- Copolymers of vinyl pyrrolidone and acrylamide or ter-polymers of vinyl pyrrolidone, acrylamide and acrylate.
- Cationic polyacrylamides polymers.
- New synthetic polymers system:
  - Hydrophobically modified water-soluble polymers.
  - Hydrophobically associative polymers.

The operating mechanism of the first three polymers of the above list is exactly the same one as for the Hydrolyzed polyacrylamide polymer gels. The aspects which differentiate them concern their fields of application. As a matter of fact each RPM treatment can be

---

[17] AMPS: 2-acrylamido-methyl-propanesulfonic acid monomers

optimized with a specific polymer that suits the reservoir physical aspects. These physical aspects are not discussed in this section.

On the other hand the new synthetic polymers system differs from classical water-soluble polymers in that they carry low amount of hydrophobic monomers capable of creating physical associations with each other [3]. These new polymers do not contain any crosslinkers. However the hydrophobic modification of the water-soluble polymer allows multiple layers of the polymer to build up because of the association of the hydrophobic groups [29]. The Figure B-2, below, illustrate the interaction between polymers chains in the absence of crosslinkers:

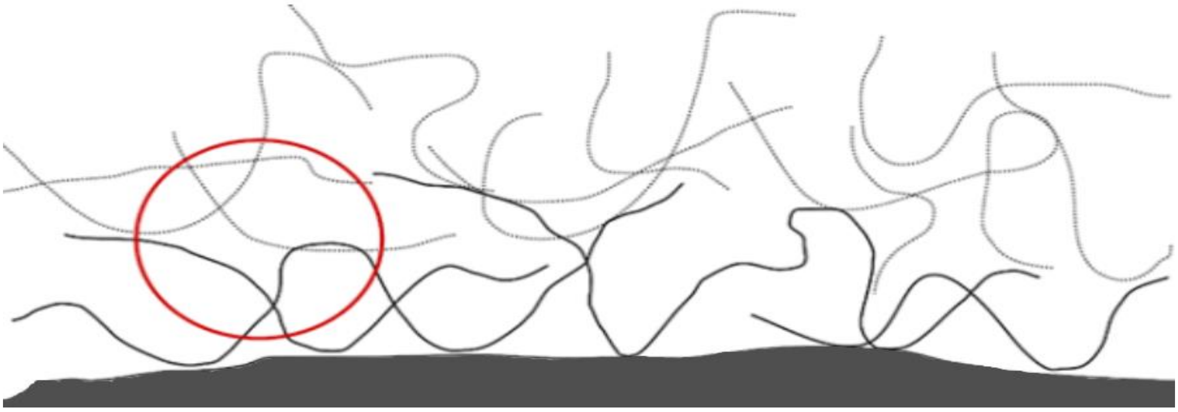

Figure B-2: RPM system base polymer; the hydrophobic modifications allow the polymer to build up because of the association of the hydrophobic groups. Vasquez J., Eoff L., A Relative Permeability Modifier Water Control: Candidate Selection, Cases Histories, and Lessons Learned after more than 3'000 Well Interventions, 2013, SPE 165091.

The associative interactions of the hydrophobic groups may lead either to lower or to higher solution viscosities. Additionally these attraction are often depicted as transient and reversible crosslinks among polymer chains that form under static or low shear stress, but rupture at high shear stress [30]. The advantages of these new polymer are multiple: they are more easily clean up from the oil and gas reservoir invaded zone [29], and they have a more selective and higher capacity to modify relative permeability.

SYMBOLS

Symbol	Description	S.I. dimensionality	Most common used dimensionality
v	Superficial velocity	$\frac{m}{s}$	$\frac{m}{s}$
v_i	Superficial velocity of the specie ‘i’	$\frac{m}{s}$	$\frac{m}{s}$
v_t	Superficial total velocity	$\frac{m}{s}$	$\frac{m}{s}$
k	Absolute permeability	m^2	Darcy [D]
$k_{r,i}$	Relative permeability of ‘i’	-	-
S_i	Rock pore saturation of ‘i’	-	-
$S_{w,\mathrm{irr}}$	Irreducible water saturation	-	-
$S_{o,r}$	Residual oil saturation	-	-
Δ	Variation parameter	-	-
δ	$k_{r,w}$ curve scaling factor	-	-
ϕ	Rock porosity	-	-
A	Area variable	m^2	m^2
t	Time variable	s	s
P	Pressure variable	Pa	bar or $Psia$

Symbol	**Description**	**S.I. dimensionality**	**Most common used dimensionality**
P_i	Pressure with relation to specie ‘i’	Pa	bar or $Psia$
μ	Viscosity	$Pa \cdot s$	cP
μ_i	Viscosity with relation to specie ‘i’	$Pa \cdot s$	cP
q_i	Volumetric flow rate of ‘i’	$\frac{m^3}{s}$	$\frac{bbl}{d}$
f_w	Fraction of flowing water	-	-
WOR	Producing water to oil ratio	-	-
P_{cow}	Water to oil Capillary pressure	$Pa \cdot s$	cP
C	Concentration of solute in solvent	$\frac{g}{L}$	$\frac{g}{L}$
σ	Superficial tension	$\frac{N}{m}$	$\frac{N}{m}$
ϑ_c	Wetting phase contact angle	°	°
R^2	Mean squared error	-	-
$F_{rr,i}$	Residual resistance facto of “i”	-	-
L	Length variable	m	m
z	Compressibility factor	-	-
T	Temperature variable	-	-
π	Pi variable	-	-
d	Diameter variable	m	m

Symbol	Description	S.I. dimensionality	Most common used dimensionality
B_i	Formation volume factor of “i”	$\frac{m_{res}^3}{m_{st}^3}$	$\frac{m_{res}^3}{m_{st}^3}$
r	Radius variable	m	m
A_d	Adsorption degree	$\frac{g_{polymer}}{g_{rock}}$	$\frac{\mu g_{polymer}}{g_{rock}}$
m_p	Mass of polymer	kg	kg
ρ_s	Solid sandstone density	$\frac{kg}{m^3}$	$\frac{kg}{m^3}$
OD_c	Casing outside diameter	m	m
r_m	Treatment invasion radius	m	m

ACRONYM GLOSSARY

Abbreviation	Acronym
DPR	Disproportionate permeability reduction
RPM	Relative permeability modifier
WC	Water cut
WOR	Water oil ratio
ppm	Part per million
PAM	Polyacrylamide
HPAM	Hydrolyzed polyacrylamide
PHPAM	Partially hydrolyzed polyacrylamide
AMPS	Acrylamide-methyl-propanesulphonic
HEC	Hydroxyethylcellulose
STHP	Static top head pressure
FTHP	Flowing top head pressure
SBHP	Static bottom hole pressure
FBHP	Flowing bottom hole pressure
TVHP	Top vertical height of the perforation

BIBLIOGRAPHY

[1] R. S. Seright, "New Mexico Petroleum Recovery Research Center," New Mexico Petroleum Recovery Research Center, New Mexico Tech, 2006. [Online]. Available: http://baervan.nmt.edu/research_groups/reservoir_sweep_improvement/. [Accessed May 2014].

[2] L. Eoff, D. Darlymple, B. R. Reddy, J. Morgan and H. Frampton, “Development of a Hydrophobically Modified Water-Soluble Polymer as a Selective Bullhead System for Water-Production Problems,” no. SPE 80206, 2003.

[3] R. D. Sydansk and L. Romero-Zeron, Reservoir Conformance Improvement, Society of Petroleum Engineers, 2011.

[4] A. H. Kabir, “Chemical Water & Gas Shutoff Technology - An Overview,” no. SPE 72119, 2001.

[5] L. Eoff and D. Darlymple, “A versatile Monomer System for Conformance Application,” Huston, Texas, 1998.

[6] R. H. Lane, *Design Placement and Field Quality Control of Polymer Gel Water & Gas Shut-off Treatments,* Huston,, 1997.

[7] Y. Feng, R. Tabary, M. Renard, C. Le Bon, A. Omari and G. Chauveteau, “Characteristics of Microgels Designed for Water Shutoff and profile Control,” no. SPE 80203, 2003.

[8] D. Rousseau, R. Tabary, A. Zaitoun, T. Pichery, P. Mallo and O. Braun, “New Microgels fo EOR - From Laboratory to Field Applications,” in *14th European Symposium on Improved Oil Recovery*, Cairo, Egypt, 2007.

[9] J.-T. Liang and R. S. Seright, “Further Investigations of Why Gels Reduce Water Permeability More Than Oil Permeability,” no. SPE-37249-PA, 1997.

[10] A. Zaitun, H. Bertin and D. Lasseux, “Two-Phase Flow Property Modifications by,” no. SPE 39631, 1998.

[11] A. Zaitoun and N. Kohler, “Thin Polyacrylamide Gels for Water Control in High-Permeability,” no. SPE 22785, 1991.

[12] S. Nilsson, A. Stavland and H. C. Jonsbraten, “Mechanistic Study of Disproportionate Permeability Reduction,” no. SPE 39635, 1998.

[13] Liang J. and R. S. Seeright, “Wall-Effect/Gel Droplet Model of Disproportionate,” no. SPE 59334, 1998.

[14] A. Stavland and S. Nilsson, “Segregated Flow is the Governing Mechanism of Disproportionate Permeability Reduction in Water and Gas shutoff,” no. SPE 71510, 2001.

[15] G. P. e. a. Willhite, “Mechanism Causing Diproportionate Permeability In Porous Media Treated With Chromium Acetate and HPAAM Gels,” no. SPE 59345, 2000.

[16] R. S. Seright, “New Mexico Petroleum Recovery Research Center,” New Mexico Petroleum Recovery Research Center, New Mexico Tech, 2004. [Online]. Available: http://baervan.nmt.edu/research_groups/reservoir_sweep_improvement/. [Accessed 05 2014].

[17] T. Q. Nguyen, D. W. Green, G. P. Willhite and C. S. McCool, “Effect of Composition of a Polyacrylamide-Chromium(III) Acetate Gel on the Magnitude of Gel Dehydration and Disproportionate Permeability Reduction,” no. SPE89404, 2004.

[18] A. Stavland, S. Ekrann, K. O. Hettervik, S. R. Jakobsen, T. Schmidt and B. Schilling, “Disproportionate Permeability Reduction Is Not a Panacea,” no. SPE-50983-PA, 1998.

[19] J. T. Liang and R. S. Seright, “Further Investigations of Why Gels Reduce Water Permeability More Than Oil Permeability,” no. SPE-37249-PA, 1997.

[20] Norwegian Petroleum Directorate, “Reservoir Utilization through advanced Technological Help,” 1996.

[21] C. A. Grattoni, P. F. Luckham, X. D. Jing, L. Norman and R. W. Zimmerman, “Polymers as Relative Permeability Modifier: Adsorption and the Dynamic Formation of a Thick Polyacrylamide Layers,” no. 45, 2004.

[22] A. Mennella, L. Chiappa, T. P. Lockhart and G. Burrafato, “Candidate and Chemical Selection Guidelines for Relative Permeability Modification (RPM) Treatment,” no. SPE 72056, 2001.

[23] Ph. Elmkies, H. Bertin, D. Lasseux, M. Murray and A. Zaitoun, “Further Investigation on Two-phase Flow Property Modification by Polymers: Wettability Effect,” no. SPE 64986, 2001.

[24] N. Blin and A. Zaitoun, “Sand Control Treatment of Gas Production Well of Offshore Field: Laboratory Study,” Poweltec, 2012.

[25] M. W. Conway, S. W. Almond, J. E. Briscoe and L. E. Harris, “Chemical model for Rheological Behaviour of Crosslinked Fluid System,” vol. SPE 9334, 1983.

[26] D. Borling, K. Chan, T. Hughes and R. D. Sydansk, “Pushing Out the Oil with Conformance Improvement,” Schlumberger, 1994.

[27] Wikipedia, [Online]. Available: http://en.wikipedia.org/wiki/Xanthan_gum. [Accessed 09 05 2014].

[28] Cargill, 09 05 2014. [Online]. Available: http://www.cargill.com/products/personal-care/ingredients/hydrocolloids/scleroglucan/.

[29] J. Vasquez and L. Eoff, “A Relative Permeability Modifier Water Control: Candidate Selection, Cases Histories, and Lessons Learned after more than 3'000 Well Interventions,” no. SPE 165091, 2013.

[30] L. Eoff, D. Darlymple, B. R. Reddy, J. Morgan and H. Frampton, “Development of a Hydrophobically Modified Water-Soluble Polymer as Selective Bullhead System for Water-Production Problems,” no. SPE 80206.

[31] Wikipedia, [Online]. Available: http://en.wikipedia.org/wiki/Completion_(oil_and_gas_wells). [Accessed 06 05 2014].

[32] Wikipedia, Wikipedia, [Online]. Available: http://en.wikipedia.org/wiki/Tieback. [Accessed 06 05 2014].

[33] Polymer-Plastics Technology and Engineering, Atalnta, Georgia: School of Chemical Engineering, The Georgia Institute of Technology, 1996.

[34] Schlumberger, [Online]. Available: http://www.glossary.oilfield.slb.com/. [Accessed 08 05 2014].

[35] C. Osuji, Yale University, 02 05 2009. [Online]. Available: http://www.eng.yale.edu/polymers/docs/classes/polyphys/lecture_notes/5/handout5_w.html#handout5_wli1.html. [Accessed 04 06 2014].

[36] G. Chauveteau and K. S. Sorbie, “Mobility Control by Polymer,” in *Basic Concepts in Oil Recovery Processes*, Ed. Marc Bavière, Elsevier Science Publisher, 1992, p. Chapter II.

[37] A. Zaitoun and T. Pichery, “New Polymer Technology for Sand COntrol of Gas Storage Wells,” *International Symposium on Oilfield Chemestry,* no. SPE 121291, 20-22 April 2009.